

Slutrapport

# Risikkvantifiering vid olyckor med föroreningsspredning i mark och grundvatten

Georgia Destouni, Klas Persson och Jerker Jarsjö  
Institutionen för naturgeografi och kvartärgeologi,  
Stockholms universitet





## Svensk sammanfattning

Vattenförvaltning i Sverige och EU organiseras numera, i enlighet med EUs Ramdirektiv för vatten (2000/60/EC), i allt större utsträckning efter avrinningsområden. För att skydda vattenresurserna i ett avrinningsområde från förorening måste vi ofta ta hänsyn till ett flertal befintliga föroreningskällor, såsom industrier, avfallsdeponier och jordbruksområden. Vi bör också ta hänsyn till risken för framtida föroreningsutsläpp till följd av olyckor (t.ex. bränder och spillolyckor med farligt gods). Från alla befintliga föroreningskällor och tänkbara framtida föroreningsolycksplatser i ett avrinningsområde kan vattenburna ämnen transporteras genom vattensystemen och därmed hota vattenkvalitén i nedströms grundvattentäkter, sjöar, vattendrag och kustområden.

Huvudsyftet med detta projekt, samt med den licentiatavhandling och publicerade vetenskapliga artiklar som utgör projektets slutrapportering, var att undersöka hur en modelleringsmetodik baserad på tiderna för vattentransport, som tidigare utvecklats och använts främst för att beräkna föroreningstransport i grundvatten, kan användas för att även uppskatta spridning av vattenburna föroreningar och föroreningsrisker genom hela avrinningsområden. Vi har även särskilt undersökt de osäkerheter som är förknippade med att använda metoden på avrinningsområdesskala.

Resultaten från studien visar att denna vattentransporttidsbaserade metodik är väl användbar för att uppskatta den andel av ett föroreningsutsläpp som kan nå en nedströms vattenrecipient (som en flod, en sjö, eller kustvatten) från olika föroreningskällor i ett avrinningsområde, såväl som sannolikheten att överskrida givna riktvärden för föroreningar vid recipienten. Vi demonstrerar också hur man genom en scenarioanalys kan undersöka effekter av olika osäkerheter, till exempel kring karakteriseringen av föroreningskällan och markens heterogenitet. Resultaten från studien visar att i många fall har dessa, vanligtvis stora osäkerheter inte en avgörande betydelse för om föroreningsrisken är acceptabel eller inte. Inom ett kritiskt intervall för förhållandet mellan en förorenings nedbrytningshastighet och dess genomsnittliga transporttid med vattnet till recipienten kan emellertid osäkerheterna ha mycket stor inverkan på föroreningsriskbedömningen. Detta kritiska parameterintervall visar för vilka typer av föroreningar och rådande mark- och vattenförhållanden som mer platsspecifik information behövs för relevant uppskattning av föroreningsrisk. Intervallet kan i förebyggande syfte identifieras för olika föroreningar och platser genom den i studien vidareutvecklade och föreslagna metodiken för spridningsmodellering och scenarioanalys.

Denna slutrapport utgörs av Klas Perssons licentiatavhandling, som i sin tur består av en sammanfattningsdel och två publicerade artiklar. Studien som ligger till grund för rapporten har finansierats av Myndigheten för samhällsskydd och beredskap (MSB), med finansieringsbidrag även från Svensk Kärnbränslehantering AB (SKB).



## **Abstract**

Water quality management on hydrological catchment scales, as is for instance required by the EU Water Framework Directive (2000/60/EC), will generally have to consider groundwater and surface water transport of pollutants and nutrients from various local and diffuse sources (e.g. industrial plants, waste water treatment plants, agricultural areas and waste deposits) to recipient surface and coastal waters. In addition, water managers must plan for the risk of future accidental release of pollutants, for instance due to fires (fire fighting wastewater may be heavily polluted) and accidents involving dangerous goods.

In this thesis, I investigate the possibility and applicability of using a solute travel time based approach for quantifying the propagation of water pollution and associated water pollution risk through groundwater to surface water and through the linked groundwater and surface water systems of entire hydrological catchments. Furthermore, I investigate some main uncertainties associated with this quantification. The results show that this modelling approach can be readily used to quantify the mass delivery fractions from different pollutant sources to sensitive surface water recipients in a catchment and the resulting probability of exceeding given environmental or health risk based maximum pollution levels at the boundaries of these recipients. Moreover, the results show how the advective travel time based modelling approach can be combined with a scenario analysis approach to account also for uncertainties that are not statistically quantifiable about the advective travel time distribution, the pollutant input and the pollutant attenuation rates. The scenario analysis approach identifies, for any given water pollution situation in a catchment, the critical range of the relation between the average time-scales of advective transport and mass attenuation, within which these uncertainties may considerably affect modelled pollutant levels and associated risk of water pollution at the boundary of a surface water recipient of special environmental concern. Outside this range, assessment of pollution risk may be unambiguous even under large such quantification uncertainties.

## List of Papers

This thesis consists of two papers, a summary of these papers and some additional results:

Paper I:

Persson, K, Destouni, G, 2009. Propagation of water pollution and risk from the subsurface to the surface water system of a catchment. *Journal of Hydrology* 277, 434-444.

Paper II:

Darracq A, Destouni G, Persson K, Prieto C, Jarsjö J, 2009. Quantification of advective solute travel times and mass transport through hydrological catchments. *Environmental Fluid Mechanics*, doi:10.1007/s10652-009-9147-2.

# 1. Introduction

## 1.1. General problem description

In recent years, there has been a growing awareness of the importance of water quality management at the scale of entire drainage basins. For instance, the EU Water Framework Directive (WFD; European Commission 2000) requires catchment-scale water management for achieving and maintaining good physical, chemical and ecological status in all the waters of the EU member states. To fulfil that requirement, water quality management within drainage basins will generally have to consider groundwater and surface water transport of pollutants and nutrients from various local and/or diffuse sources (e.g. industrial plants, waste water treatment plants, agricultural areas and waste deposits). In addition, water managers must plan for the risk of future accidental release of contaminants, fires (fire fighting wastewater may be heavily polluted) and accidents involving dangerous goods.

Figure 1 illustrates a typical water pollution situation with various present or potential future sources of pollutants of different spatial extents at a number of locations within a catchment area (hypothetical pollutant sources are marked as black fields on the map). Some of the pollutants released from these sources may dissolve quickly in the water, whereas others may leak during a long period of time. Even after abatement and restoration measures have been taken, some pollutant fraction may reach the groundwater table below or within a pollutant source zone. From the source zone, pollutants may subsequently be transported by the groundwater into the nearest surface water body, and then further through the stream network towards some downstream surface water recipient (which in the example shown in Figure 1 is a stretch of coastal waters).

Surface water pollution risk includes the environmental and health consequences of different levels of pollution, in conjunction with the likelihood or probability that these pollution levels will occur. In this study, the focus is on the latter component of the total risk assessment problem, whereas the former component (ecosystem and health consequences associated with different water pollution levels) is considered in terms of maximum pollution levels that may be allowed by society and targeted by water quality management and pollution abatement. Such levels should be established by water quality regulation and water management plans, for instance based on toxicological studies.

The level of water pollution can be quantified as concentrations, mass flow rates, or as the total cumulative pollutant mass load from a pollutant source to a recipient. The fraction of the pollutant mass input at the source that eventually reaches a downstream recipient of special environmental concern will in the following be referred to as the mass delivery fraction. Estimates of mass delivery fractions for each pollutant source in a catchment indicate which sources have the greatest impact on a certain recipient, and, consequently, where pollution reduction measures are most needed (Darracq and Destouni 2005, Baresel et al. 2006). If the mass input is constant over time, the mass delivery fraction represents the steady-state mass flow rate into the recipient relative to the mass input rate. If the mass input varies in time, the mass delivery fraction is time-dependent, and its definition must include a time specification or, alternatively, only refer to the total cumulative pollutant mass loading to the recipient relative to the total cumulative pollutant mass input at the source.

To quantify mass delivery fractions for different sources of water pollution upstream of a surface water recipient, and the resulting future pollutant concentration, mass flow rate and cumulative mass load at the recipient boundary, we need to model the pollutant transport and mass exchange that takes place along the transport pathways from the sources to the recipient. However, such modelling and its pollution level predictions are associated with uncertainty that needs to be accounted for. Most model parameters are impossible to determine precisely due to large and irregular variability in time and space (O'Hagan and Oakley 2004). In

addition, even the site-specific information that could in principle be obtainable is commonly not available, and there is also uncertainty about whether the model representation of the dominant pollutant transport processes is adequate given the modelling purpose (e.g. Kavanaugh et al. 2003, Beven 2006, Baresel and Destouni 2007).

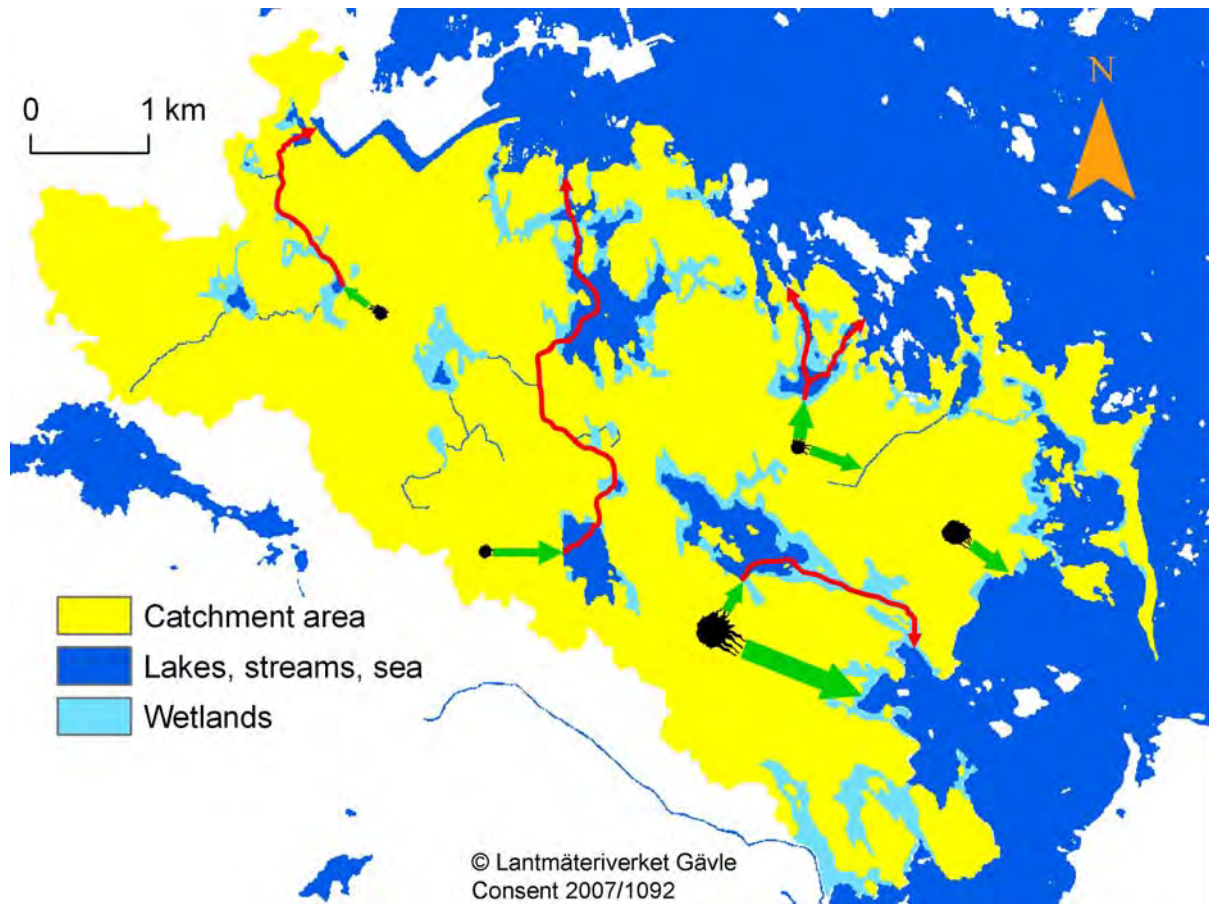


**Figure 1.** Illustration of a typical water pollution situation in a catchment area. Within a catchment area, like the Swedish coastal catchment area of Forsmark, which is here used as our illustration example, there may be various present or potential future sources of pollutants (the hypothetical sources that are here marked as black fields in the Forsmark catchment area example) from which contaminants may be transported by groundwater (green arrows) into the nearest inland surface water body, and then by surface water (red arrows) in the stream network towards a surface water recipient downstream of the catchment area.

In the typical situation of waterborne pollutant transport illustrated in Figure 1, one important aim should be to guarantee good water quality in the different surface water systems of the catchment area. As mentioned above, at the nearest groundwater–surface water boundary downstream of each source of water pollution, environmental or health risk based threshold values of pollutant concentration, mass flow rate or total mass load may be given from an independent toxicological assessment of the environmental and health consequences that are associated with different pollutant exposure levels in the surface water systems. Because the mass transport of any compound through the water systems is spatially variable at small and large scales (Dagan 1989, Rubin 2003), pollutant concentrations, mass flow rates and total mass loads at a groundwater–surface water boundary will vary in time and space. As

a result, the probability of a threshold pollution level to be exceeded somewhere on the groundwater–surface water boundary at some point in time may always be greater than zero (Andersson and Destouni 2001). In this study, we investigate the possible quantification of this exceedence probability, which constitutes an essential component of pollution risk assessment in hydrological catchments. Furthermore, we explore the possible quantification of mass delivery fractions. These fractions determine to large degree the catchment-scale pollutant transport and mass loading to downstream recipients and may also constitute a fundamental step of the exceedence probability quantification in water pollution risk assessments.

## **1.2. Catchment-scale pollutant transport modelling based on distributions of advective solute travel times**

The purely physical, advective travel time of solute along an individual transport pathway from any point of solute input to a given downstream recipient boundary depends on the pathway length and the water velocity along that pathway. Due to the variability of transport velocities and pathway lengths from different source input points to the recipient, and the generally irregular character of aquifer heterogeneity, advective solute travel times through the subsurface to the surface waters of a catchment will generally vary. The variability along and among the different transport pathways from source to recipient includes both deterministic and essentially random (Dagan 1989, Rubin 2003) components. With regard to both components, the resulting total advective solute travel time variability may be represented by a statistical distribution. This distribution is solute-independent because the advection of any solute depends by definition only on the transport length and purely physical hydraulic properties (hydraulic gradient, hydraulic conductivity, water content, porosity, etc.) that determine the water flow in different water systems.

Quantification of the statistical distributions of advective solute travel times constitutes a basic first step in a widely used approach to model solute transport in soil and groundwater systems (Shapiro and Cvetkovic 1988, Cvetkovic et al. 1992, Destouni 1992, Cvetkovic and Dagan 1994, Destouni and Graham 1995, Simmons et al. 1995, Andricevic and Cvetkovic 1996, Cvetkovic et al. 1996, Destouni and Graham 1997, Eriksson and Destouni 1997, Graham et al. 1998, Yabusaki et al. 1998, Gupta et al. 1999, Kaluarachchi et al. 2000, Andersson and Destouni 2001, Destouni et al. 2001, Foussereau et al. 2001, Tompson et al. 2002, Malmström et al. 2004). Once the solute-independent distribution of advective solute travel times is computed, it can be coupled with relevant models of other transport, mass transfer and reaction processes (such as hydrodynamic dispersion, diffusive mass transfer between mobile and immobile water zones, sorption–desorption, biodegradation, and decay) that may affect water pollution propagation from the sources within a catchment to the downstream recipient. This coupling approach has been referred to as the Lagrangian stochastic advective–reactive (LaSAR) modelling approach, and has recently been used to model solute transport in the groundwater–surface water systems of entire catchments (Lindgren et al. 2004, Lindgren and Destouni 2004, Botter et al. 2006, Rinaldo et al. 2006).

The relevant advective solute travel time distribution for entire catchments cannot be readily determined experimentally (McGuire and McDonnell 2006). Its quantification at catchment scales must often rely on available Geographic Information System (GIS) information and data, such as soil and land use maps, from which hydraulic properties may be estimated. For solute input distributed over entire catchment areas, results from previous studies (e.g. White et al. 2004, McGuire et al. 2005, Wörman et al. 2007, Fiori and Russo 2008, Fiori et al. 2009) have shown that the distribution of advective solute travel time to a given recipient may be governed by the distribution of pathway lengths and gradients, rather than by the randomness in flow velocity due to heterogeneity.

### 1.3. Objectives

The overall aim of this study is to investigate the possibility and applicability of using the LaSAR approach, and its solute travel time basis, for quantifying the propagation of water pollution and associated water pollution risk through groundwater to surface water and through the linked groundwater and surface water systems of entire hydrological catchments. More specific study objectives are to investigate how:

- pollutant mass delivery fractions and resulting probability of exceeding given environmental or health risk based maximum pollution levels can be quantified with the LaSAR modelling approach.
- different groundwater system characterisations and parameterisations affect estimated catchment-scale advective travel time distributions and model results of pollutant transport
- model results of pollutant mass transport and associated water pollution uncertainty and risk in hydrological catchments are affected by uncertainty about the pollutant mass input and biogeochemical attenuation along the different transport pathways to sensitive recipients.

To address these objectives, Paper I in this thesis develops a LaSAR based methodology to assess the probability of exceeding some given pollutant concentration limit or threshold at the groundwater–surface water boundaries downstream of present and possible future pollutant sources in hydrological catchments. In this LaSAR methodology development, Paper I accounts for and investigates the modelled water pollution uncertainty that arises from statistically quantifiable pollutant transport randomness, and from additional, not statistically quantifiable uncertainty about the total pollutant release level, the advective travel time variability (where necessary statistical input is unavailable), and the biogeochemical attenuation rate along transport pathways.

In Paper II and some new extensions to Paper II presented in this thesis summary, advective solute travel time distributions for different groundwater system characterisations and parameterisations are quantified for two specific Swedish catchment areas (Forsmark and Norrström) based on GIS data and hydrological modelling. The LaSAR modelling approach is subsequently used in order to quantify solute mass transport in the two case study catchments. As an extension of Papers I–II, I also use the estimated advective travel time distributions for the Forsmark catchment area (Paper II) in the risk propagation methodology developed in Paper I to further clarify the linkages between these two main thesis components.

## 2. Materials and methods

### 2.1. Case study areas

The sparsely populated 29.5 km<sup>2</sup> Forsmark catchment area drains to a stretch of the Baltic Sea coast about 100 km north of Stockholm. Along this coastal stretch there are multiple surface water outlets (streams and wetlands) as well as coastal catchment zones with mainly groundwater flow to the coast. Forsmark is the main candidate site for the final repository of nuclear waste in Sweden; thus the prevailing hydrological conditions in the area have been extensively investigated in the past years (e.g. Johansson et al. 2005, SKB 2005, Werner et al. 2007), and uniquely high-resolved (10×10 m) measured and modelled geographic and hydrological data is available (Jarsjö et al. 2007, 2008). The terrain is mildly undulating, and elevations range from 0 to 50 m above sea level (Brydsten and Strömngren 2004). The depth to the groundwater table is generally less than 1 m, and there is a strong correlation between

small-scale topography and groundwater level. The undulating landscape appears to generate various small recharge areas of local groundwater flow systems (Werner et al. 2007). Quaternary deposits dominated by till cover the bedrock in almost the entire area. Most recharged groundwater can be expected to follow shallow flow paths in the quaternary deposits or in the highly conductive quaternary deposits–bedrock interface, which normally is located at a depth of less than 5 m (Johansson et al. 2005). Infiltration excess overland flow may occur, but only over short distances (SKB 2005).

The landscape is characterised by forest, some small agricultural areas and a large number of lakes and wetlands. None of the lakes and wetlands is larger than  $0.5 \text{ km}^2$ , many are smaller than a hectare, but altogether they constitute 19% of the total catchment area. Some of these lakes and wetlands are connected to each other and to the Baltic Sea by streams. Others do not have any outlet and thus no surface water connection to the sea. The streams are all tiny with a cross section area of around  $0.3 \text{ m}^2$ , and they are all dry during dry periods (Nilsson and Borgiel 2004).

The  $22000 \text{ km}^2$  Norrström drainage basin, with more than 1.7 million inhabitants, contains the third and the fourth largest lakes in Sweden: Lake Mälaren and Lake Hjälmaren. Around these lakes the mildly undulating landscape is dominated by agricultural and urban areas, while the hilly north-western part of the drainage basin is mostly covered by forests. Right in the historic centre of Stockholm the drainage basin has its single coastal outlet, Norrström, which connects Lake Mälaren with the Baltic Sea. The available geographic data and hydrologic model resolution in the Norrström drainage basin is  $1 \times 1 \text{ km}$ . At this resolution, the drainage basin consists of 1.5% wetlands and 9.5% major inland surface waters. The previous hydrological model studies of the Norrström basin (Darracq and Destouni 2005, Darracq et al. 2005, Darracq and Destouni 2007, Destouni and Darracq 2006, Lindgren et al. 2007, Darracq et al. 2008) have estimated that about 25% of the total precipitation surplus in the basin runs off as surface water without passing through the groundwater system. Some of the runoff in the  $1 \times 1 \text{ km}$  model grid cells classified as land is then considered to go directly into small lakes and streams that form an unresolved surface water network within the model cell. As in Forsmark, the pure surface runoff contribution to the total runoff from the catchment is negligible.

## **2.2. Methodology for assessing the propagation water pollution uncertainty and risk from subsurface pollutant sources**

Paper I outlines a methodology that can be used for pollution risk assessment in hydrological catchments. The methodology uses the advective travel time based LaSAR modelling approach to estimate the probability  $P_R$  that a given, environmental or health risk based, pollutant concentration limit  $C_T$  will at any time  $t$  be exceeded by any local concentration value at a surface water recipient boundary downstream of a groundwater pollution source. The exceedence probability  $P_R$  is determined by the probability density function (pdf) of the local concentration  $f(C(t))$  at the surface water recipient boundary. The pdf  $f(C(t))$  may be of any realistic type or form but is, for simplicity, exemplified as lognormal in Paper I. Thereby,  $f(C(t))$  is fully determined by the two most readily quantifiable statistics of concentration  $C$ : the expected value  $E[C(t)]$  and variance  $V[C(t)]$ .

As an extension of Paper I, I also quantify the probability  $P_R$  of exceeding a given, environmental or health risk based limit mass delivery fraction  $\alpha_T$  for pollutant input in each one of the  $10 \times 10 \text{ m}$  model grid cells classified as land in the Forsmark catchment area. The limit mass delivery fraction  $\alpha_T$  can for instance be related to a limit mass flow rate at the surface water recipient boundary downstream of the source. As for the local concentration in Paper I, I assume for simplicity that the pdf of the mass delivery fraction  $\alpha$  is lognormal.

Two different cases of contaminant release from the source zone are considered in Paper I: (1) a short-pulse release scenario, which may for instance represent the first, fast release phase of easily soluble contaminant fraction after a pollution accident at the soil surface; and (2) a continuous release scenario, which may for instance represent a long-term industrial leakage, or the second, slow leakage phase after a pollution accident, when some hydrophobic pollutant fraction that has been retained in the accidental source zone slowly dissolves into the water phase during a long period of time. For both contaminant release cases, the local concentration statistics ( $E[C(t)]$  and  $V[C(t)]$ ) and the resulting exceedence probability  $P_R$  are quantified for different scenarios to account for uncertainties that are not statistically quantifiable.

To account for the effect of the statistically quantifiable randomness in aquifer heterogeneity, the exceedence probability  $P_R$  is quantified for lognormally distributed hydraulic conductivity  $K$  with different variance,  $V[\ln K]$ , but the same mean value of  $\ln K$ . The effect of  $V[\ln K]$  translates then differently into the solute travel time and  $C$  statistics depending on which spatial correlation structure of aquifer heterogeneity that prevails in the field.

To investigate the effect of the often large quantification uncertainty (e.g. Kavanaugh et al. 2003) about the input concentration  $C_0$  from the source zone, the exceedence probability  $P_R$  is quantified for a range of different scenarios of relative input concentration,  $C_0/C_T$ , where  $C_T$  is a given environmental or health risk based pollutant concentration limit.

To investigate the effect of quantification uncertainty about the average degree of biogeochemical attenuation between the source zone and the surface water recipient boundary, we also consider different scenarios for the relation between the average rates (or time-scales) of mass attenuation and advective transport (quantified as the product of the attenuation rate and a characteristic mean advective solute travel time through the pollutant source zone).

To investigate the effect of quantification uncertainty about the spatial correlation structure of aquifer heterogeneity we consider two extreme aquifer structure scenarios. The first scenario is a stratified aquifer (in Paper I generally referred to as 1D aquifer), where the advective velocity of groundwater transport is constant in the mean flow direction along any individual streamline, or streamtube, between the source zone and the surface water recipient boundary, but varies randomly due to random variation of hydraulic conductivity among the different streamlines (i.e. infinite correlation length in the flow direction). The second scenario is an isotropic aquifer (in Paper I generally referred to as 3D aquifer), where hydraulic conductivity and advective groundwater transport velocity vary randomly with equal spatial correlation lengths in all three spatial directions. The resulting variance of advective solute travel time is, for any given magnitude of hydraulic conductivity heterogeneity (i.e. hydraulic conductivity variance  $V[\ln K]$ ), much higher for the stratified than the isotropic aquifer case.

In general, the variability of advective solute travel times is a result of various processes that are difficult or impossible to quantify with accuracy and precision in real field situations. Examples of such processes are pore-scale dispersion and molecular diffusion (Dagan and Fiori 1997), as well as diffusive mass transfer between mobile and immobile groundwater zones (Lindgren et al. 2004). The travel time pdfs that correspond to the considered stratified and isotropic aquifer cases are so different that they are likely to bound a quite wide range of possible travel time pdfs for more complex field-process situations. The present aquifer scenario analysis may therefore implicitly give a good indication of the practical importance of different quantification uncertainties associated with the pdf of the physical solute travel time through a geological formation.

### 2.3. Calculation of travel times and mass delivery fractions in Forsmark and Norrström

In the methodology presented in Paper I, the quantification of advective travel time distributions is the basic first step to estimate water pollution propagation from pollutant sources and the exceedence probability  $P_R$  at downstream surface water recipient boundaries. In Paper II, we quantify and map the spatial distribution of advective travel times through the coupled groundwater–surface water systems of the coastal Swedish catchment areas of Forsmark and Norrström. Advective travel times are quantified for different groundwater system representations, including different scenarios of the distribution of flow paths between fast (shallow) and slow (deep) groundwater subsystems (Norrström), and of the relation between local ground slope and hydraulic gradient (Forsmark). As an extension of Paper II, different scenarios of the spatial variability of hydraulic conductivity in Forsmark are also considered in this thesis summary. Based on the estimated advective travel time distributions, pollutant mass delivery fractions are quantified from these catchments for different scenarios of the relation between the average time-scales of advective transport and pollutant attenuation.

The advective solute travel time through the stream network is quantified from the total pathway length and the effective water flow velocity along the pathway. For Norrström, effective water flow velocities through the lakes and streams that compose the stream network are quantified by empirical equations including the mean annual flow rate and the lake surface area (Darracq and Destouni 2007). As described in Jarsjö et al. (2007) and Persson et al. (2008), effective water flow velocities and travel times in lakes, wetlands and streams in Forsmark are estimated based on lake/wetland surface areas, modelled water flow rates, and available measurements of mean lake/wetland depths, stream cross-section areas, water content in wetlands, and stream flow rates.

For each 1×1 km model grid cell classified as land in the Norrström model, average flow velocity and average flow path length to the nearest stream within the grid cell are quantified for shallow and deep groundwater, respectively, using the PolFlow approach (e.g. de Wit et al. 2000). In the high-resolution (10×10 m) Forsmark model, the advective solute travel time from each model grid cell is quantified from the actual horizontal pathway length to the nearest stream network and the estimated groundwater flow velocity along the pathway. Pathways through deep groundwater are not considered in the Forsmark model. For simplicity, vertical solute transport is neglected in the modelling of advective solute travel times for both catchment areas, in which groundwater levels are generally very shallow (typically around 1–2 m or even less).

For both Forsmark and Norrström, the shallow groundwater flow velocity in each model grid cell is calculated as the product of hydraulic conductivity and gradient divided by the effective porosity. The hydraulic gradient in Norrström is assumed to equal the mean ground slope in each model grid cell. In the Forsmark modelling, we consider two alternative scenarios for the relation between ground slope and hydraulic gradient: (1) the hydraulic gradient equals the arithmetic average local ground slope within each one of the sub-catchments of the total 8783 outlets to the stream network or directly to the sea, and (2) the hydraulic gradient equals the local ground slope.

Hydraulic conductivity and porosity are modelled to vary between grid cells in the Norrström drainage basin, depending on the available data of soil characteristics (Darracq and Destouni 2005, Darracq et al. 2005, Darracq and Destouni 2007, Destouni and Darracq 2006, Lindgren et al. 2007, Darracq et al. 2008). For Forsmark, by contrast, uniform values of hydraulic conductivity and porosity are used in Paper II to mainly represent the solute transport through a high-conductivity layer at the interface between the quaternary deposits and the bedrock (Jarsjö et al. 2007), where measured conductivity values (reported e.g. in Johansson et al. 2005) were highly variable but did not correlate with soil cover.

As an extension to the results of Paper II, I quantify the spatial distribution of advective travel times through the groundwater systems of Forsmark for solute transport also in a more superficial layer in the quaternary deposits in Forsmark. Different hydraulic conductivity values (based on the measurements reported in Johansson et al. 2005) are assigned to areas corresponding to different soil texture classes in Jarsjö et al. (2008). In this scenario of hydraulic conductivity variability, the conductivity is thus assumed variable in space but locally uniform.

In addition, I quantify advective travel times through the groundwater systems of Forsmark for two scenarios of randomly variable, statistically stationary  $K$ . I then consider solute transport at the soil–bedrock interface for lognormally distributed  $K$  with uniform mean and variance. I quantify a lognormal pdf  $g(\tau)$  of the advective travel time  $\tau$  from each model grid cell to the downstream surface water recipient boundary, for the two extreme aquifer structure scenarios considered in Paper I (a stratified aquifer with infinite correlation length in the flow direction, and an isotropic aquifer with equal correlation length in all directions). A relatively small correlation length ( $I = 1\text{m}$ ) in the isotropic aquifer case and large degree of heterogeneity ( $V[\ln K] = 1$ ) are used, implying generally a very large difference between the resulting cell-specific travel time pdfs.

In the scenarios of constant and deterministically variable hydraulic conductivity, the advective travel time  $\tau$  from each model grid cell to a downstream recipient is constant, and the mass delivery fraction from each cell to the recipient can be quantified as  $\alpha = \exp[-\lambda\tau]$ , where  $\lambda$  is a first-order biogeochemical attenuation rate. In the scenarios of randomly variable, statistically stationary  $K$ , the advective travel time  $\tau$  from each cell varies randomly among different pathways to the recipient. The resulting mass delivery to the recipient will then also vary randomly among different pathways. The mean and variance of the mass delivery fraction from each model cell can be quantified as  $E[\alpha] = \int_0^{\infty} \exp[-\lambda\tau]g(\tau)d\tau$  and  $V[\alpha] = \int_0^{\infty} \exp[-2\lambda\tau]g(\tau)d\tau - (E[\alpha])^2$ , respectively. The assumed lognormal delivery fraction pdf can subsequently be quantified from  $E[\alpha]$  and  $V[\alpha]$ .

### 3. Catchment-scale water pollution risk assessment based on advective travel time distributions

#### 3.1. General results based on hypothetical advective travel time distributions

In Paper I, we show that the probability  $P_R$  of exceeding a given, environmental or health risk based, concentration limit can be readily assessed by a combined methodology, including an advective travel time based LaSAR modelling approach, which accounts for statistically quantifiable pollutant transport randomness, and a scenario analysis approach, which accounts for additional, not statistically quantifiable quantification uncertainty about the total pollutant release level, the advective travel time variability (where necessary statistical input is unavailable), and the biogeochemical attenuation rate along transport pathways.

The specific  $P_R$  results in Paper I show that uncertainty about the prevailing magnitude and correlation structure of aquifer heterogeneity generally affects the  $P_R$  propagation more for continuous than for short-pulse pollutant input. However, for both these scenarios of contaminant release, the aquifer heterogeneity details may be important for whether or not the risk of water pollution exceeds a threshold risk level (for instance the risk level that is judged acceptable by environmental managers and other stakeholders) only for a relatively narrow value range of a characteristic average attenuation rate–transport rate relation (quantified as the product of the solute-dependent biogeochemical attenuation rate and a characteristic mean

advective solute travel time through the pollutant source zone). Outside of this range, the water pollution risk may in many cases be judged unambiguously as acceptable or unacceptable (below or above a threshold risk level) essentially regardless of actual input concentration and correlation structure and magnitude of aquifer heterogeneity.

### 3.2. Quantification of advective travel time distributions in the catchment areas of Forsmark and Norrström

While the advective travel time distributions that underlie the exceedence probability  $P_R$  calculations in Paper I are purely hypothetical, we quantify in Paper II spatial distributions of the advective solute travel time through the coupled groundwater–surface water systems of the coastal Swedish catchment areas of Forsmark and Norrström using site-specific geographical and hydrological data. The results of Paper II show that transport in groundwater generally dominates advective travel times through both catchments. Nonetheless, stream networks in Forsmark and Norrström include various lakes with relatively long hydraulic turnover times. As a consequence, travel times in these stream networks are far from insignificant, in particular for the Forsmark model, where most estimated travel times through the inland surface water systems are in the order of months, and about  $\frac{1}{4}$  even in the order of one year (to compare with the average advective travel time through the coupled groundwater–surface water systems of Forsmark  $\bar{T}_C = 1.7$  years). This result indicates the importance of realistic representation, not only of the groundwater system, but also of the surface water systems for quantification of solute transport through the water systems of catchments with similar characteristics as those in Forsmark and Norrström.

For the catchment area of Forsmark, Paper II shows how different assumptions about the relation between local ground slope and hydraulic gradient yield large differences both in the estimated advective travel times from individual model grid cells to the sea and in the spreading of the resulting travel time distribution of the entire catchment area. For the Norrström drainage basin, the results illustrate how alternative model representations that neglect or account for the possible contribution of slow (deep) groundwater flow yield largely different catchment-scale travel distribution.

Figure 2 shows the catchment-scale cumulative distributions of the advective travel time in groundwater to a surface water recipient (the sea and the stream networks connected with the sea) in Forsmark resulting from the four considered cases of spatial variability of hydraulic conductivity  $K$ : (1) constant  $K$  in the entire catchment (the scenario used in Paper II); (2) randomly variable, statistically stationary  $K$  for a stratified aquifer; (3) randomly variable, statistically stationary  $K$  for an isotropic aquifer; and (4) deterministically variable, locally constant  $K$ . For direct comparison between the resulting travel time distributions, the travel times in the deterministically variable  $K$  scenario (corresponding to solute transport through the quaternary deposits) are scaled to yield the same catchment-average travel time as the other three scenarios (corresponding to solute transport in the high-conductivity layer at the soil–bedrock interface).

Figure 2 shows that the isotropic aquifer case results in almost identical catchment-scale travel time distribution as the constant  $K$  case, while the stratified aquifer case (which implies much larger cell-specific travel time variance than the isotropic aquifer) results in slightly larger spreading of travel times. The deterministically variable  $K$  case (i.e. non-stationary but locally uniform  $K$ ) yields a rather differently shaped travel time distribution with a much larger fraction of relatively short travel times than the other three scenarios. The coefficient of variation  $CV(\tau) = 190\%$  in the deterministically variable  $K$  scenario, compared to  $CV(\tau) = 110\%$  in the constant  $K$  scenario. In the Norrström model, where the hydraulic conductivity is also assumed deterministically variable depending on available soil texture maps, the coefficient of variation of the advective travel time through the catchment is considerably

larger,  $CV(\tau) = 330\%$ , even though the variability in groundwater flow path lengths is much larger in the fine-resolution ( $10 \times 10$  m) Forsmark model, than in the course-resolution Norrström model, where one single flow length in groundwater is used for each  $1 \times 1$  km model grid cell.

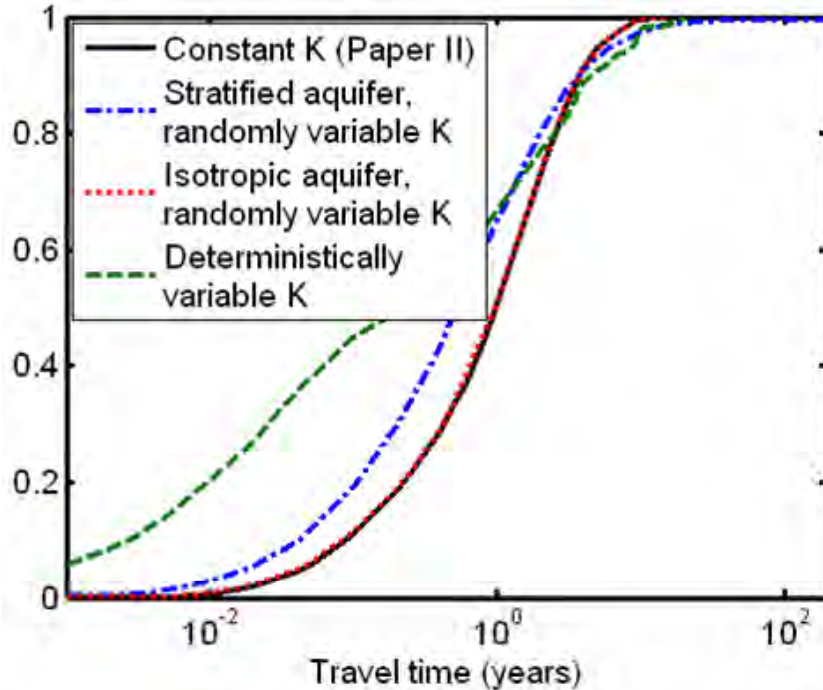


**Figure 2.** Cumulative distribution of the whole population of advective solute travel times from all model grid cells upstream of the considered surface water recipient (i.e. the sea or a stream network that is connected with the sea) to the nearest recipient boundary in the Forsmark catchment area for different scenarios of hydraulic conductivity,  $K$ , variability: (1) constant  $K$  in the entire catchment; (2) randomly variable ( $V[\ln K] = 1$ ), statistically stationary  $K$  for a stratified aquifer; (3) randomly variable ( $V[\ln K] = 1$ ), statistically stationary  $K$  for an isotropic aquifer; and (4) deterministically variable, locally constant  $K$ . The conductivity correlation length in the isotropic aquifer case is  $I = 1\text{m}$ .

### 3.3 Quantification of catchment-scale pollution uncertainty and risk: application Forsmark

Figure 3 shows the probability  $P_R$  of exceeding an example limit mass delivery fraction  $\alpha_T = 0.01$  to a surface water recipient (the sea and the stream networks connected with the sea) for pollutant input in each one of the model grid cells classified as land in the Forsmark catchment area. The exceedence probability  $P_R$  is quantified based on the advective travel time distributions resulting from the two considered scenarios of randomly variable, statistically stationary hydraulic conductivity  $K$  (i.e. a stratified aquifer structure scenario with large cell-specific travel time variance (Figs. 3a–c), and an isotropic aquifer structure scenario with small cell-specific travel time variance (Figs. 3d–f); the resulting catchment-scale distributions of advective travel time from these two scenarios of aquifer heterogeneity structure are shown in Figure 2). Furthermore, different scenarios of the relation between the average time-scales of advective transport and attenuation are considered. This average attenuation–transport relation is quantified as the product of catchment-average physical travel

time  $\bar{T}_C$  and first-order biogeochemical attenuation rate  $\lambda$  (which for exemplification simplicity is assumed constant for all groundwater sub-systems of the catchment).

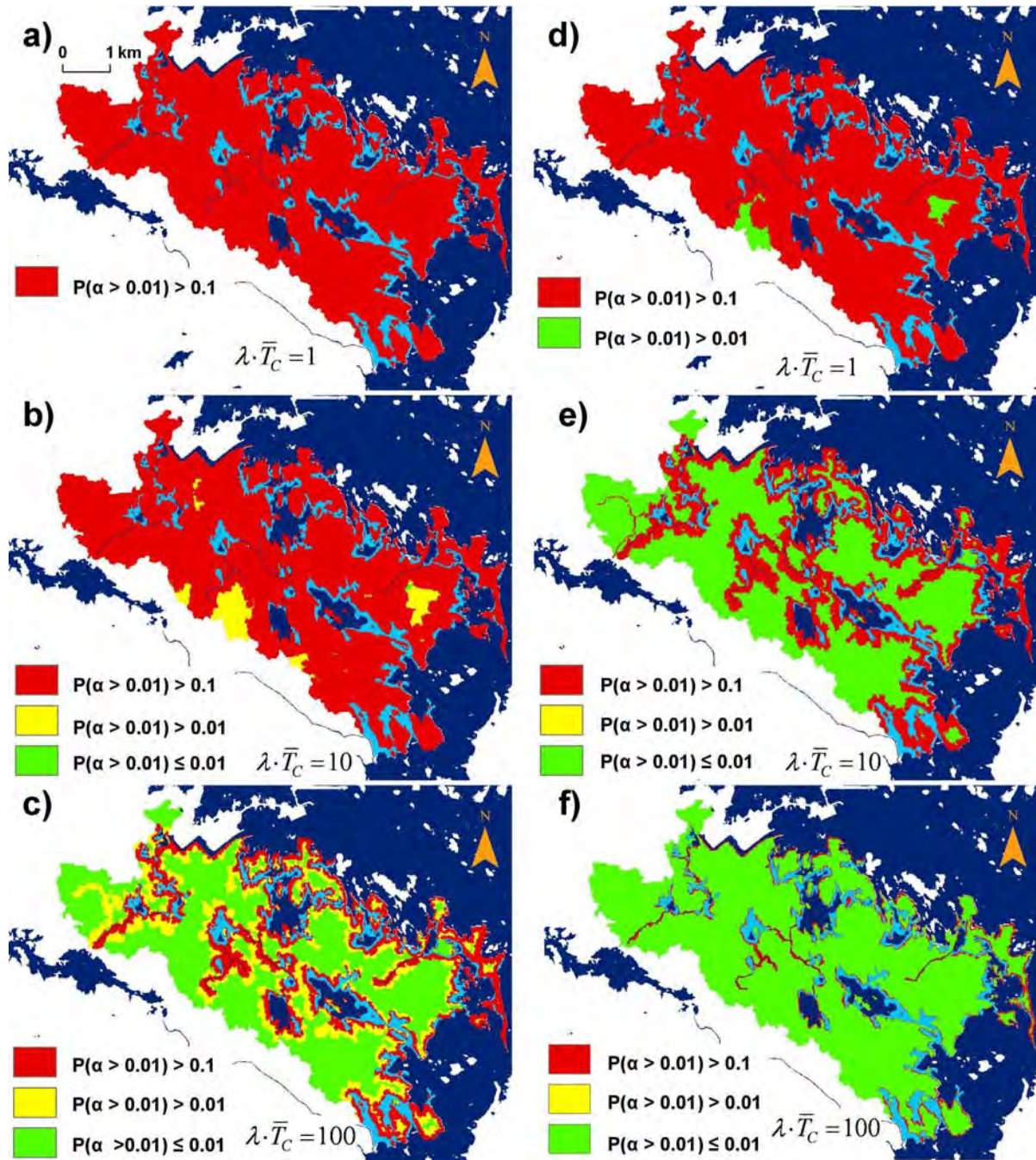


**Figure 3.** The probability that the delivered mass fraction  $\alpha$  from each grid cell location to the considered surface water recipient (i.e. the sea or a stream network that is connected with the sea) exceeds 0.01 for different scenarios of the product of the catchment-average advective travel time and first-order attenuation rate ( $\lambda\bar{T}_C = 1, 10$  and  $100$ ) and for two different scenarios of hydraulic conductivity,  $K$ , variability: (1) randomly variable ( $V[\ln K] = 1$ ), statistically stationary  $K$  for a stratified aquifer (a–c); and (2) randomly variable ( $V[\ln K] = 1$ ), statistically stationary  $K$  for an isotropic aquifer (d–f). The conductivity correlation length in the isotropic aquifer case is  $I = 1m$ .

The results from this scenario analysis example show that if there is sufficient site-specific information to at least estimate the average catchment-scale attenuation–transport relation  $\lambda\bar{T}_C$  to be in the order of 1 or smaller (Figs. 3a and 3d), the exceedence probability  $P_R$  is higher than 0.1 for contaminant release at most grid cell locations upstream of the recipient, regardless of prevailing aquifer heterogeneity structure. For  $\lambda\bar{T}_C$  in the order of 100 or larger (Figs. 3c and 3f), both scenarios yield instead an exceedence probability  $P_R$  lower than 0.01 for contaminant input to groundwater anywhere in the catchment, except for sources in the immediate vicinity of the recipient. For  $\lambda\bar{T}_C \approx 10$  (Figs. 3b and 3e), by contrast, the exceedence probability  $P_R$  results are highly sensitive to aquifer structure scenario and resulting cell-specific travel time variance. The exceedence probability  $P_R$  is then lower than 0.01 for most model cells in the isotropic aquifer case and higher than 0.1 for most cells in the stratified aquifer case.

#### 4. Effects of different groundwater system representations on estimated mass delivery fractions in the catchment areas of Forsmark and Norrström

This section includes results of modelled mass delivery fractions for the catchment areas of Forsmark and Norrström. The mass delivery fractions are quantified based on different advective travel time distributions resulting from alternative groundwater system representations, including the different considered scenarios of spatial variability of the hydraulic conductivity  $K$  explained in Section 2.3.

Figure 4 shows mass delivery fractions from different input locations in the Forsmark catchment area for the two considered scenarios of deterministic variability in the hydraulic conductivity: the constant  $K$  case (Figs. 4a–c) and the deterministically variable  $K$  case (Figs. 4d–f). The deterministically variable  $K$  case implies considerably larger mass delivery to the considered surface water recipient (i.e. the sea and the stream networks connected with the sea) than the constant  $K$  case from large parts of the catchment area for a quite wide range of average catchment-scale attenuation–transport relations,  $0.1 < \lambda\bar{T}_C < 1000$ . For instance, for  $\lambda\bar{T}_C = 10$  (Figs. 3b and 3e), the mass delivery is significant only from model cells in the immediate vicinity of the recipient in the constant  $K$  case, whereas the mass delivery to the recipient is more than 50% for a large part of the area in the case of deterministically variable  $K$ .

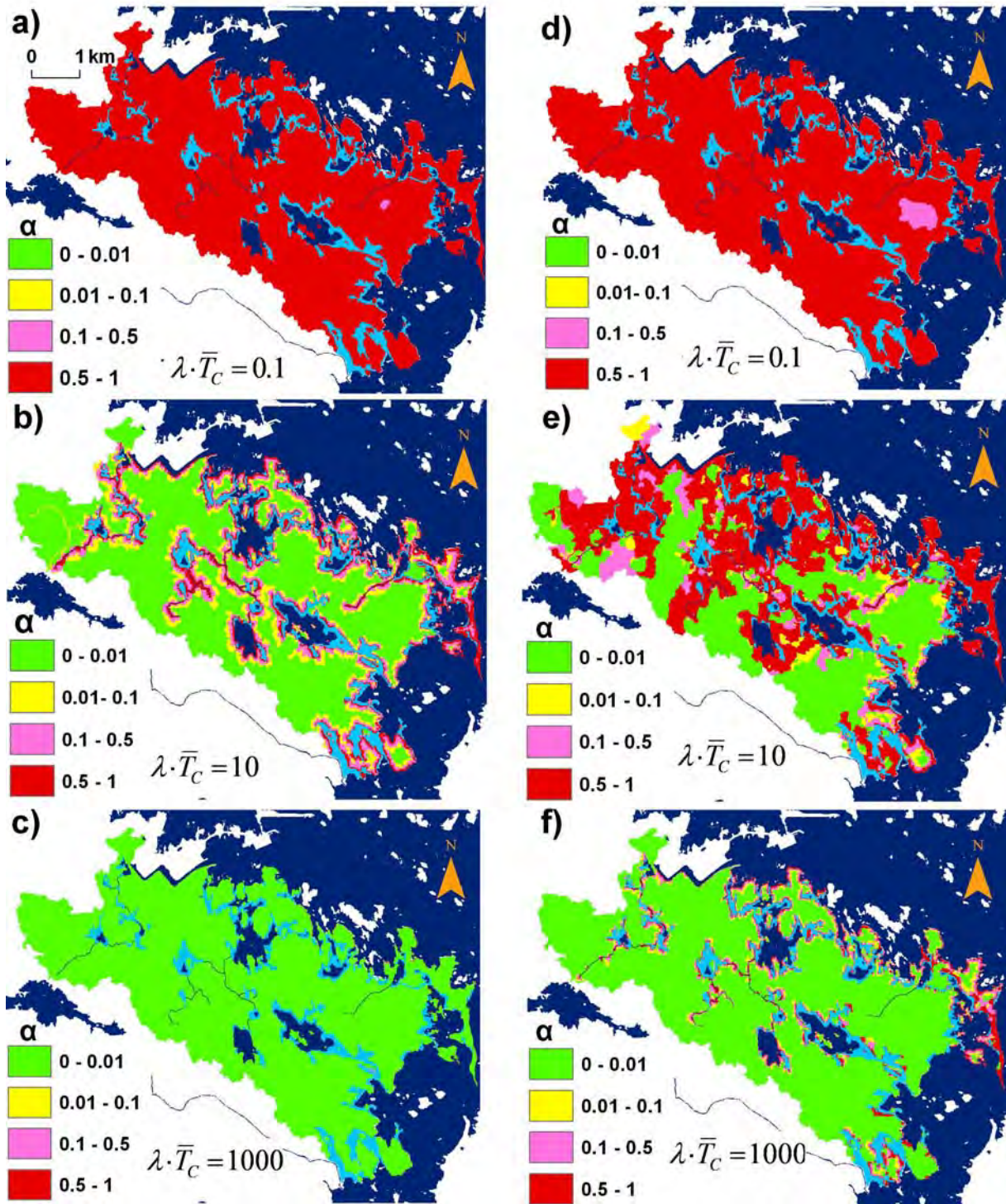
Figure 4 also shows that the solute mass delivery fractions differ considerably also within small areas. This is due to small-scale differences in advective travel time, which may be attributed mainly to different flow lengths, but also, in some cases, to differences in gradient. In deterministically variable  $K$  case, the spatial variability in hydraulic conductivity is an additional factor of importance.

Figure 5 shows average mass delivery fractions  $\bar{\alpha}_C$  for the entire area upstream of the considered surface water recipient in Forsmark (i.e. the sea and the stream networks connected with the sea) for the four considered scenarios of  $K$  variability. The deterministically variable  $K$  scenario yields generally the largest catchment-average mass delivery. This is because in that scenario there is a large fraction of flow paths along which the advective travel time to the recipient is much smaller than the catchment average travel time  $\bar{T}_C$ . In the calculation of the total catchment-scale delivery fraction  $\bar{\alpha}_C$  for time-dependent mass attenuation, the relatively large mass delivery contribution of these flow paths has greater statistical weight than the relatively small mass (or insignificant) delivery

contribution of flow paths along which the advective travel time is longer than average. For the same reason, the stratified aquifer structure scenario of randomly variable  $K$  also yields larger catchment-average mass than the isotropic aquifer and constant  $K$  scenarios (where the spreading of advective travel times around  $\bar{T}_C$  is smaller and there are fewer pathways with advective travel time  $\tau \ll \bar{T}_C$ ).

However, in analogy with the  $P_R$  results in Figure 3, Figures 4 and 5 show that a correct representation of heterogeneity and travel time variability is primarily important for mass delivery if the average relation between the time-scales of attenuation and advective transport lies within a specific critical interval  $0.1 < \lambda\bar{T}_C < 1000$ . For an attenuation–transport relation  $\lambda\bar{T}_C$  in the order of 0.1 or lower, Figures 4 and 5 show that most of a solute mass that is transported through the groundwater systems of the Forsmark catchment area can be expected to reach the recipient, regardless of the prevailing spatial variability of  $K$ , and essentially regardless of contaminant input location. Also for an attenuation–transport situation where  $\lambda\bar{T}_C$  is in the order of 1000 or larger, the travel time variability differences resulting from the different scenarios of  $K$  variability have a relatively minor impact on solute mass delivery. With the exception of contaminant input in model cells just next to the recipient, the mass delivery from any solute input location upstream of the recipient is insignificant for all four  $K$  variability scenarios.

In Paper II, we investigate how the difference in estimated advective travel time variability between the model cases of Forsmark (considering the constant  $K$  scenario) and Norrström (deterministically variable  $K$ ), affects the catchment-average delivery factor  $\bar{\alpha}_C$  for different scenarios of the average attenuation–transport relation  $\lambda\bar{T}_C$ . The Norrström model case, with its larger travel time variability ( $CV(\tau) = 330\%$ ), yields generally larger  $\bar{\alpha}_C$  than the Forsmark model case ( $CV(\tau) = 110\%$ ), but, interestingly, the difference in resulting  $\bar{\alpha}_C$  is significant only for a relatively narrow range of the average attenuation–transport relation  $1 < \lambda\bar{T}_C < 10$ . In fact, the deterministically variable  $K$  scenario for Forsmark ( $CV(\tau) = 190\%$ ) results in significantly larger  $\bar{\alpha}_C$  for some attenuation–transport relations  $\lambda\bar{T}_C$  than the Norrström model case, even though the travel time variability is larger in the Norrström model, in terms of coefficient of variation. For instance, for  $\lambda\bar{T}_C = 10$ , the catchment-average mass delivery fraction  $\bar{\alpha}_C = 0.12$  in the Norrström model case, whereas  $\bar{\alpha}_C = 0.43$  in the most directly comparable Forsmark model case of deterministically variable  $K$ . This result shows that it is not the travel time variability per se that affects the magnitude of mass delivery, but the fraction of pathways with much lower than average advective travel time. In the Forsmark model case of deterministically variable  $K$ , more than 20% of the advective travel times are smaller than 1% of the catchment-average travel time  $\bar{T}_C$ . In the Norrström model, the corresponding fraction of very short travel times is insignificant.



**Figure 4.** The fraction of solute mass released at each grid cell location upstream of the considered surface water recipient (i.e. the sea or a stream network that is connected with the sea) that reaches the nearest recipient boundary in the Forsmark catchment area for different scenarios of the product of the catchment-average advective travel time and first-order attenuation rate ( $\lambda \bar{T}_C = 0.1, 10$  and  $1000$ ) and for different scenarios of hydraulic conductivity,  $K$ , variability: (1) constant  $K$  in the entire catchment (a–c); and (2) deterministically variable, locally constant  $K$  (d–f).

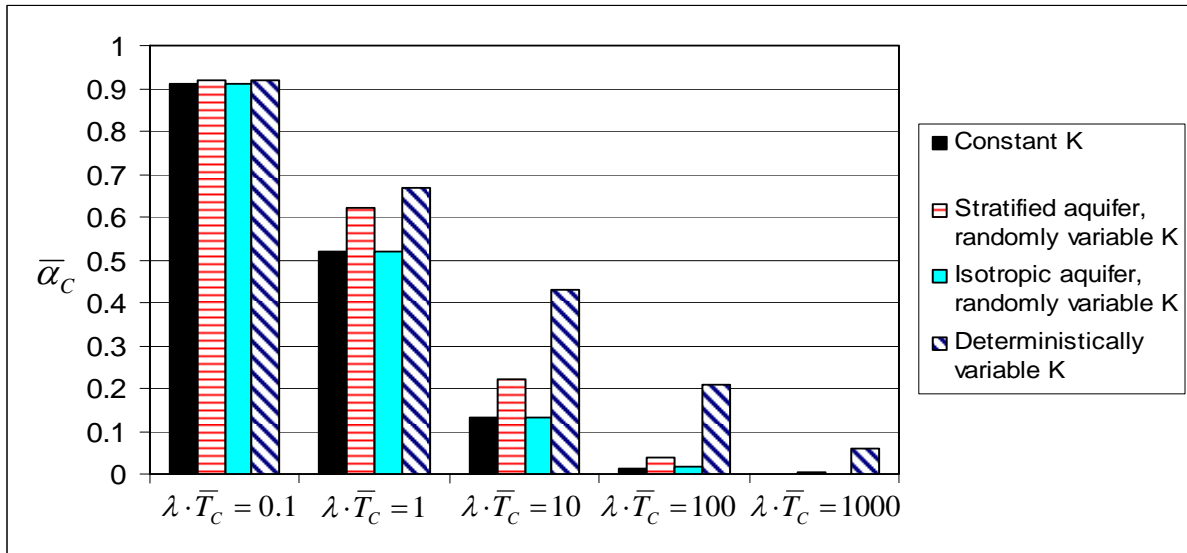


**Figure 5.** The catchment-average mass delivery  $\bar{\alpha}_C$  for the entire area upstream of the considered surface water recipient (i.e. the sea or a stream network that is connected with the sea) in the Forsmark catchment area for different scenarios of the product of the catchment-average advective travel time and first-order attenuation rate ( $\lambda \bar{T}_C = 0.1-1000$ ) and for different scenarios of hydraulic conductivity,  $K$ , variability: (1) constant  $K$  in the entire catchment; (2) randomly variable ( $V[\ln K] = 1$ ), statistically stationary  $K$  for a stratified aquifer; (3) randomly variable ( $V[\ln K] = 1$ ), statistically stationary  $K$  for an isotropic aquifer; and (4) deterministically variable, locally constant  $K$ .

## 6. Discussion

Models of catchment-scale solute transport can provide an overview of the potential impact of various sources of pollutants, nutrients, or tracers within a drainage basin that may be of great value for regional planning and management. For instance, model results of mass delivery from different pollutant sources to a sensitive surface water recipient can help environmental managers assess the economic efficiency of alternative pollution reduction measures (Baresel et al. 2006). The value of catchment-scale transport models for water quality management depends on how well the dominating processes are reproduced by the model. In this context, the account of model uncertainty is a crucial issue, because site-specific information may not be available at all for some key factors of catchment-scale solute transport and others can be measured only at a limited number of discrete points in time and space.

In this study, we have developed a methodology to assess catchment-scale transport of pollutant (or any solute) and associated uncertainty and risk using a LaSAR based modelling approach. In this methodology, the advective travel time distribution expresses both deterministic variability and statistically quantifiable randomness of transport pathway lengths and velocities within catchment areas in a compact and consistent way. Furthermore, a scenario analysis approach is used to account for additional, not statistically quantifiable uncertainty, with particular focus on the uncertainty about the total pollutant release level, the advective travel time variability (where necessary statistical input is unavailable), and the average mass attenuation rate along transport pathways. To further investigate the usefulness and limitations of the methodology for assessing mass delivery fractions and probability of exceeding given pollution level limits in hydrological catchments, we have also quantified

catchment-specific advective travel time distributions for the relatively well-investigated Swedish catchment areas of Forsmark and Norrström.

An important issue throughout this thesis has been the quantification uncertainty of advective travel time distributions. For pollutant that undergoes irreversible attenuation, underestimation of the fraction of transport pathways with relatively short advective travel time leads to underestimation of the non-attenuated pollutant mass that ultimately reaches a recipient from upstream sources. For essentially conservative pollutant, an assumed greater travel time spreading around the mean advective travel time from the input location results in increased modelled dilution of pollutants and lower modelled average pollutant concentration. For the applicability of the LaSAR approach to solute transport modelling, it is thus important to accurately quantify the relevant advective travel time variability in different field situations.

In this thesis, I have particularly investigated the influence of the heterogeneity of hydraulic properties on the distributions of advective solute travel time and resulting pollutant transport under different source extent conditions within a catchment. For pollutant transport from a local source, the magnitude and correlation structure of random hydraulic conductivity greatly affect the travel time distribution. For solute input distributed over an entire catchment area, such as that of Forsmark, the characteristics of this random heterogeneity were found to have much smaller impact on the total catchment-scale travel time distribution. The catchment-scale travel time distribution was then governed more by the distribution of pathway lengths than by random heterogeneity, as found also for other catchments (e.g. White et al. 2004, McGuire et al. 2005, Wörman et al. 2007, Fiori and Russo 2008). However, the present Forsmark results show that the risk-related probability of exceeding a given maximum level of pollution at a recipient boundary may be more sensitive to the characteristics of random heterogeneity than to pathway length for some critical interval of the relation between the average time scale of advective solute transport and the biogeochemical attenuation rate. Neglect of random heterogeneity and resulting random travel time variability may then result in considerable underestimation of pollution mass delivery and associated water pollution risks in a catchment.

Moreover, the results for deterministically variable hydraulic conductivity in Forsmark show that spatial non-stationarity of aquifer heterogeneity in terms of variable mean hydraulic conductivity (due to the presence of various soil types and geological formations within the catchment area) may have large effect on the catchment-scale travel time distribution, beyond the effects of the pathway length variability and the local randomness in hydraulic conductivity and advective groundwater transport velocity. Neglect of this spatial non-stationarity may yield misleading predictions of pollutant transport from both local and distributed sources. For the latter, such neglect may lead to systematic underestimation of the total pollutant loading into surface water.

Another critical factor of catchment-scale advective travel times and resulting pollutant mass transport is the groundwater hydraulic gradient. Measurements of groundwater levels are typically only available for a relatively small number of discrete points within a catchment area, and hydraulic gradients are mostly estimated based on topography data for the land surface. In humid climates, the groundwater surface is generally assumed to follow the ground surface (Wörman et al. 2007), but an important modelling issue is at which spatial resolution this assumption is valid. On the one hand, the hydraulic gradient fluctuations can be expected to be somewhat damped relative to small-scale land–surface fluctuations. On the other hand, in an undulating landscape, such as in the studied Forsmark and Norrström catchment areas, an assumed hydraulic gradient based on average regional ground slope may lead to considerable underestimation of the hydraulic gradient in areas where local ground slopes in opposite directions average each other out. The results in Paper II illustrate how different

assumptions about the relation between local ground slope and hydraulic gradient may yield large effects on the modelled travel time distributions for both local and distributed sources.

In Paper II, advective solute travel times and pollutant mass delivery fractions for the Norrström drainage basin were quantified using relatively coarse-resolution data (1×1 km). Model results for the much smaller catchment area of Forsmark, where high-resolution data (10×10 m) were available, show that small-scale spatial variability in, for instance, transport pathway lengths and hydraulic conductivity and gradient may have a major impact on catchment-scale mass delivery and associated water pollution risks. For larger catchments such fine model representation as in Forsmark is greatly limited by computational and data availability constraints. Critical modelling issues are then if variability within the smallest modelling unit (which may be for instance square units or subcatchments covering areas in the order of km<sup>2</sup> or larger) is important given the modelling purpose (Dehotin and Braud 2008), and, if so, how such small-scale variability should be accounted for. For spatially uniform solute input, heterogeneity and transport length variability within the smallest modelling unit may be represented by spatially stationary statistics. For spatially variable input, by contrast, the specific geographical location of the heterogeneity statistics is important and a coarse-resolution model might produce misleading results of water pollution risks.

In this thesis, I have focused on the investigation of different model representations and associated uncertainty regarding the groundwater rather than the surface water systems of hydrological catchments. In the studied Swedish catchment areas (Forsmark and Norrström), solute travel times in the stream networks, which are composed by various lakes and wetlands with relatively long hydraulic turnover times, however, are far from insignificant in comparison with the travel times in groundwater. Different model representations of the surface water systems could therefore also have a large impact on resulting total travel time distributions for the catchment. This merits further investigation because the travel times through the stream networks are often ignored in estimations of catchment-scale travel time distributions (McGuire and McDonnell 2006).

An exhaustive analysis of catchment-scale water pollution risk and uncertainty must further also consider various other factors, such as temporally variable travel time distributions (Fiori and Russo 2008), multi-directional flow in flat areas (McGuire et al. 2005), and reversible sorption–desorption and other reactive processes (Destouni and Graham 1997, Eriksson and Destouni 1997, Yabusaki et al. 1998, Kalaurachchi et al. 2000, Malmström et al. 2004). Additional factors that could significantly affect solute transport include spatial and temporal variability of solute-specific mass attenuation rate. Temperature commonly influences these rates, and they may also be highly dependent on the geological media. Studies on the biodegradation of different pollutants in different subsurface environments have found evidence of both negative and possible correlation between biodegradation rate and hydraulic conductivity (e.g. Jardin 2008 and references therein). Several studies have shown the importance of variability in local mass attenuation rate and its correlation with the hydraulic properties for pollutant transport from local sources in groundwater (e.g. Cunningham and Fadel 2007 and references therein). Further research is required to investigate the effects of such variability and correlations on solute transport in the linked groundwater and surface water systems of whole hydrological catchments.

While the focus of this thesis is primarily on the quantification of advective travel time and its distribution, the biogeochemical attenuation has, as a first step and for illustrative simplicity, been represented by a constant first-order rate. Under these conditions, the thesis results have shown that the product of the (field or catchment) characteristic average advective solute travel time and the average attenuation rate largely determines total pollutant

mass delivery and associated pollution risk if this product falls within two identified, open value ranges.

In general, it is difficult to estimate mass attenuation rates, particularly for pollutants such as petroleum products that are mixtures of hundreds of different constituents with different biodegradation properties (Fagerlund and Niemi 2007). In addition, reported degradation rates often vary over various orders of magnitude for the same organic compound (Suarez and Rifai 1999, Washington and Cameron 2001, Mulligan and Yong 2004). There are also other important parameters of irreversible solute mass attenuation than just the first-order rate constant used in the quantification examples of this thesis. For instance, at relatively high pollutant concentrations, the biodegradation kinetics may be better approximated by a zero-order rate expression (Bekins et al. 1998). Hence, there are various open research questions related to the accurate representation of dominant mass attenuation processes in catchment-scale solute transport modelling.

## 7. Conclusions

In this thesis, I have investigated the possibility and applicability of using the LaSAR approach, and its solute travel time basis, for quantifying the propagation of water pollution and associated water pollution risk through groundwater to surface water and through the linked groundwater and surface water systems of entire hydrological catchments. Furthermore, I have investigated some main uncertainty associated with this quantification. The results show that the LaSAR modelling approach can be readily used to quantify mass delivery fractions from different pollutant sources to sensitive surface water recipients in a catchment and the resulting probability of exceeding given environmental or health risk based maximum pollution levels at the boundaries of these recipients. The basic advective travel time distributions in this approach express then in a compact and consistent way both deterministic variability and statistically quantifiable randomness of transport lengths and velocities along and among the different transport pathways through the catchment to the recipient.

Moreover, the thesis has shown how the advective travel time based LaSAR modelling approach can be combined with a scenario analysis approach to account also for uncertainties that are not statistically quantifiable about the advective travel time distribution, the pollutant input and the pollutant attenuation rates in a catchment. The scenario analysis approach identified, for different water pollution problems, the critical range of the relation between the average time-scales of advective transport and mass attenuation, within which these uncertainties may considerably affect modelled pollutant levels and associated risk of water pollution at the boundary of a surface water recipient of special environmental concern. Outside this range, assessment of pollution risk may be unambiguous even under large such quantification uncertainties.

The main focus of this thesis has been on the quantification of solute transport through linked groundwater–surface water systems, neglecting for simplicity the transport component through the unsaturated zone, from the land surface to the saturated groundwater zone. Water quality management within a catchment, however, should also protect the groundwater from pollution, requiring future studies to also particularly consider: (1) the essentially vertical pollutant transport from the land surface to the groundwater zone. Other key issues for future research include further investigations of the effects of: (2) different model representations of the surface water systems, (3) different representations of the variability within the smallest modelling unit of course-resolution models, and (4) spatial variability of biogeochemical

attenuation rates and their correlation with the hydraulic properties of the linked groundwater and surface water systems of whole catchments.

## Tack

Jag vill först och främst rikta ett stort tack till min huvudhandledare Gia Destouni. Hennes roll i det arbete som har lett fram till den här licentiatavhandlingen kan inte nog framhävas. Under arbetets alla faser har jag även haft turen att kunna luta mig mot min biträdande handledare Jerker Jarsjö, som alltid är tillmötesgående och hjälpsam. Jag tackar även Amélie Darracq och Carmen Prieto för deras bidrag samt medlemmarna i MSB-projektets referensgrupp för givande diskussioner om tillämpbarheten av mina forskningsresultat.

Myndigheten för samhällsskydd och beredskap (MSB) och Svensk Kärnbränslehantering (SKB) har finansierat min forskning.

## References

- Andricevic, R., Cvetkovic, V., 1996. Evaluation of risk from contaminants migrating by ground water. *Water Resources Research*, 32, 611-621.
- Andersson, C., Destouni, G, 2001. Risk–cost analysis in ground water contaminant transport: the role of random spatial variability and sorption kinetics. *Ground Water* 39(1), 35–48.
- Baresel C., Destouni G., Gren I.-M., 2006. The influence of metal source uncertainty on cost-effective allocation of mine water pollution abatement in catchments. *Journal of Environmental Management* 78, 138–148, doi:10.1016/j.jenvman.2005.03.013.
- Bekins B.A., Warren E., Godsy E.M., 1998. A comparison of zero-order, first-order, and Monod biotransformation models. *Ground Water*, 36(2), 261–268.
- Botter G.; Settin T.; Marani M.; Rinaldo A., 2006. A stochastic model of Nitrate transport and cycling at basin scale, *Water Resources Research* 42, W04415.
- Brydsten L.; Strömgren M. Digital elevation models for site investigation programme in Forsmark. Swedish Nuclear Fuel and Waste Management Company Report P-04-70, Stockholm, 2004.
- Cunningham J.A., Fadel Z.J., 2007. Contaminant degradation in physically and chemically heterogeneous aquifers. *Journal of Contaminant Hydrology* 94, 293–304.
- Cvetkovic, V.; Dagan, G. Shapiro, A. M., 1992. A solute flux approach to transport in heterogeneous formations, 2, Uncertainty analysis, *Water Resources Research* 28, 137–1388.
- Cvetkovic V.; Dagan G., 1994. Transport of kinetically sorbing solute by steady random velocity in heterogeneous porous formations, *Journal of Fluid Mechanics* 265, 189–215.
- Cvetkovic V.; Ceng H.; Wen, X.-H., 1996 Analysis of non-linear effects on tracer migration in heterogeneous aquifers using Lagrangian travel time statistics. *Water Resources Research* Vol. 32, NO. 6, 1671–1680.
- Dagan G., 1989. *Flow and Transport in Porous Formations*. Springer Verlag, Berlin.
- Dagan G; Fiori A., 1997. The influence of pore-scale dispersion on concentration statistical moments in transport through heterogeneous aquifers. *Water Resources Research* 33(7), 1595–1606.
- Darracq A., Destouni G., 2005. In-stream nitrogen attenuation: model-aggregation effects and implications for coastal nitrogen impacts. *Environmental Science and Technology* 39(10):3716–3722.

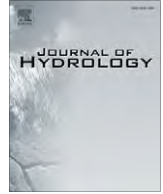
- Darracq A., Greffe F., Hannerz F., Destouni G., Cvetkovic V., 2005. Nutrient transport scenarios in a changing Stockholm and Mälaren valley region. *Water Science and Technology* 51(3–4):31–38.
- Darracq A., Destouni G., 2007. Physical versus biogeochemical interpretations of nitrogen and phosphorus attenuation in streams and its dependence on stream characteristics. *Global Biogeochemical Cycles*, doi:10.1029/2006GB002901.
- Darracq A., Lindgren G.A., Destouni G., 2008. Long-term development of phosphorus and nitrogen loads through the subsurface and surface water systems of drainage basins, *Global Biogeochemical Cycles*, doi:10.1029/2007GB003022.
- De Wit M., Meinardi C., Wendland F., Kunkel R., 2000. Modelling water fluxes for the analysis of diffuse pollution at the river basin scale. *Hydrological Processes* 14, 1707–1723.
- Dehotin J., Braud, I., 2008. Which spatial discretization for distributed hydrological models? Proposition of a methodology and illustration for medium to large-scale catchments. *Hydrology and Earth System Sciences*, 12, 769–796.
- Destouni G., 1992. Prediction uncertainty in solute flux through heterogeneous soil. *Water Resources Research*, Vol. 28, NO. 3, 793–801.
- Destouni G.; Graham W., 1995. Solute transport through an integrated heterogeneous soil–groundwater system. *Water Resources Research*, Vol. 31, 1935–1944.
- Destouni, G.;Graham, W., 1997. The influence of observation method on local concentration statistics in the subsurface. *Water Resources Research* 33(4), 663–676.
- Destouni, G.; Simic, E.; Graham, W., 2001. On the applicability of analytical methods for estimating solute travel time statistics in nonuniform groundwater flow. *Water Resources Research* 37, 2303–2308.
- Destouni G., Darracq A., 2006. Response to comment on "In-stream nitrogen attenuation: model aggregation effects and implications for coastal nitrogen impacts". *Environmental Science and Technology* 40(7):2487–2488.
- Destouni G.; Lindgren G.; Gren I.-M., 2006. Effects of inland nitrogen transport and attenuation modeling on coastal nitrogen load abatement. *Environmental Science and Technology* 40 (20), 6208–6214.
- Eriksson N., Destouni G., 1997. Combined effects of dissolution kinetics, secondary mineral precipitation, and preferential flow on copper leaching from mining waste rock. *Water Resources Research* 33, 471–483.
- European Commission, 2000. Directive 2000/60/EC of the European Parliament and of the Council establishing a framework for Community action in the field of water policy. *Official Journal of the European Communities* L 41, 26–32.
- Fagerlund F., Niemi A., 2007. A partially coupled, fraction-by-fraction modelling approach to the subsurface migration of gasoline spills. *Journal of Contaminant Hydrology* 89, 174–198.
- Fiori A., Russo D., Di Lazzaro M., 2009. Stochastic analysis of transport in hillslopes: Travel time distribution and source zone dispersion, *Water Resources Research* 45, W08435, doi:10.1029/2008WR007668.
- Foussereau X.; Graham W.; Aakpoji A.; Destouni G.; Rao P.S.C., 2001. Solute transport through a heterogeneous coupled vadose–saturated zone system with temporally random rainfall. *Water Resources Research*, Vol. 36, 911–921.
- Graham W., Detsouni G., Demmy G., Foussereau X., 1998. Prediction of local concentration statistics in variably saturated soils : Influence of observation scale and comparison with field data. *Journal of Contaminant Hydrology* 32, 177–199.
- Gupta A., Destouni G., Bergen Jenssen M., 1999. Modelling tritium and phosphorus transport by preferential flow in structured soil. *Journal of Contaminant Hydrology* 35, 389–407.

- Jardin P.M., 2008. Influence of coupled processes on contaminant fate and transport in subsurface environments. *Advances in Agronomy*, Vol. 99, doi: 10.1016/S0065-2113(08)00401-X
- Jarsjö J.; Destouni G.; Persson K.; Prieto C., 2007. Solute transport in coupled inland–coastal water systems. General conceptualization and application to Forsmark. Swedish Nuclear Fuel and Waste Management Co Report R-07-65, Stockholm.
- Jarsjö J.; Shibuo Y.; Destouni G., 2008. Spatial distribution of unmonitored inland water flows to the sea. *Journal of Hydrology*, 348, 59–72.
- Johansson P.-O., 2003. Drilling and sampling in soil. Installation of groundwater monitoring wells and surface water level gauges. Swedish Nuclear Fuel and Waste Management Company Report P-03-64, Stockholm.
- Johansson P.-O.; Werner K.; Bosson E.; Juston J., 2005. Description of climate, surface hydrology, and near-surface hydrology. Preliminary site description. Forsmark area – version 1.2. Swedish Nuclear Fuel and Waste Management Co Report R-05-06.
- Kaluarachchi J. J., Cvetkovic V., Berglund S., 2000. Stochastic analysis of oxygen- and nitrate-based biodegradation of hydrocarbons in aquifers. *Journal of Contaminant Hydrology*, 41, 335–365.
- Kavanaugh M. C.; Rao P. S. C. K.; Abriola L.; Cherry J.; Destouni G.; Falta R.; Major D.; Mercer J.; Newell C.; Sale T.; Shoemaker S.; Siegrist R.; Teutsch G.; Udell, K., 2003. *The DNAPL remediation challenge: is there a case of source depletion?* Expert panel report EPA/600/R-03/143, Environmental Protection Agency (EPA), U.S.A.
- Lindgren G. A., Destouni G., 2004. Nitrogen loss rates in streams: Scale-dependence and up-scaling methodology. *Geophysical Research Letters* 31, L13501, doi:10.1029/2004GL019996.
- Lindgren G. A., Destouni G., Miller A. V., 2004. Solute transport through the integrated groundwater-stream system of a catchment. *Water Resources Research*, Vol. 40, doi:10.1029/2003WR002765.
- Lindgren G.A., Destouni G., Darracq A., 2007. The inland subsurface water system role for coastal nitrogen load dynamics and abatement responses. *Environmental Science and Technology* 41(7):2159–2164.
- Malmström M.E., Destouni G., Martinet P., 2004. Modeling expected solute concentration in randomly heterogeneous flow systems with multicomponent reactions. *Environmental Science and Technology*, Vol. 38, 2673–2679.
- McGuire K.J., McDonnell J.J., 2006. A review and evaluation of catchment transit time modeling. *Journal of Hydrology* 330:543–563.
- Mulligan C.N., Yong R.N., 2004. Natural attenuation of contaminated soils. *Environment International*, 30, 587–601.
- Nilsson A.-C., Borgiel M., 2004. Sampling and analyses of surface waters. Results from sampling in the Forsmark area, March 2003 to March 2004. Swedish Nuclear Waste Management Company Report P-04-146, Stockholm.
- O’Hagan, A.; Oakley, J. E., 2004. Probability is perfect, but can we elicit it perfectly? *Reliability Engineering and System Safety* 85, 239–248.
- Persson K., Jarsjö J., Prieto C., Destouni G., 2008. Propagation of environmental risk from contaminant transport through groundwater and stream networks. Risk Analysis VI: Simulation and Hazard Mitigation”, 5–7 May 2008, Cephalonia, Greece.
- Rinaldo A., Botter G., Bertuzzo E., Uccelli A., Settin T., Marani M., 2006. Transport at basin scales: 1. Theoretical framework. *Hydrology and Earth System Sciences* 10, 19–30.
- Rubin Y., 2003. *Applied Stochastic Hydrogeology*. Oxford University Press, New York.
- SKB., 2005. Description of surface systems. Preliminary site description. Forsmark area – version 1.2. Swedish Nuclear Fuel and Waste Management Co Report R-05-03.

- Shapiro A.M., Cvetkovic V., 1988. Stochastic analysis of solute arrival time in heterogeneous porous media. *Water Resources Research*, Vol. 24, 1711–1718.
- Simmons C.S., Ginn T.R., Wood B.D., 1995. Stochastic–convective transport with nonlinear reaction: Mathematical framework. *Water Resources Research*, Vol. 31, 2675–2688.
- Sonsten L., 2005. Chemical characteristics of surface waters in the Forsmark area. Evaluation of data from lakes, streams, and coastal sites. Swedish Nuclear Fuel and Waste Management Co Report R-05-41.
- Suarez M.P., Rifai, H.S., 1999. Biodegradation Rates for Fuel Hydrocarbons and Chlorinated Solvents in Groundwater. *Bioremediation Journal*, Vol. 3, 337–362.
- Tompson A.F.B., Bruton C.J., Pawloski G.A., Smith D.K., Bourcier W.L., Shumaker D.E., Kersting A.B., Carle S.F., Maxwell R.M., 2002. On the evaluation of groundwater contamination from underground nuclear tests. *Environmental Geology*, Vol. 42, 235–247.
- Tröjbom M., Söderbäck B., 2006. Chemical characteristics of surface systems in the Forsmark area. Visualisation and statistical evaluation of data from shallow groundwater, precipitation, and regolith. Swedish Nuclear Fuel and Waste Management Co Report R-06-19.
- Yabusaki S.B.; Steefel C.I.; Wood B.D, 1998. Multidimensional, multicomponent, subsurface reactive transport in nonuniform velocity fields: code verification using an advective reactive streamtube approach. *Journal of Contaminant Hydrology*, Vol. 30, NO. 3, 299–331.
- Van Deursen W. P. A., 1995 *Geographical information systems and dynamic models; development and application of a prototype spatial modelling language*; Ph.D. Thesis, Utrecht University, Utrecht, 1995, available electronically through [www.carthago.nl](http://www.carthago.nl).
- Washington J.W., Cameron B.A., 2001. Evaluating degradation rates of chlorinated organics in groundwater using analytical models. *Environmental Toxicology and Chemistry*, 20(9), 1909–1915.
- Werner K., Johansson P., Brydsten L., Bosson, E., Berglund, S., Tröjbom, M., Nyman, H., 2007. Recharge and discharge of near-surface hydrology. Swedish Nuclear Fuel and Waste Management Co Report R-07-08.
- Wörman A., Packman A.I., Marklund L., Harvey J., Stone S., 2007. Fractal topography and subsurface water flows from fluvial bedforms to the continental shield. *Geophysical Research Letters*, Vol 34, L07402, doi:10.1029/2007GL029426.

# Paper I





## Propagation of water pollution uncertainty and risk from the subsurface to the surface water system of a catchment

Klas Persson \*, Georgia Destouni

Department of Physical Geography and Quaternary Geology, Stockholm University, SE-106 91, Stockholm, Sweden

### ARTICLE INFO

#### Article history:

Received 22 September 2008

Received in revised form 9 June 2009

Accepted 2 September 2009

This manuscript was handled by L. Charlet, Editor-in-Chief, with the assistance of Chong-yu Xu, Associate Editor

#### Keywords:

Water pollution

Risk assessment

Contaminant transport

Stochastic modelling

### SUMMARY

This paper investigates the propagation of quantifiable probability and quantification uncertainty of water pollution from local pollutant sources at and below the land surface, through the groundwater system, to downstream surface water recipients. Methodologically, the study shows how the risk and uncertainty of surface water pollution within a catchment may be assessed by a combined methodology of a Lagrangian stochastic advective-reactive modelling approach, which accounts for the quantifiable pollutant transport randomness, and a scenario analysis approach, which accounts for different quantification uncertainties. The results show that, in general, unambiguous risk assessment requires at least a reliable order-of-magnitude quantification of the prevailing relation between the average rate of physical pollutant transport from source to recipient and the average rate of pollutant attenuation. If this average relation can be reliably estimated to fall within two identified, relatively wide open value ranges, the assessment of pollution risk to surface waters from localised sources at or below the soil surface may be unambiguous even under otherwise large quantification uncertainty. For a relatively narrow, closed value range of this average rate relation, however, risk assessment must either rely on conservative assumptions, or else be based on a more detailed and resource demanding quantification of pollutant transport.

© 2009 Elsevier B.V. All rights reserved.

### Introduction

Various contaminated land sites and groundwater pollutant plumes may be located within the catchment areas of sensitive water recipients, such as drinking water supplies, lakes, streams and coastal waters. The pollutant releases from such sites and plumes, and from possible future releases in the catchments (for instance from planned or present industrial and transportation activities and pollution accidents), pose pollution risks to the downstream surface water environments. These risks need to be assessed, for instance according to the EU Water Framework Directive (WFD; European Commission, 2000), which requires catchment-scale water management for achieving and maintaining good physico-chemical and ecological status in all the waters of the EU member states.

To assess the water pollution risks posed by present and potential future pollutant releases within a catchment area, we need to model the pollutant transport and mass exchange that take place along the transport pathways from the sources to the water recip-

ients within and downstream of the considered catchment area. However, model predictions are associated with uncertainty that needs to be accounted for in this catchment-scale risk assessment. Most model parameters cannot be precisely determined due to large and irregular variability in time and space combined with measurement errors, a general lack of data and site-specific information, and uncertainty about whether the model itself constitutes an adequate mathematical representation of the real-world pollutant transport process (e.g. Kavanaugh et al., 2003; O'Hagan and Oakley, 2004; Beven, 2006; Baresel and Destouni, 2007).

Numerous studies have in the past decades developed stochastic modelling approaches to account for the physical spreading effect of random spatial aquifer heterogeneity on subsurface solute transport (see for instance Dagan, 1989 and Rubin, 2003 for reviews of different approaches to stochastic solute transport modelling in randomly heterogeneous formations). Some of these approaches use probability density functions (pdfs) of advective solute travel times as a basis for deriving the statistics of solute concentrations and mass flows. Such travel time-based, Lagrangian stochastic approaches have been applied to solute transport through subsurface water systems (soil water, groundwater; e.g. Shapiro and Cvetkovic, 1988; Destouni, 1992; Cvetkovic and Dagan, 1994; Destouni and Graham, 1995; Simmons et al., 1995; Yabusaki et al., 1998; Foussereau et al., 2001; Tompson et al.,

\* Corresponding author. Tel.: +46 8 164778; fax: +46 8 154794.

E-mail addresses: [klas.persson@natgeo.su.se](mailto:klas.persson@natgeo.su.se) (K. Persson), [georgia.destouni@natgeo.su.se](mailto:georgia.destouni@natgeo.su.se) (G. Destouni).

2002; Malmström et al., 2004) and catchments (Simic and Destouni, 1999; Lindgren et al., 2004; Lindgren and Destouni, 2004; Botter et al., 2005). The travel time pdfs that must be quantified in these approaches are commonly unknown and approximated by assuming some common pdf type (e.g. lognormal, inverse Gaussian) based only on knowledge about the travel time mean and variance (e.g. Cvetkovic et al., 1998; Destouni et al., 2001). The physical solute travel time statistics can further be coupled with relevant pollutant reaction models. This coupled Lagrangian stochastic advective-reactive (LaSAR) modelling approach can be used for quantifying the transport of reactive pollutants in terms of both expected transport (e.g. Destouni and Graham, 1995; Lindgren et al., 2004; Lindgren and Destouni, 2004; Malmström et al., 2004) and transport variance (e.g. Destouni, 1992; Andricevic and Cvetkovic, 1996; Destouni and Graham, 1997; Andersson and Destouni, 2001; Baresel and Destouni, 2007). The expected transport accounts then for the physical solute spreading effect of aquifer heterogeneity in a statistically quantifiable population of random heterogeneity outcomes, and the transport variance is a measure of the uncertainty implied by this randomness with regard to the actual field outcome from the whole statistical population.

However, pollutant transport uncertainty does not only result from the statistically quantifiable randomness of aquifer heterogeneity. Even if the mean and variance of solute travel time can be quantified from some, relatively readily obtainable field statistics of measurable groundwater hydraulics (e.g. Destouni and Graham, 1997; Simic and Destouni, 1999; Destouni et al., 2001), the further derivation of solute concentration and mass flux statistics requires more field knowledge, for example about the spatial correlation structure of groundwater hydraulics, which is more difficult and resource demanding to assess than independent population statistics. Furthermore, also other essential factors, such as pollutant release from the source zone and biogeochemical reaction rates, may be quite difficult and resource demanding to measure in the field. Our uncertainty about all these factors leads to additional pollutant transport uncertainty to that from the statistically quantifiable randomness in aquifer heterogeneity.

In this paper, we develop a combined methodology for quantifying the propagation of both the statistically quantifiable probability and the quantification uncertainty of water pollution through the groundwater system to downstream surface water recipients. The methodology combines a LaSAR modelling approach, which accounts for statistically quantifiable randomness in aquifer heterogeneity, with a scenario analysis approach, which accounts for quantification uncertainty about: (1) the spatial correlation structure of aquifer heterogeneity, (2) the pollutant release from the source zone, and (3) the biogeochemical pollutant attenuation rate. This combined approach is used for investigating the main effects of these different types of quantification uncertainties and statistically quantifiable randomness on the probability of exceeding a given, environmental or health-based, pollutant concentration limit at a surface water recipient boundary downstream of a short-term accidental (e.g. resulting from accidents involving dangerous goods), or a long-term continuous (e.g. resulting from contaminated land sites) pollutant release. Furthermore, the practical usefulness of this approach is finally also demonstrated for assessments of surface water pollution risk posed by existing or possible future local source releases within a catchment area.

### General problem and methodology description

Fig. 1 illustrates schematically the general water pollution problem considered in this study: in a catchment area there may be

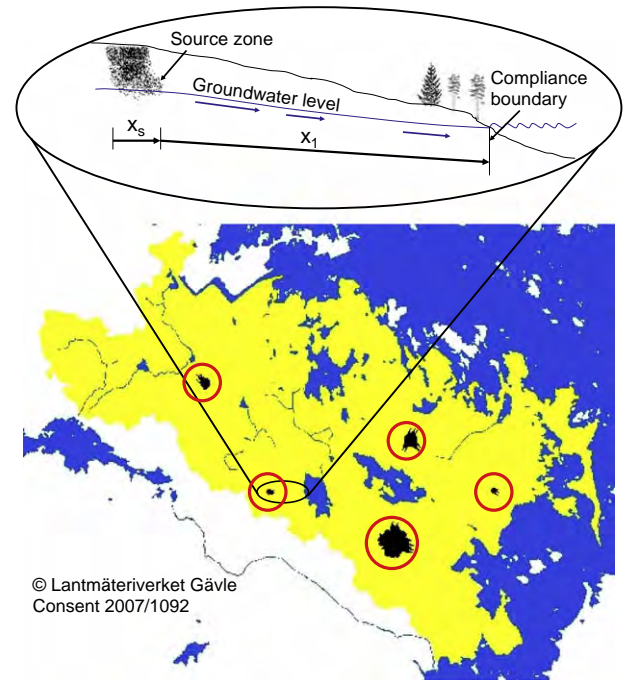


**Fig. 1.** Illustration of a hypothetical case for pollution risk assessment at catchment-scale. In a catchment area, like the coastal catchment area in Forsmark, Sweden, which is here used as our illustration example, there may be various present or potential future sources of pollutants (e.g. the hypothetical sources that are here marked as black dots and fields in the Forsmark catchment area example) from which contaminants may be transported by the groundwater towards the nearest downstream groundwater–surface water interaction boundary, which in the figure and in the main text is referred to as the ‘compliance boundary’.

various present or potential future sources of pollutants of various spatial extents and locations (a number of hypothetical pollutant sources are marked as black dots and fields with red circles around them on the map). Some of the pollutants released from these sources may dissolve quickly in the water, whereas others may leak during a long period of time. Even after abatement measures have been taken, some pollutant fraction may reach the groundwater table below or within a pollutant source zone of arbitrary extent  $x_s$  along the mean groundwater flow direction. This pollutant fraction may then be transported by the groundwater towards a groundwater–surface water interaction boundary at distance  $x_1$  downstream of the source zone along the mean groundwater flow direction. At that boundary, which may for instance be associated with a stream or a lake, as exemplified in Fig. 1, an environmental or health-based pollutant concentration limit  $C_T$  may be given from an independent assessment of the ecosystem and the toxicological risks that are associated with different pollutant exposure levels in the surface water system. In the following, we refer to the groundwater–surface water interaction boundary as the compliance boundary for meeting the given concentration limit  $C_T$ .

The probability  $P_R$  that the concentration limit  $C_T$  will, at any time  $t$ , be exceeded by any local concentration value  $C$  in the groundwater that flows through the nearest compliance boundary downstream from the source zone may then be estimated from the concentration pdf  $f(C(t, x_1))$  as

$$P_R(t, x_1) = P(C > C_T) = 1 - \int_0^{C_T} f(C(t, x_1)) dC \quad (1)$$

The pdf  $f(C(t, x_1))$  may be of any realistic type or form but will, for simplicity, in the following calculations be exemplified as log-

normal, following similar assumption examples in previous stochastic contaminant spreading and abatement management studies (Andricevic and Cvetkovic, 1996; Batchelor et al., 1998; Andersson and Destouni, 2001; Gren et al., 2002). Thereby,  $f(C(t, x_1))$  is fully determined by the two most readily quantifiable statistics of concentration  $C$ : the expected value  $E[C(t, x_1)]$  and variance  $V[C(t, x_1)]$ . We consider here  $C$  to be the local concentration, sampled at any point for comparison with the given concentration limit  $C_T$ . Destouni and Graham (1997) showed that the sampling size and method will affect the statistics of locally measured concentration  $C$ . For simplicity, we quantify here  $C$  only as a point concentration, neglecting the sampling size-method effect to generally decrease the variance  $V[C(t, x_1)]$  relative to a corresponding point concentration variance.

Two different cases of contaminant release from the source zone are considered in the assessment of the exceedence probability  $P_R$ : (i) a short-pulse release scenario, which may for instance represent the first, fast release phase of easily soluble contaminant fraction after a pollution accident at the soil surface, and (ii) a continuous release scenario, which may for instance represent a long-term industrial leakage, or the second, slow leakage phase after a pollution accident, when some hydrophobic pollutant fraction that has been retained in the accidental source zone slowly leaks out during a long period of time. For both release cases, we quantify the local concentration statistics  $E[C]$  and  $V[C]$ , which fully determine the example lognormal pdf  $f(C)$  in (1).

In the continuous release case,  $E[C]$  and  $V[C]$  will be constant in time after the continuously fed pollutant plume has reached its steady-state condition, and the associated concentration pdf  $f(C)$  and exceedence probability  $P_R$  will then also remain constant. In the short-pulse release case,  $E[C(t, x_1)]$  and  $V[C(t, x_1)]$ , and through them also  $f(C(t, x_1))$  and  $P_R$ , will vary in time at the compliance boundary at  $x_1$  as the finite pollutant plume that is bounded by the short-pulse input passes through the boundary. In all the transport-attenuation scenarios considered here for the short-pulse release case, the peak values of the concentration statistics  $E[C(t, x_1)]$  and  $V[C(t, x_1)]$  coincide in time, in accordance with the model results reported by Andersson and Destouni (2001). The timing of the peak values of  $E[C(t, x_1)]$  and  $V[C(t, x_1)]$  is then also the timing of the maximum exceedence probability  $P_R$ . However, for strongly asymmetrical expected BTCs (occurring, for instance, if the pollutant undergoes slow reversible non-equilibrium sorption–desorption), the peak  $E[C]$  and  $V[C]$  values may not coincide in time and the timing of the maximum exceedence probability must be found by calculating  $P_R$  from Eq. (1) as a function of time (Andersson and Destouni, 2001). In the following, the notation  $P_R$  will generally refer to the maximum probability of concentration  $C$  exceeding the given concentration limit  $C_T$ , which for the short-pulse release case occurs at the time of the peak  $E[C]$  and  $V[C]$  values at the compliance boundary location  $x_1$ .

To account for the effect of the statistically quantifiable randomness in aquifer heterogeneity, we quantify  $P_R$  in Eq. (1) based on the LaSAR approach to solute transport modelling. The groundwater velocity field is then assumed to be essentially stationary or unidirectional, implying that transport pathways coincide with groundwater streamlines or streamtubes. The mixing that may occur between different streamtubes due to pore-scale dispersion and molecular diffusion is often neglected for simplicity; previous results imply that this neglect should not affect the expected concentration much, but may lead to overestimation of the concentration variance (Dagan and Fiori, 1997; Fiori and Dagan, 2000; Fiori et al., 2002; Janssen et al., 2006). For non-reactive solute in the short-pulse release case, the expected value  $E[C(t, x_1)]$  and the variance  $V[C(t, x_1)]$  of the point concentration may then be expressed as (adapted from Destouni and Graham, 1997 for explicit expression of the source input concentration  $C_0$ )

$$E[C(t, x_1)] = \int_0^\infty \left( \frac{M_0}{A_0 n v_0} \right) \delta(t - T) g(T; x_1) dT \\ = C_0 x_s \int_0^\infty \left( \frac{1}{v_0} \right) \delta(t - T) g(T; x_1) dT \quad (2)$$

$$V[C(t, x_1)] = E[C(t, x_1)](C_0 - E[C(t, x_1)]) \quad (3)$$

where  $A_0$  is the cross-sectional area normal to the mean groundwater flow through the source zone,  $M_0 \delta(t)/A_0$  is the assumed instantaneous release of pollutant mass  $M_0$  per unit of cross-sectional area at running time  $t = 0$ ,  $\delta$  is the Dirac delta function,  $C_0 \equiv M_0/(A_0 n x_s)$  is the average pollutant concentration within the source zone pore water,  $n$  is the assumed constant porosity,  $g(T; x_1)$  is the pdf of the spatially variable advective solute travel time  $T$  from the source zone boundary at  $x_s$  to the compliance boundary at  $x_1$ , and  $v_0$  is the groundwater velocity along the mean groundwater flow direction at  $x_s$ .

For the continuous release case, the corresponding statistics of  $C$  are obtained as

$$E[C(t, x_1)] = C_0 \int_0^\infty H(t - T) g(T; x_1) dT \quad (4)$$

$$V[C(t, x_1)] = C_0^2 \int_0^\infty H(t - T) g(T; x_1) dT - E[C(t, x_1)]^2 \quad (5)$$

where  $H$  is the Heaviside step function and  $C_0$  is in this case the temporally constant input concentration from the source zone at  $x_s$ . In the following, we will for simplicity also for the continuous release case refer to the average pollutant concentration within the source zone pore water,  $C_0 \equiv M_0/(A_0 n x_s)$ , as the input concentration, but note that the local input concentration values vary (because  $v_0$  varies) and the  $C_0 \equiv M_0/(A_0 n x_s)$  definition is only an approximation of the average input concentration in that case.

The expressions (3) and (5) quantify the variance of  $C$  in the bounding case of zero pore-scale dispersion and concentration measurement at a true point, i.e., for measurement volume approaching zero (Dagan, 1989). In such a case, the concentration of non-reactive solute in an individual streamtube is either  $C = 0$  or  $C = C_0$ , i.e., the true point concentration is bi-modally distributed. Real local concentrations, however, are always measured in finite sampling volumes, wherein the solute mass is mixed, destroying the bi-modality of hypothetical point concentration values. This mixing does not much affect the expected concentration value, but it decreases the local concentration variance relative to the point variance expressed in (3) and (5). In applications with specific sampling information, the variance expressions (3) and (5) can be exchanged to corresponding ones that account for the mixing effect of finite sampling volume on the concentration variance, for example as suggested by Destouni and Graham (1997). In generic pollution risk studies like the present one, however, one may conservatively choose to overestimate the local concentration variance by use of the upper limit point variance expressions (3) and (5), even though the local concentration pdf  $f(C)$  in (1) is not assumed to be bi-modal.

For reactive pollutant transport, relevant reaction functions (here accounting for irreversible first-order attenuation and reversible linear equilibrium sorption–desorption) extend the basic non-reactive  $\delta$  and  $H$  transport functions in the above  $E[C]$  and  $V[C]$  expressions, as outlined in the Appendix 1. For simplicity, the results illustrated in the following include only the effects of irreversible first-order attenuation, but a reversible sorption–desorption process may also readily be accounted for by the use of the full  $E[C]$  and  $V[C]$  expressions given in the Appendix 1.

To account for the effect of the statistically quantifiable randomness in aquifer heterogeneity, we quantify the exceedence probability  $P_R$  (1) for lognormally distributed hydraulic conductivity  $K$  with different variance,  $V[\ln K]$ , but the same mean value of

In  $K$ . The effect of  $V[\ln K]$  translates then differently into the solute travel time and  $C$  statistics depending on which spatial correlation structure of aquifer heterogeneity that prevails in the field.

To investigate the effect of quantification uncertainty about the spatial correlation structure of aquifer heterogeneity (i.e., quantification uncertainty 1 in the Introduction) on  $P_R$ , we will in the following consider two extreme correlation structure scenarios. The first scenario is a perfectly stratified aquifer (in the following referred to as a 1D aquifer), where the advective velocity of groundwater transport is constant in the mean flow direction along any individual streamline, or streamtube, between the source zone and the compliance boundary at  $x_1$ , but varies randomly due to random variation of hydraulic conductivity among the different streamlines. The second scenario is a three-dimensional isotropic aquifer (in the following referred to as a 3D aquifer), where hydraulic conductivity and advective groundwater transport velocity vary randomly with equal spatial correlation lengths in all three spatial directions.

Appendix 1 outlines the expressions for the mean and variance of solute travel time  $T$  and concentration  $C$  in the 1D and 3D aquifer scenarios. For lognormal hydraulic conductivity, the resulting travel time pdf  $g(T; x_1)$  is lognormal in the 1D aquifer scenario. For simplicity, we assume here that  $g(T; x_1)$  is lognormal also in the 3D aquifer scenario (see e.g. Destouni et al., 2001 for justification of this assumption). Fig. 2 further shows the very different normalised lognormal solute travel time pdfs  $g_1(T)(nx_1)/(K_g J)$  resulting for the two different correlation structure scenarios, even for the same  $V[\ln K]$  value. The normalising term  $(nx_1)/(K_g J)$  corresponds to the geometric mean travel time  $T_g$  from the source zone to  $x_1$  in the 1D aquifer scenario, and to the expected travel time  $E[T]$  from the source zone to  $x_1$  in the 3D aquifer scenario. Moreover,  $K_g$  is the geometric mean hydraulic conductivity, and  $J$  is the constant hydraulic gradient in the 1D aquifer scenario and the mean hydraulic gradient (denoted  $\bar{J}$  in the Appendix 1) in the 3D aquifer scenario.

In general, the variability of physical solute travel times is a result of various processes that are difficult or impossible to quantify with accuracy and precision in real field situations. Examples of such processes are pore-scale dispersion and molecular diffusion

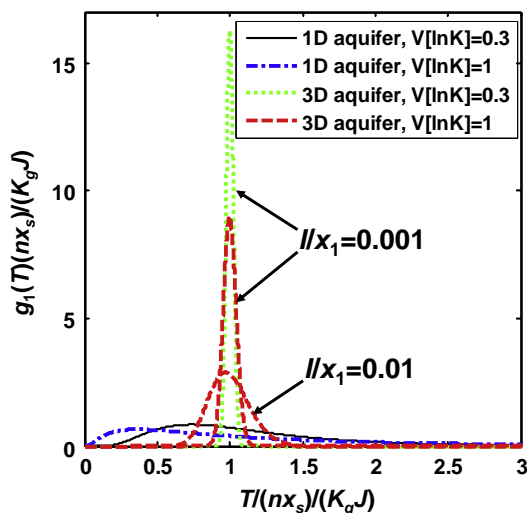


**Fig. 2.** Effects of uncertainty in the correlation structure of aquifer heterogeneity (perfectly stratified aquifer scenario, denoted 1D aquifer, or three-dimensional isotropic aquifer scenario, denoted 3D aquifer), the relative hydraulic conductivity correlation length  $l/x_1$  (in the 3D aquifer), and the log-conductivity variance  $V[\ln K]$ , on the probability density function (pdf) of the advective solute travel time  $g(T)$ . Both  $g(T)$  and  $T$  are normalised with characteristic mean travel time  $(nx_1)/(K_g J)$  (see further notation explanations in the main text).

(Dagan and Fiori, 1997), as well as diffusive mass transfer between mobile and immobile groundwater zones (Lindgren et al., 2004). The travel time pdfs illustrated in Fig. 2, which correspond to the 1D and 3D aquifer scenarios considered in the following calculations, are so different that they are likely to bound a quite wide range of possible travel time pdfs for more complex field-process situations. The present aquifer scenario analysis may therefore implicitly give a good indication of the practical importance of different quantification uncertainties associated with the physical solute travel time pdf.

To investigate the effect of the often large quantification uncertainty (e.g. Kavanaugh et al., 2003) about the input concentration from the source zone (i.e., quantification uncertainty 2 in the Introduction), we will in the following quantify the exceedence probability  $P_R$  for a range of different scenarios of relative input concentration,  $C_0/C_T$ . To investigate finally the effect of quantification uncertainty about the prevailing biogeochemical attenuation rate (i.e., quantification uncertainty 3 in the Introduction) we will also consider different scenarios for such attenuation rate. These will be represented by the relation between average characteristic attenuation and transport rates (or time scales), quantified as  $\lambda(nx_s)/(K_g J)$ , where  $\lambda$  is the rate of attenuation and the term  $(nx_s)/(K_g J)$  corresponds to the arithmetic and the geometric mean advective solute travel time through the source zone extent  $x_s$  in the 3D aquifer and the 1D aquifer scenario, respectively. The constant source zone extent  $x_s$  is included here instead of the variable transport distance  $x_1$  in order for the normalising term to be constant.

## Results and discussion

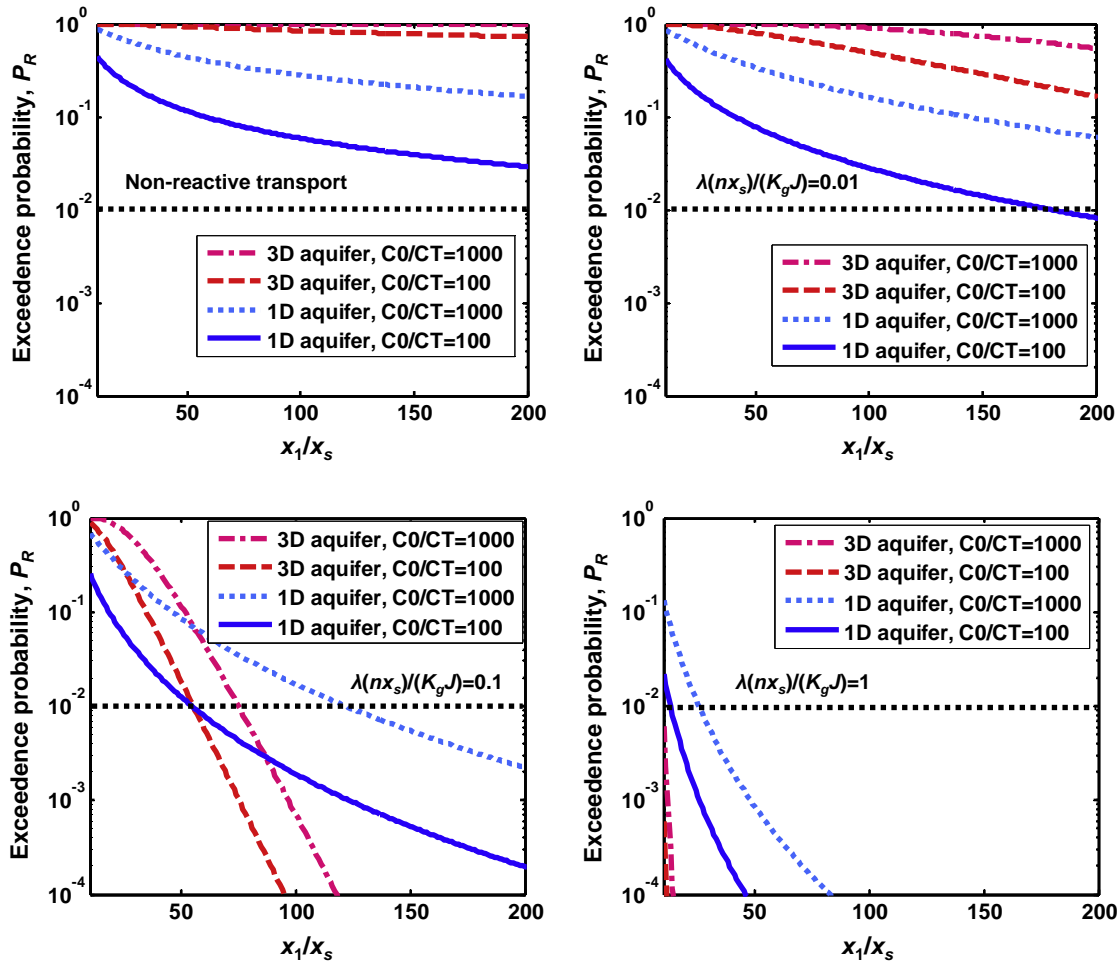
### The short-pulse release case

Fig. 3 shows the resulting probability  $P_R$  to exceed the concentration limit  $C_T$  downstream of a short-pulse contaminant release for different scenarios of aquifer correlation structure (1D or 3D aquifer), relative source input concentration ( $C_0/C_T = 100$  and 1000), and relation between average characteristic attenuation and transport rates ( $\lambda(nx_s)/(K_g J) = 0, 0.01, 0.1$  and 1).

For illustrative clarity, Fig. 3 shows  $P_R$  results only for one value of the hydraulic conductivity variance,  $V[\ln K] = 1$ . Lower hydraulic conductivity variance reduces the difference between the 1D and 3D aquifer structure cases (see Fig. A-1 in Appendix 2, which shows  $P_R$  results for both  $V[\ln K] = 0.3$  and  $V[\ln K] = 1$ ). The results in Fig. 3 and in all the following figures and tables are further based on the example relative correlation length of hydraulic conductivity  $l/x_s = 0.1$  for the 3D aquifer. The travel time pdfs in Fig. 2 that underlie the  $P_R$  results for the 3D aquifer at the relative distances  $x_1/x_s = 10$  and  $x_1/x_s = 100$  are thus the curves for  $V[\ln K] = 1$  and  $l/x_1 = 0.01$   $l/x_1 = 0.001$ , respectively. For the 1D aquifer, the shape of the travel time pdf does not depend on  $x_1$  and the travel time pdf that underlies the  $P_R$  results for this aquifer scenario is that for  $V[\ln K] = 1$  in Fig. 2.

As one possible example of a water pollution risk level that might be considered acceptable by environmental managers and other stakeholders, Fig. 3 emphasises the 1%  $P_R$  level (dashed line). Table 1 shows the relative distance  $x_1/x_s$  at which the exceedence probability  $P_R$  falls below the 1% level in different analysed scenarios. Table 1 shows more results than Fig. 3, including both  $V[\ln K] = 0.3$  and  $V[\ln K] = 1$  and a wider range of source input concentration scenarios of  $C_0 = 10-1000C_T$ .

The obtained  $P_R$  results for the very differently shaped travel time pdfs resulting from the two extreme 1D (infinite correlation length in  $x_1$ ) and 3D isotropic (equal correlation length in all directions) aquifer scenarios are likely to bound corresponding results for intermediate, more realistic anisotropic aquifer scenarios,



**Fig. 3.** Effects of uncertainty in the correlation structure of aquifer heterogeneity (perfectly stratified aquifer, denoted 1D aquifer, or three-dimensional isotropic aquifer, denoted 3D aquifer), relative solute input concentration  $C_0/C_T$  and attenuation-transport rate relation  $\lambda(nx_s)/(K_g J)$  on the probability  $P_R$  to exceed the concentration limit  $C_T$  at different relative distances  $x_1/x_s$  from the source zone in a short-pulse pollutant release case. The log-conductivity variance is  $V[\ln K] = 1$  and the relative conductivity correlation length in the 3D aquifer is  $l/x_s = 0.1$ .

**Table 1**

The relative transport distance  $x_1/x_s$  at which the probability  $P_R$  to exceed the concentration limit  $C_T$  falls below 1% for different scenarios of aquifer heterogeneity, relative input concentration  $C_0/C_T$ , and attenuation-transport rate relation  $\lambda(nx_s)/(K_g J)$  in a short-pulse pollutant release case.

$C_0/C_T$	Aquifer scenario	$\lambda(nx_s)/(K_g J)$		
		$\leq 0.01$	0.1	$\geq 1$
10	1D aquifer	$>40^a$ $>60^b$	$\approx 20^{a,b}$	$<10^{a,b}$
	3D aquifer	$>200^{a,b}$	$\approx 40^{a,b}$	
100	1D aquifer	$>180^a$ $>200^b$	$\approx 60^a$ $\approx 50^b$	$<10^{a,b}$
	3D aquifer	$>200^{a,b}$	$\approx 60^{a,b}$	
1000	1D aquifer	$>200^{a,b}$	$\approx 120^a$ $\approx 80^b$	$<30^a$ $<10^b$
	3D aquifer		$\approx 80^{a,b}$	$<10^{a,b}$

<sup>a</sup>  $V[\ln K] = 1$ .

<sup>b</sup>  $V[\ln K] = 0.3$ .

where correlation lengths in the essentially horizontal  $x_1$  direction are commonly greater than in the vertical direction. The present aquifer scenario analysis may therefore indicate the practical importance of the greatest possible quantification uncertainty about the correlation structure of aquifer heterogeneity, i.e., of essentially not knowing anything about the prevailing correlation

structure. Such large uncertainty may be relevant for instance in pollution accidents with very limited available site-specific information and with fast abatement measure decisions that must be made in spite of these limitations.

As we have seen in Fig. 2, the resulting variance of advective solute travel time is, for any given  $V[\ln K]$  value, much higher for the 1D than the 3D aquifer. Large travel time variability implies that the travel time along many streamlines deviates significantly from the mean travel time. Attenuation along the fastest streamlines will then be much lower than along streamlines that are closer to the mean, whereas the transport along streamlines with much longer than average travel times will not affect the total pollutant mass delivery much, since the mean travel time is there already large enough for most of the pollutant mass to be attenuated. On the one hand, the large travel time variability in the 1D aquifer scenario thus implies less pollutant mass attenuation than in the 3D aquifer scenario, which has smaller travel time variability for the same conductivity variance  $V[\ln K]$ . On the other hand, however, the larger travel time variability in the 1D aquifer scenario also implies greater spreading of the migrating pollutant plume, so that the pollutant becomes more diluted in the short-pulse release case. These two counteracting effects of the larger travel time variance in a 1D than in a 3D aquifer explain the results shown in Fig. 3, where the 1D aquifer scenario generally implies high  $P_R$  for the relatively large attenuation-transport rate relation  $\lambda(nx_s)/(K_g J) = 1$  (for

which the reducing effect of larger travel time variability on mass attenuation dominates the result), whereas the 3D aquifer scenario generally implies high  $P_R$  for the scenarios of non-reactive solute and solute with the relatively small attenuation-transport rate relation  $\lambda(nx_s)/(K_gJ) \leq 0.01$  (i.e., for relatively non-reactive solute, for which the dilutive effect of larger travel time variability dominates the result). For the intermediate attenuation-transport rate relation  $\lambda(nx_s)/(K_gJ) = 0.1$ , the 3D aquifer implies high  $P_R$  close to the source zone, while the 1D aquifer implies high  $P_R$  further downstream, where the pollutant attenuation has had sufficient time to yield significant effects.

We see then in Fig. 3 and Table 1 (and in Fig. A-1, Appendix 2) that in many cases, neither the quantifiable aquifer heterogeneity degree nor the quantification uncertainty about its correlation structure may be very important with regard to whether or not the risk of water pollution exceeds some given or agreed upon acceptable risk level. Generally, the quantification uncertainty about the average attenuation-transport rate relation  $\lambda(nx_s)/(K_gJ)$  seems to be the key for this type of risk level acceptability assessment.

For a high attenuation-transport rate relation of  $\lambda(nx_s)/(K_gJ) \geq 1$ , the  $C_T$  exceedence probability  $P_R$  declines below 1% at distances closer than  $x_1/x_s = 30$  (i.e., 30 times the source zone extent) for any input concentration  $C_0 \leq 1000C_T$ . This applies regardless of the aquifer heterogeneity details, as long as the log-conductivity variance is, as often assumed, about 1 or less (Dagan, 1989; Rubin, 2003), which indicates a possibility to give remediation and prevention needs relatively lower priority if one can know with some certainty that  $\lambda(nx_s)/(K_gJ) \geq 1$ , even though there might be large quantification uncertainty about the precise  $\lambda$  and advection parameter values.

For an attenuation-transport rate relation of  $\lambda(nx_s)/(K_gJ) \leq 0.01$ , the  $C_T$  exceedence probability  $P_R$  is highly likely to remain above 1% at distances up to 200 times the source zone extent for any input concentration  $C_0 \geq 100C_T$  and aquifer heterogeneity assumption. This indicates a need to prioritise prevention measures and remediation efforts if such conditions of  $\lambda(nx_s)/(K_gJ) \leq 0.01$  can be expected, even in the face of otherwise large uncertainty. Only for a small relative input concentration,  $C_0/C_T = 10$  in the extreme 1D aquifer scenario, does  $P_R$  decline below 1% at a relatively short distance  $x_1/x_s$  if  $\lambda(nx_s)/(K_gJ) \leq 0.01$ .

For the intermediate attenuation-transport rate relation of  $\lambda(nx_s)/(K_gJ) \approx 0.1$ , the distance at which  $P_R$  declines below 1%

ranges between 20 and 120 times the source zone extent, mostly depending on the magnitude of relative input concentration  $C_0/C_T$ . For a given  $C_0/C_T$ , the distance  $x_1/x_s$  of  $P_R < 1\%$  is relatively insensitive to the assumed aquifer heterogeneity scenario (within the limit  $V[\ln K] \leq 1$ ).

The continuous release case

Fig. 4 shows the probability  $P_R$  to exceed the concentration limit  $C_T$  downstream of a continuous contaminant release for the example hydraulic conductivity variance  $V[\ln K] = 1$ . As in the short-pulse release case, lower hydraulic conductivity variance reduces the difference between the 1D and 3D aquifer structure cases (see Fig. A-2 in Appendix 2, which shows  $P_R$  results for both  $V[\ln K] = 0.3$  and  $V[\ln K] = 1$ ). Table 2 further shows the relative distance  $x_1/x_s$  at which  $P_R$  falls below the example 1% risk acceptance level. In the continuous release case, the travel time variability does not affect the contaminant plume dilution after steady-state is reached, but larger travel time variability may still imply smaller overall pollutant mass attenuation (see discussion above in “The short-pulse release case”). The latter effect explains why  $P_R$  generally declines below the 1% level at greater relative distance  $x_1/x_s$  from the source zone in the 1D than in the 3D aquifer scenario.

Table 2

The relative transport distance  $x_1/x_s$  at which the probability  $P_R$  to exceed the concentration limit  $C_T$  falls below 1% for different scenarios of aquifer heterogeneity, relative input concentration  $C_0/C_T$ , and attenuation-transport rate relation  $\lambda(nx_s)/(K_gJ)$  in a continuous pollutant release case.

$C_0/C_T$	Aquifer scenario	$\lambda(nx_s)/(K_gJ)$		
		$\leq 0.01$	0.1	$\geq 1$
10	1D aquifer	>200 <sup>a,b</sup>	$\approx 170^a$ $\approx 70^b$	<20 <sup>a</sup> <10 <sup>b</sup>
	3D aquifer	>200 <sup>a,b</sup>	$\approx 30^{a,b}$	<50 <sup>a</sup> <20 <sup>b</sup>
100	1D aquifer	>200 <sup>a,b</sup>	$\approx 150^b$ $\approx 50^{a,b}$	<90 <sup>a</sup> <20 <sup>b</sup>
	3D aquifer	>200 <sup>a,b</sup>	>200 <sup>a,b</sup>	<20 <sup>b</sup> <10 <sup>a,b</sup>
1000	1D aquifer	>200 <sup>a,b</sup>	>200 <sup>a,b</sup>	<20 <sup>b</sup> <10 <sup>a,b</sup>
	3D aquifer	>200 <sup>a,b</sup>	$\approx 80^{a,b}$	<10 <sup>a,b</sup>

<sup>a</sup>  $V[\ln K] = 1$ .

<sup>b</sup>  $V[\ln K] = 0.3$ .

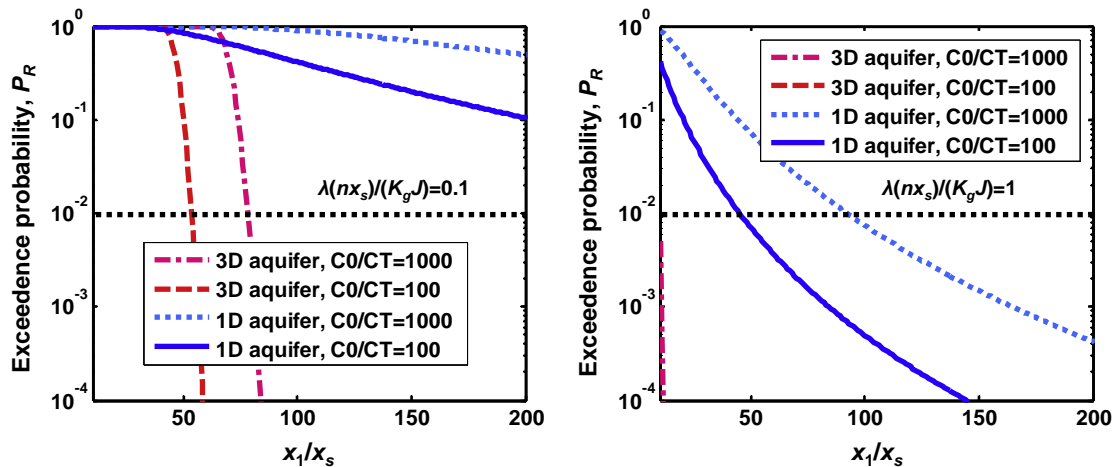


Fig. 4. Effects of uncertainty in the correlation structure of aquifer heterogeneity (perfectly stratified aquifer, denoted 1D aquifer, or three-dimensional isotropic aquifer, denoted 3D aquifer), relative solute input concentration  $C_0/C_T$ , and attenuation-transport rate relation  $\lambda(nx_s)/(K_gJ)$  on the probability  $P_R$  to exceed the concentration limit  $C_T$  at different relative distances  $x_1/x_s$  from the source zone in a continuous pollutant release case. The log-conductivity variance is  $V[\ln K] = 1$  and the relative conductivity correlation length in the 3D aquifer is  $l/x_s = 0.1$ .

In general, uncertainty about the correlation structure of aquifer heterogeneity affects the  $P_R$  propagation more in the continuous than in the short-pulse release case. However, also in the continuous release case, the aquifer heterogeneity details may be important for whether or not the risk of water pollution exceeds an acceptable risk level only for a relatively narrow value range of the average attenuation-transport rate relation  $\lambda(nx_s)/(K_gJ)$ .

Specifically, for  $\lambda(nx_s)/(K_gJ)$  values around 0.1, the distance at which  $P_R$  declines below the example of 1% risk acceptance level varies greatly depending on the prevailing correlation structure and also on the degree of heterogeneity (Fig. A-2, Appendix 2) in the 1D aquifer scenario. For  $\lambda(nx_s)/(K_gJ)$  outside of this range, however, the water pollution risk may in many cases be judged unambiguously as acceptable or unacceptable (below or above the example 1% risk level) regardless of actual input concentration ( $C_0 = 10\text{--}1000C_T$ ) or correlation structure and magnitude of aquifer heterogeneity. For  $\lambda(nx_s)/(K_gJ) \leq 0.01$ , the probability  $P_R$  to exceed the limit  $C_T$  is highly likely to remain above 1% even at greater distances from the source zone than  $x_1/x_s = 200$ . As in the short-pulse release case, this may serve as a clear indication to prioritise prevention measures and remediation efforts if one has reason to expect  $\lambda(nx_s)/(K_gJ) \leq 0.01$ , even under otherwise large uncertainty. For  $\lambda(nx_s)/(K_gJ) \geq 1$ ,  $P_R$  is instead highly likely to decline below 1% at shorter distances than  $x_1/x_s = 50$  for all input concentrations  $C_0 \leq 100C_T$  and independently of aquifer heterogeneity details. Similarly to the short-pulse release case, this indicates a possibility to give remediation and prevention relatively low priority in expected conditions of  $\lambda(nx_s)/(K_gJ) \geq 1$ .

#### The risk of surface water pollution in a catchment area

We use the relatively well investigated (e.g. Johansson et al., 2005; Lindborg, 2005; Jarsjö et al., 2008) 29.5 m<sup>2</sup> Swedish coastal catchment area of Forsmark, north of Stockholm (Figs. 1 and 5) as an example of how scenario analysis results like those presented

in the above sections may be used for assessing the risk of surface water pollution, for instance for the nearest lake or stream, downstream of different groundwater pollution sources within a catchment area. We relate here such an analysis to the risk assessment requirements of the WFD (European Commission, 2000) and exemplify its use for continuous pollutant releases (using the results in Table 2). We consider local source zone extents of  $x_s = 10$  m, which correspond to the finest pixel resolution of reported hydrological modelling of the Forsmark catchment area (e.g. Jarsjö et al., 2008). Smaller sources can anyhow not be spatially resolved beyond the finest available model resolution, and analogous risk assessment analysis can be readily extended to larger source extents.

The basic WFD demand is for good ecological status to be achieved or maintained in all the waters of the EU member states. In order to meet this demand, the WFD requires the member states to characterise the present status of their waters and assess the future risk of declining water status. In this context, the concentration limit  $C_T$  may represent a regulatory pollutant concentration limit, which is set for maintaining or achieving good ecological water status and must not be exceeded at any compliance boundary of a surface or coastal water body. However, the present scenario analysis shows that the probability  $P_R$  of the concentration limit  $C_T$  to be exceeded at some point in time, somewhere on a compliance boundary, may always be greater than zero (Figs. 3 and 4). There must therefore exist some non-zero probability of pollutant concentrations to exceed  $C_T$  sometime and somewhere in a catchment, which is tacitly or openly acceptable to environmental managers and other stakeholders. If this acceptable probability level is not explicitly stated and agreed upon, it may differ considerably among different stakeholders and constitute an important, unresolved cause of stakeholder conflict and ineffective environmental management.

In this study, we consider the example of an acceptable  $P_R$  level of 1%, corresponding to an expectation that the water status will

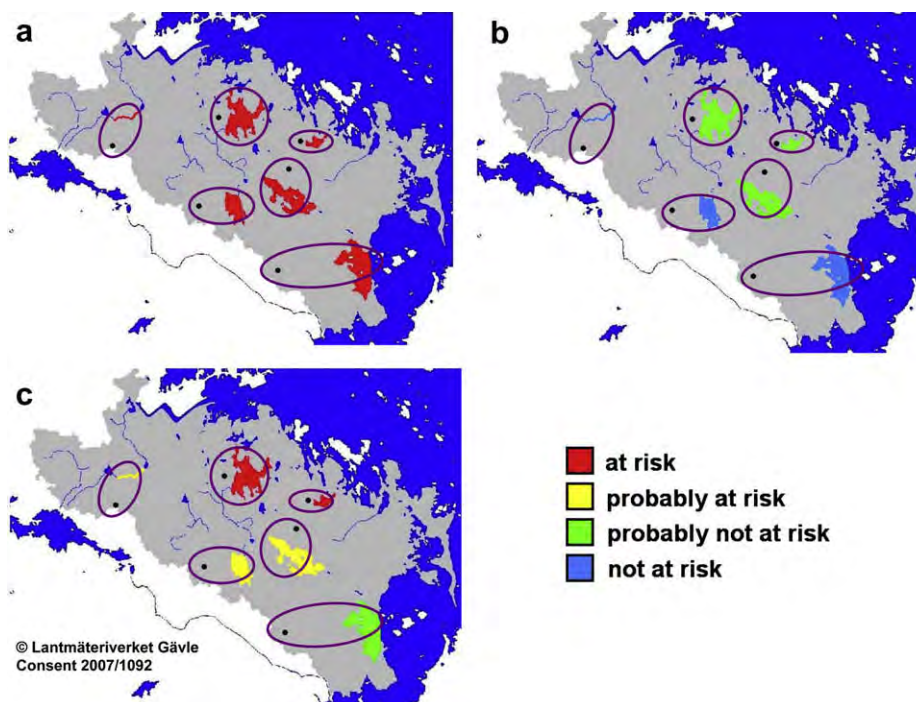


**Fig. 5.** Pollution risk at the nearest surface water system downstream of some hypothetical groundwater pollution sources (marked as black dots) for an average attenuation-transport rate relation of: (a)  $\lambda(nx_s)/(K_gJ) \leq 0.01$ ; (b)  $\lambda(nx_s)/(K_gJ) \geq 1$ ; and (c)  $\lambda(nx_s)/(K_gJ) \approx 0.1$ . The corresponding risk categories are indicated by: red colour = at risk; yellow colour = probably at risk; green colour = probably not at risk; blue colour = not at risk.

remain acceptably good even if about 1% of the groundwater that flows through a surface water compliance boundary at different points in space and time has greater pollutant concentration than the regulatory concentration limit  $C_T$ . In general, the results in Table 2 for continuous pollutant releases (as well as in Table 1 for short-pulse releases) indicate that quantification uncertainty about the average attenuation-transport rate relation  $\lambda(nx_s)/(K_gJ)$  is the key to whether and where  $P_R$  declines to 1% (or some other possible acceptable  $P_R$  level) within a catchment. To evaluate how this uncertainty affects the pollution risk at the nearest surface water compliance boundaries of the different hypothetical pollutant source locations that are illustrated in Fig. 5, we can then use the scenario results for each value range of  $\lambda(nx_s)/(K_gJ)$  in Table 2, along with the following definitions of four different risk categories: (1) *at risk* – if  $P_R > 1\%$  in all or nearly all the investigated source input concentration and aquifer heterogeneity scenarios for each  $\lambda(nx_s)/(K_gJ)$  value range; (2) *probably at risk* – if  $P_R > 1\%$  in most or in the most probable investigated scenarios; (3) *probably not at risk* – if  $P_R < 1\%$  in most or in the most probable investigated scenarios; (4) *not at risk* – if  $P_R < 1\%$  in all or nearly all the investigated scenarios. The flow paths from each source to the nearest surface water compliance boundary are determined from a high-resolution (10 m) digital elevation model of the area, as explained in more detail by Jarsjö et al. (2008). The lengths of the flow paths from the different hypothetical sources in Fig. 5 to their nearest surface water recipient range between 100 and 1300 m.

Fig. 5a shows that if there is sufficient site-specific information to at least estimate the average attenuation-transport rate relation to be in the range  $\lambda(nx_s)/(K_gJ) \leq 0.01$ , the nearest surface water bodies to all of the six source locations are unambiguously *at risk*, across a wide value range of all other scenario parameters, which determine the pollutant input concentration and the physical transport through the heterogeneous groundwater system. For a possible reliable quantification of  $\lambda(nx_s)/(K_gJ) \geq 1$ , Fig. 5b shows that the nearest surface waters are unambiguously *not at risk* for three of the sources and *probably not at risk* for the other three sources; if the 1D aquifer scenario can further be reliably estimated as unlikely, based on the available site information, all surface water bodies can be unambiguously judged as *not at risk*. For  $\lambda(nx_s)/(K_gJ) \approx 0.1$ , Fig. 5c finally shows that the risk may vary widely among the different sources and their nearest surface water bodies, implying that the result is here sensitive to the details of pollutant input and/or aquifer heterogeneity scenario parameters and their quantification uncertainty. Decisions about whether any and which pollutant abatement measures that are necessary for the different sources then rely heavily on the accuracy of the quite specific estimate of  $\lambda(nx_s)/(K_gJ) \approx 0.1$  and require in addition reliable judgement and quantifications of the actual probability of different possible pollutant input and/or aquifer heterogeneity scenarios.

In general, all risk assessments depend on the chosen definitions of the different risk categories. In practice, such as in real WFD implementation situations, the risk category definitions will commonly be decided by the competent water management authorities, after consultations with different stakeholders and the interested public. In this study, we have exemplified how the risk definitions can be directly related to a scenario analysis, which accounts for quantifiable variability and randomness as well as quantification uncertainty in essential risk-determining parameters. If sufficient and accurate information is not available about the key average attenuation-transport rate relation, or about the other pollutant input and groundwater transport parameters for some specific  $\lambda(nx_s)/(K_gJ)$  conditions, the results in Fig. 5 demonstrate that the risk of surface water pollution may be assigned any possible category value, depending on which subjective assumptions are made about these parameters.

## Conclusions

This paper has investigated the propagation of quantifiable probability and quantification uncertainty of water pollution from local sources at and below the land surface, through the groundwater system, to downstream surface water recipients. Methodologically, the study has shown how the risk and uncertainty of surface water pollution within a catchment may be assessed by a combined methodology, including a LaSAR modelling approach, which accounts for quantifiable pollutant transport randomness, and a scenario analysis approach, which accounts for quantification uncertainty. The investigated latter uncertainty regards the correlation structure of aquifer heterogeneity, the released pollutant concentration from the source zone, and the pollutant attenuation rate along the transport from the source to the surface water compliance boundary.

The application results of this methodology have shown that, in general, unambiguous risk assessment for any pollutant source requires at least a reliable order-of-magnitude quantification of the prevailing average attenuation-transport rate relation, quantified here as  $\lambda(nx_s)/(K_gJ)$ . If this average parameter value can reliably be estimated to fall within any of the open ranges of  $\lambda(nx_s)/(K_gJ) < 0.01$  or  $\lambda(nx_s)/(K_gJ) > 1$ , the assessment of pollution risk to surface waters may be unambiguous even under otherwise large quantification uncertainty. If even such range estimates are uncertain, so that the prevailing average  $\lambda(nx_s)/(K_gJ)$  value can possibly be of the order of 0.1, additional investigations may be necessary for reducing the quantification uncertainty about the additional investigated factors of pollutant input concentration and transport through the heterogeneous groundwater system. If such investigations are not possible within the time and resources available for the pollution abatement effort, or if their costs are greater than the possible pollution abatement measures, one should conservatively assume and plan abatement measures for the relatively non-reactive scenario of  $\lambda(nx_s)/(K_gJ) < 0.01$ .

## Acknowledgements

We gratefully acknowledge the financial support for this study from the Swedish Civil Contingencies Agency (MSB) and the Swedish Nuclear Fuel and Waste Management Company (SKB).

## Appendix

### Statistics of travel times and local concentrations

In the short-pulse release case, the local solute concentration at time  $t$  and location  $x_1$  along the mean flow direction in an individual streamtube can be expressed as  $C(t, x_1) = C_0 x_s \delta(t - T(x_1)) / v_0$ . If the solute along its transport through the individual streamtube undergoes first-order irreversible attenuation from the aqueous phase at the rate  $\lambda$  and linear equilibrium sorption-desorption with the resulting retardation factor  $R$ , the local concentration becomes instead  $C(t, x_1) = C_0 x_s \exp(-\lambda T) \delta(t - RT(x_1)) / (v_0)$  (adapted from Destouni and Graham, 1997; Destouni and Cvetkovic, 1991 for explicit expression of both  $C_0$  and  $R$ ). In the 1D aquifer scenario, the advective velocity along a streamtube is constant so that  $v_0 = x_1 / T$  and the expected concentration  $E[C(t, x_1)]$  in the ensemble of streamtubes in the aquifer becomes (adapted from Destouni and Graham, 1997 (Eq. (9)) and Destouni and Cvetkovic, 1991 (Eq. (6)) for explicit expression of both  $C_0$  and  $R$ )

$$E[C(t, x_1)] = \int_0^\infty \frac{C_0 x_s}{v_0} \exp[-\lambda T] \delta(t - RT) g_1(T; x_1) dT \\ = \frac{C_0 x_s t}{x_1 R^2} \exp[-\lambda t / R] g_1\left(\frac{t}{R}; x_1\right) \quad (A1)$$

The statistics of  $T$  in the 1D aquifer scenario can further be derived from the statistics of the lognormally distributed  $K$  as

$$T_g = \frac{n x_1}{K_g \bar{J}}$$

$$V[\ln T] = V[\ln K] \tag{A2}$$

where  $J$ , in this aquifer scenario, is the constant hydraulic gradient in the mean flow direction  $x_1$ ,  $T_g \equiv \exp(E[\ln T])$  is the geometric mean travel time,  $K_g \equiv \exp(E[\ln K])$  is the geometric mean hydraulic conductivity,  $V[\ln T]$  is the variance of  $\ln T$ , and  $V[\ln K]$  is the variance of  $\ln K$ .

In the 3D aquifer scenario, with equal correlation length of hydraulic conductivity in all three directions,  $E[C(t, x_1)]$  becomes instead (adapted from Destouni and Graham, 1997 (Eqs. (15) and (16)) and Destouni and Cvetkovic, 1991 (Eq. (6)) for explicit expression of both  $C_0$  and  $R$ )

$$E[C(t, x_1)] = \frac{C_0 x_s}{R} \frac{n(1 + 11V[\ln K]/30)}{K_g \bar{J}} \exp[-\lambda t/R] g_1\left(\frac{t}{R}; x_1\right) \tag{A3}$$

The mean travel time  $E[T]$  and variance  $V[T]$  can in this aquifer scenario be derived from the statistics of the lognormally distributed  $K$  for far-field transport,  $x_1 \gg l$ , as

$$E[T] = \frac{n x_1}{K_g \bar{J}} \quad x_1 \rightarrow \infty$$

$$V[T] = \frac{2l}{x_1} V[\ln K] \left(\frac{n x_1}{K_g \bar{J}}\right)^2 \quad x_1 \rightarrow \infty \tag{A4}$$

where  $\bar{J}$  is the mean hydraulic gradient in the mean flow direction,  $x_1$ , and  $l$  is the correlation length of the hydraulic conductivity. As explained in the appendix of Destouni and Graham (1997), the expression of  $E[T]$  in Eq. (A4) is a consistent (with the following first-order expression of  $V[T]$ ) first-order approximation of mean arrival time, as discussed by Cvetkovic et al. (1992). The expression for  $V[T]$  is identical to Eq. (23) of Shapiro and Cvetkovic (1988).

Note that if contaminant attenuation takes place in both the aqueous phase and at the sorption sites, the local concentration along an individual streamtube is  $C = C_0 x_s \exp(-\lambda RT) \delta(t - RT) / (v_0)$  instead of  $C = C_0 x_s \exp(-\lambda T) \delta(t - RT) / (v_0)$  because the solute is attenuated all the time  $RT$  that it travels and stays sorbed along the streamtube and not only during the travel time  $T$ . The expected concentration expressions (A1) and (A3) must also then be modified accordingly.

For the continuous release case, the local concentration in an individual streamtube can be expressed as  $C = C_0 \exp(-\lambda T) H(t - RT)$ , where  $H(t)$  is the Heaviside step function. The statistics of  $C$  are then for both the 1D and the 3D aquifer scenarios obtained as

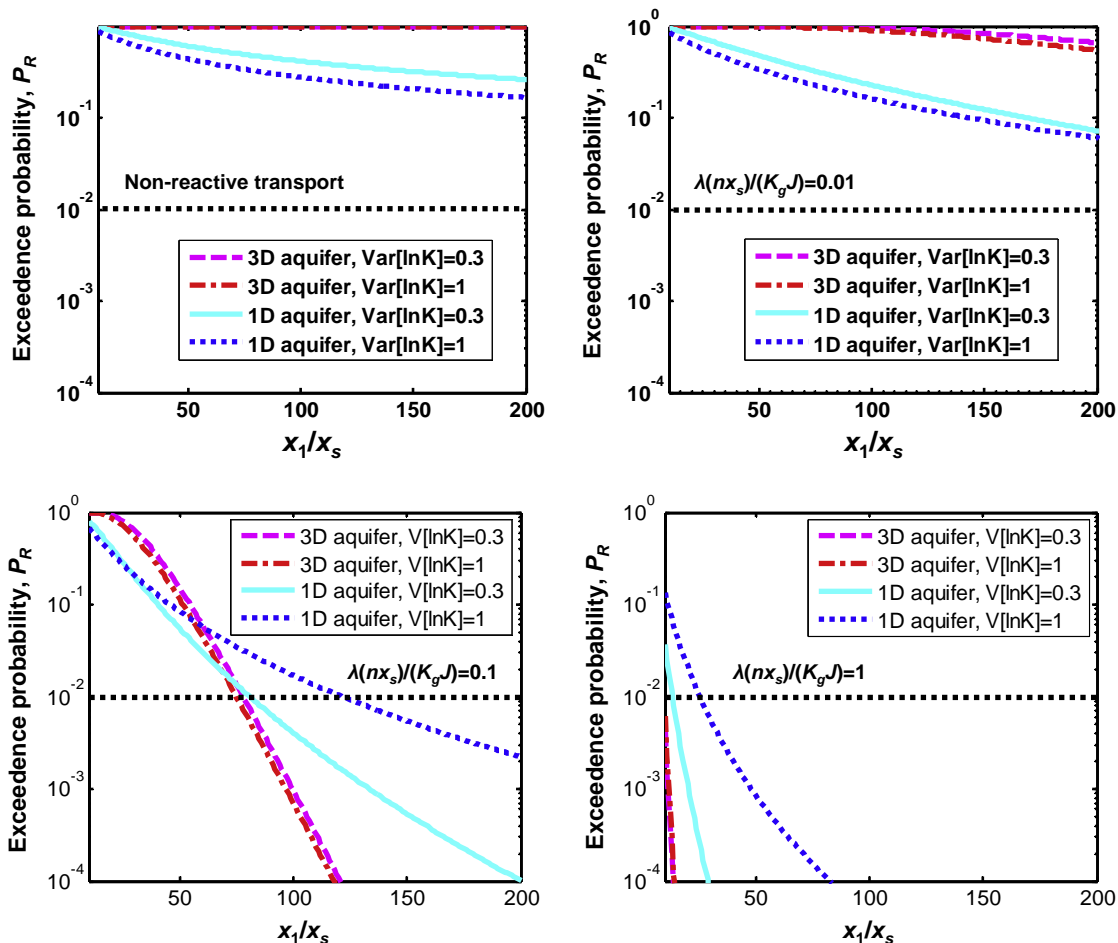


**Fig. A-1.** Effects of uncertainty in the aquifer heterogeneity magnitude (log-conductivity variance,  $V[\ln K]$ ), correlation structure (perfectly stratified aquifer, denoted 1D aquifer, or three-dimensional isotropic aquifer, denoted 3D aquifer), and attenuation-transport rate relation  $\lambda(n x_s)/(K_g \bar{J})$  on the probability  $P_R$  to exceed the concentration limit  $C_T$  at different relative distances  $x_1/x_s$  from the source zone in a short-pulse pollutant release case. The relative source input concentration is  $C_0/C_T = 1000$  and the relative conductivity correlation length in the 3D aquifer is  $l/x_s = 0.1$ .

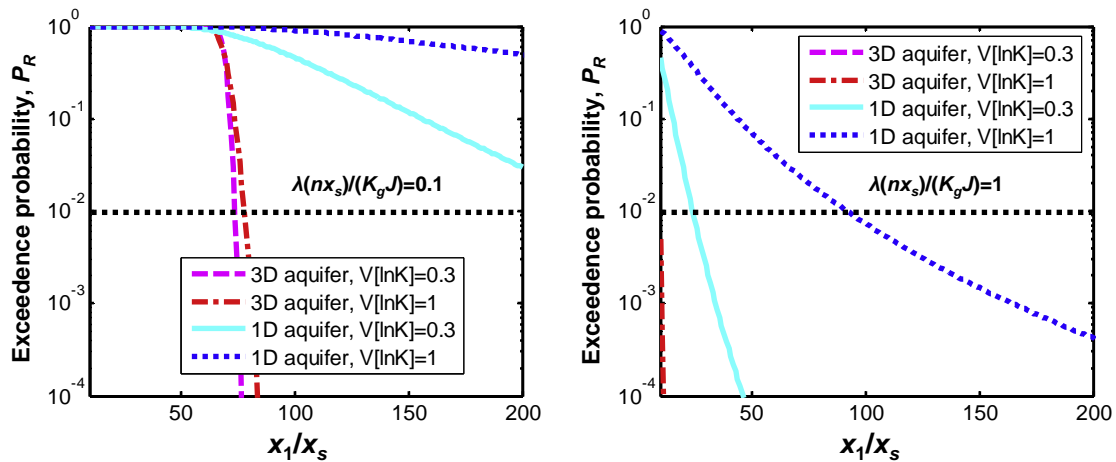


**Fig. A-2.** Effects of uncertainty in the aquifer heterogeneity magnitude (log-conductivity variance,  $V[\ln K]$ ), correlation structure (perfectly stratified aquifer, denoted 1D aquifer, or three-dimensional isotropic aquifer, denoted 3D aquifer), and attenuation-transport rate relation  $\lambda(nx_s)/(K_g J)$  on the probability  $P_R$  to exceed the concentration limit  $C_T$  at different relative distances  $x_1/x_s$  from the source zone in a continuous pollutant release case. The relative source input concentration is  $C_0/C_T = 1000$  and the relative conductivity correlation length in the 3D aquifer is  $l/x_s = 0.1$ .

$$E[C(t, x_1)] = C_0 \int_0^\infty \exp(-\lambda T) H(t - RT) g(T; x_1) dT$$

$$V[C(t, x_1)] = C_0^2 \int_0^\infty \exp(-2\lambda T) H(t - RT) g(T; x_1) dT - E[C(t, x_1)]^2 \quad (\text{A5})$$

with the travel time statistics also given here by Eq. (A2) for the 1D aquifer scenario and by Eq. (A4) for the 3D aquifer scenario. If attenuation takes place in both the aqueous phase and at the sorption sites, the local concentration would further in this scenario be  $C = C_0 \exp(-\lambda RT) H(t - RT)$  instead of  $C = C_0 \exp(-\lambda T) H(t - RT)$  and the concentration statistics in Eq. (A5) would be modified accordingly.

The effects of the reversible sorption–desorption process are for simplicity not included in any of the results presented in the main paper, i.e.,  $R = 1$  in the equations above.

#### Propagation of exceedence probability for different magnitude of heterogeneity

As complements to Figs. 3 and 4 in the main paper, Figs. A-1 and A-2 show  $P_R$  results for both  $V[\ln K] = 0.3$  and  $V[\ln K] = 1$  in a short-pulse and continuous pollutant release case, respectively.

#### References

- Andersson, C., Destouni, G., 2001. Risk-Cost analysis in ground water contaminant transport: the role of random spatial variability and sorption kinetics. *Ground Water* 39 (1), 35–48.
- Andricevic, R., Cvetkovic, V., 1996. Evaluation of risk from contaminants migrating by ground water. *Water Resources Research* 32, 611–621.
- Baresel, C., Destouni, G., 2007. Uncertainty-accounting environmental policy and management of water systems. *Environmental Science and Technology* 41, 3653–3659.
- Batchelor, B., Valdés, J., Araganth, V., 1998. Stochastic risk assessment of sites contaminated by hazardous waste. *Journal of Environmental Engineering* 124, 380–388.
- Beven, K., 2006. A manifesto for the equifinality thesis. *Journal of Hydrology* 320, 18–36.
- Botter, G., Bertuzzo, E., Bellin, A., Rinaldo, A., 2005. On the Lagrangian formulations of reactive solute transport in the hydrologic response. *Water Resources Research* 41, W04008. doi:10.1029/2004WR003544.
- Cvetkovic, V., Dagan, G., Shapiro, A.M., 1992. A solute flux approach to transport in heterogeneous formations, 2. Uncertainty analysis. *Water Resources Research* 28, 137–1388.
- Cvetkovic, V., Dagan, G., 1994. Transport of kinetically sorbing solute by steady random velocity in heterogeneous porous formations. *Journal of Fluid Mechanics* 265, 189–215.
- Cvetkovic, V., Cheng, H., Dagan, G., 1998. Contaminant transport in aquifers with spatially variable hydraulic and sorption properties. *Proceedings of the Royal Society of London A* 454, 2173–2207.
- Dagan, G., 1989. *Flow and Transport in Porous Formations*. Springer Verlag, Berlin.
- Dagan, G., Fiori, A., 1997. The influence of pore-scale dispersion on concentration statistical moments in transport through heterogeneous aquifers. *Water Resources Research* 33 (7), 1595–1606.
- Destouni, G., 1992. Prediction uncertainty in solute flux through heterogeneous soil. *Water Resources Research* 28 (3), 793–801.
- Destouni, G., Cvetkovic, V., 1991. Field scale mass arrival of sorptive solute into the groundwater. *Water Resources Research* 27 (6), 1315–1325.
- Destouni, G., Graham, W., 1995. Solute transport through an integrated heterogeneous soil-groundwater system. *Water Resources Research* 31, 1935–1944.
- Destouni, G., Graham, W., 1997. The influence of observation method on local concentration statistics in the subsurface. *Water Resources Research* 33 (4), 663–676.
- Destouni, G., Simic, E., Graham, W., 2001. On the applicability of analytical methods for estimating solute travel time statistics in nonuniform groundwater flow. *Water Resources Research* 37, 2303–2308.
- European Commission, 2000. Directive 2000/60/EC of the European parliament and of the council establishing a framework for community action in the field of water policy. *Official Journal of the European Communities L* 41, 26–32.
- Fiori, A., Dagan, G., 2000. Concentration fluctuations in aquifer transport: a rigorous first-order solution and applications. *Journal of Contaminant Hydrology* 45, 139–163.
- Fiori, A., Berglund, S., Cvetkovic, V., Dagan, G., 2002. A first-order analysis of solute flux statistics in aquifers: the combined effect of pore-scale dispersion, sampling, and linear sorption kinetics. *Water Resources Research* 38. doi:10.1029/2001WR000678.
- Foussereau, X., Graham, W., Aakpoji, A., Destouni, G., Rao, P.S.C., 2001. Solute transport through a heterogeneous coupled vadose-saturated zone system with temporally random rainfall. *Water Resources Research* 36, 911–921.
- Gren, I.-M., Destouni, G., Tempone, R., 2002. Cost effective policies for alternative distributions of stochastic water pollution. *Journal of Environmental Management* 66, 145–157.
- Janssen, G.M.C.M., Cirpka, O.A., van der Zee, E.A.T.M., 2006. Stochastic analysis of nonlinear biodegradation in regimes controlled by both chromatographic and dispersive mixing. *Water Resources Research* 42. doi:10.1029/2005WR004042.
- Jarsjö, J., Shibuo, Y., Destouni, G., 2008. Spatial distribution of unmonitored inland water flows to the sea. *Journal of Hydrology* 348, 59–72.
- Johansson, P.-O., Werner, K., Bosson, E., Juston, J., 2005. Description of climate, surface hydrology, and near-surface hydrology. Preliminary site description. Forsmark area – version 1.2. Swedish Nuclear Waste Management Company Report R-05-06.
- Kavanaugh, M.C., Rao, P.S.C.K., Abriola, L., Cherry, J., Destouni, G., Falta, R., Major, D., Mercer, J., Newell, C., Sale, T., Shoemaker, S., Siegrist, R., Teutsch, G., Udell, K., 2003. The DNAPL remediation challenge: is there a case of source depletion? Expert Panel Report EPA/600/R-03/143. Environmental Protection Agency (EPA), USA.
- Lindborg, T. (Ed.), 2005. Description of surface systems. Preliminary site description Forsmark area – version 1.2. Swedish Nuclear Waste Management Company Report R-05-03.
- Lindgren, G.A., Destouni, G., 2004. Nitrogen loss rates in streams: scale-dependence and up-scaling methodology. *Geophysical Research Letter* 31, L13501. doi:10.1029/2004GL019996.

- Lindgren, G.A., Destouni, G., Miller, A.V., 2004. Solute transport through the integrated groundwater-stream system of a catchment. *Water Resources Research* 40. doi:10.1029/2003WR002765.
- Malmström, M.E., Destouni, G., Martinet, P., 2004. Modeling expected solute concentration in randomly heterogeneous flow systems with multicomponent reactions. *Environmental Science Technology* 38, 2673–2679.
- O'Hagan, A., Oakley, J.E., 2004. Probability is perfect, but can we elicit it perfectly? *Reliability Engineering and System Safety* 85, 239–248.
- Rubin, Y., 2003. *Applied Stochastic Hydrogeology*. Oxford University Press, New York.
- Shapiro, A.M., Cvetkovic, V., 1988. Stochastic analysis of solute arrival time in heterogeneous porous media. *Water Resources Research* 24, 1711–1718.
- Simic, E., Destouni, G., 1999. Water and solute residence times in a catchment: stochastic model interpretation of  $^{18}\text{O}$  transport. *Water Resources Research* 35, 2109–2119.
- Simmons, C.S., Ginn, T.R., Wood, B.D., 1995. Stochastic-convective transport with nonlinear reaction: mathematical framework. *Water Resources Research* 31, 2675–2688.
- Tompson, A.F.B., Bruton, C.J., Pawloski, G.A., Smith, D.K., Bourcier, W.L., Shumaker, D.E., Kersting, A.B., Carle, S.F., Maxwell, R.M., 2002. On the evaluation of groundwater contamination from underground nuclear tests. *Environmental Geology* 42, 235–247.
- Yabusaki, S.B., Steefel, C.I., Wood, B.D., 1998. Multidimensional, multicomponent, subsurface reactive transport in nonuniform velocity fields: code verification using an advective reactive streamtube approach. *Journal of Contaminant Hydrology* 30 (3), 299–331.



# Paper II



# Quantification of advective solute travel times and mass transport through hydrological catchments

Amélie Darracq · Georgia Destouni · Klas Persson ·  
Carmen Prieto · Jerker Jarsjö

Received: 29 March 2009 / Accepted: 10 August 2009  
© Springer Science+Business Media B.V. 2009

**Abstract** This study has investigated and outlined the possible quantification and mapping of the distributions of advective solute travel times through hydrological catchments. These distributions are essential for understanding how local water flow and solute transport and attenuation processes affect the catchment-scale transport of solute, for instance with regard to biogeochemical cycling, contamination persistence and water quality. The spatial and statistical distributions of advective travel times have been quantified based on reported hydrological flow and mass-transport modeling results for two coastal Swedish catchments. The results show that the combined travel time distributions for the groundwater-stream network continuum in these catchments depend largely on the groundwater system and model representation, in particular regarding the spatial variability of groundwater hydraulic parameters (conductivity, porosity and gradient), and the possible contributions of slower/deeper groundwater flow components. Model assumptions about the spatial variability of groundwater hydraulic properties can thus greatly affect model results of catchment-scale solute spreading. The importance of advective travel time variability for the total mass delivery of naturally attenuated solute (tracer, nutrient, pollutant) from a catchment to its downstream water recipient depends on the product of catchment-average physical travel time and attenuation rate.

**Keywords** Hydrology · Travel time · Solute transport · Natural attenuation · Catchment · Groundwater–surface water interactions

## 1 Introduction

Travel time distributions (or also called transit time distributions, system response functions, weighting functions [1]) are useful descriptors of how small-scale physical transport processes and their dynamics combine to determine larger-scale transport behavior in

---

A. Darracq (✉) · G. Destouni · K. Persson · C. Prieto · J. Jarsjö  
Department of Physical Geography and Quaternary Geology, Stockholm University, Stockholm, Sweden  
e-mail: amelie.darracq@natgeo.su.se

catchments. A travel time distribution can be determined from the mass flow response or breakthrough of an instantaneous, conservative tracer input in a catchment area with zero background tracer concentration [2]. This integrates the physical transport of tracer in all the pathways that carry it through the catchment into a single distribution of the timescales of the tracer transport through the catchment. This distribution quantifies the physical spreading of tracer mass in that catchment-scale transport process and can aid significantly in the understanding and quantification of the processes involved in the catchment-scale water flow and solute (tracer, nutrient, pollutant) transport [3–7]. These processes control also biogeochemical cycling, contamination persistence and water quality [8].

Purely physical, advective solute travel times through a catchment depend on the transport velocities and transport pathway lengths between the solute input and output locations. These physical transport quantities and associated solute travel times may vary widely for different solute input locations, an influence that may be referred to as geomorphologic dispersion in the stream networks [9] and analogously in the subsurface transport process from the land surface to the streams [3, 5]. Even for solute input at a single well-defined point-source location in a stream, the downstream solute transport and travel times through the stream network are subject to dispersion due to transport velocity variations among and along different transport pathways [10, 11]. The solute may also undergo diffusive mass transfer between mobile and immobile water in the hyporheic [12] and dead zones [13].

Different factors and mechanisms may control the dynamics and timescales of hydrological mass transport through drainage basins [14–17]. The travel time variability that exists at all scales in all catchments may to smaller or greater degree mask some important effects of these factors and mechanisms and lead to disparities between different solute transport models and results for different measurement and model scales [4, 18–20]. Such disparities limit our capability to incorporate field knowledge and to interpret and transfer results in and between different modeling frameworks and catchments.

In general, realistic distributions of solute travel times in catchments have been pointed out as essential information for accurately representing the catchment-scale process of solute transport, yet commonly difficult to quantify and constrain [1]. In this paper, we investigate the possible quantification of solute travel time distributions in catchments, by the use of reported results on catchment-scale hydrological flow and mass transport modeling in two well-investigated, coastal Swedish catchments areas (Fig. 1): the Norrström drainage basin [19–24] and the Forsmark catchment area [25–28]. In particular, we investigate here the role of different possible groundwater system representations for the quantification of solute travel times through catchments. We further investigate the effects of different travel time distribution quantifications for the resulting solute mass transport from the catchments to downstream recipients.

## 2 Materials and methods

This section describes the general approach to quantify travel times and their spatial and statistical distributions in catchments, and the solute mass delivery from the catchments. The modeling details for the two specific investigated catchment areas are given in the Appendix.

### 2.1 General quantification approach

Numerous studies have in the past decades developed and used theoretical conceptualization and quantification approaches that account for the large-scale, physical spreading of solute

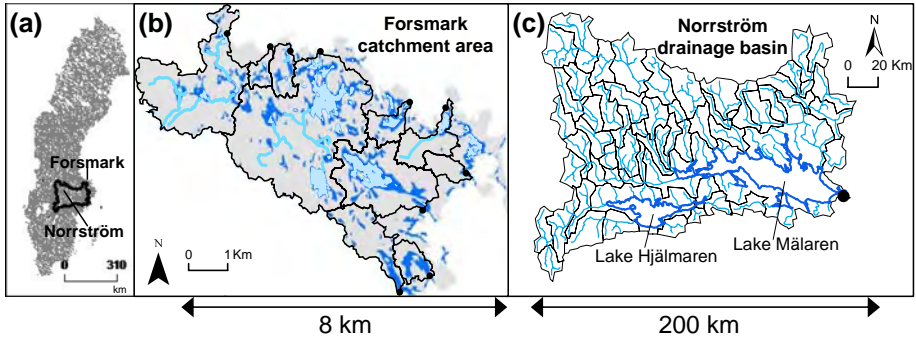


**Fig. 1** **a** Location of the Forsmark and Norrström catchment areas within Sweden; **b** the Forsmark catchment area with its: surface water system, including streams (blue lines), lakes (soft blue), wetlands (dark blue) and ten main stream outlets to the coast (black dots), the subcatchment boundaries of which are drawn with black lines; and **c** the Norrström drainage basin with its: river network (soft blue), major lakes (dark blue) and subcatchment boundaries (black lines), and outlet to the sea (black dot). The small near-coastal zones in between the main stream outlets of the Forsmark catchment area discharge mainly groundwater to the sea

transport in heterogeneous geological formations in terms of prevailing advection variability; see for instance Dagan [29] and Rubin [30] for reviews of such different approaches. Some of these approaches have particularly developed the use of advective solute travel times and their distributions as a main basis for Lagrangian conceptualizations and derivations of field-scale solute transport and spreading in different subsurface water systems (unsaturated soil and groundwater, e.g. [2, 31–47]). Parallel studies also extended the theoretical basis of the Lagrangian travel time-based approaches to link the solute transport through the different water subsystems (unsaturated soil, groundwater, streams and stream networks) that are hydraulically connected at the larger scales of hydrological catchments [4, 5, 44, 48–50].

The advective travel time distributions that have been used in most previous studies have been approximated by assuming some common type of probability density function (e.g., log-normal, inverse Gaussian), which can be fully parameterized based on knowledge of only the possible mean and variance of solute travel times in the considered transport system. In this study, we adopt the Lagrangian advective travel time-based approach and extend it to quantify and investigate entire distributions of advective solute travel times in the two Swedish catchment cases and their different water subsystems, by the use of the flow and mass transport results that have already been modeled, tested against all available monitoring data and reported in a series of previous published studies of these catchment areas [19–28].

In general, studies that use Lagrangian advective travel time-based approaches do so because they focus on the macro-dispersion of solute transport due to large-scale advection variability. In such large-scale contexts, the local mixing that occurs between and along different advection pathways due to pore-scale dispersion and molecular diffusion in mobile water is often neglected [29, 30]. However, if and where account of these processes is needed, they can be linked to the advective travel-time based model representations, with such linked studies showing that neglecting local dispersion and diffusion within mobile water does not much affect the large-scale mean mass flow rate or concentration, but may lead to the overestimation of local mass flux and concentration variances [51–54].

Jarsjö et al. [26] have also specifically investigated the effect of local random variability around mean advective travel time, e.g. due to local dispersion and diffusion, for the Forsmark catchment area, which constitutes one of the two specific catchment cases of the present

study. The results of Jarsjö et al. [26] confirm that also in this specific catchment case, the effect of such local variability within mobile water is small on the expected large-scale solute transport. The present paper therefore focuses on the quantification of advective solute travel times as the main, first and necessary step towards quantifying catchment-scale pollutant transport and its dominant timescales.

With regard to more significant effects of diffusive mass transfer between mobile and immobile water zones, it is one of the main advantages of Lagrangian travel time-based approaches that their first-step quantification of advective solute travel time distributions can readily be coupled with relevant process models of diffusive mass transfer [5,33,34,36,37,46,49], as well as with biogeochemical reaction process models of various degrees of complexity [34,38–43,45,47,50,55]. The resulting coupled advection-sorption and/or advection-reaction models account then both for the physical solute spreading effect of advection variability and the diffusive mass transfer and/or biogeochemical reaction process effects on large-scale pollutant transport. In this study, this extension possibility will only be illustrated for a generic, hypothetical and simple case of solute undergoing first-order attenuation. This illustration is made to show some general first-order effects of the advective solute travel time variability and distributions on the large-scale solute mass delivery from different parts of a catchment area and the whole catchment to a downstream water recipient. More complex investigations of diffusive mass transfer and/or reactive transport of specific pollutants are outside the scope of the present study, but we note with reference to the above-cited diffusive-reactive transport studies that such investigations are facilitated by the present, first-step quantification of advective solute travel time distributions.

In the present quantification of these distributions, we further neglect the travel time components in the essentially vertical transport from the soil surface down to the groundwater table, for simplicity and in comparison to the dominant, large travel times in the groundwater system, from the groundwater table to the groundwater–stream interface. This is by no means any necessary neglect requirement in the Lagrangian advective travel time-based approach. On the contrary, this approach has already been developed and used for linking the travel times and travel time distributions of the essentially vertical unsaturated zone transport with the essentially horizontal transport in the groundwater zone and its travel times and travel time distributions, in order to represent the large-scale solute transport through the integrated soil–groundwater system [44,49]. If and where the advective travel times through the unsaturated zone are quantified or expected to be significant in relation to the groundwater travel times, the same methodology can readily be used to extend the present quantification results to consider and integrate the unsaturated zone travel time components in the combined catchment-scale travel time distribution.

Furthermore, the previously reported flow and transport modeling of the specific two Swedish catchment cases considered in this study certainly include soil properties and processes [19–28]. The main reason and motivation for the present primary focus on quantifying and linking the groundwater and stream network travel times is that the soil depth of quaternary deposits above the bedrock is generally small (around 1–2 m, up to maximum 5 m) in both these catchment areas, with the groundwater table being on average about one meter below the soil surface. In contrast, the horizontal transport lengths are three to five orders of magnitude greater in both the small Forsmark catchment area of 30 km<sup>2</sup> and the much larger Norrström catchment area of 22000 km<sup>2</sup> (Fig. 1). We believe that these conditions justify a primary focus on the advective travel times of the horizontal transport through the groundwater–surface water continuum, especially with the particular aim of the present study to investigate the role of different possible groundwater system characterizations and model representations for the quantification of solute travel times through catchments. Also in this

respect, the present results facilitate follow-up studies that can incorporate the additional travel time components of vertical transport through the unsaturated zone and investigate their effects on the combined total distributions of travel times through whole catchments.

### 2.2 General travel time and mass delivery fraction calculations

We consider solute mass releases from different sources on the land surface and/or directly into the streams, lakes of each catchment area, which discharges its water and waterborne solute mass flows into a downstream recipient. This recipient is the coastal water for both catchment areas investigated here, with a single coastal outlet in the Norrström basin, and multiple stream outlets as well as zones of direct groundwater discharge to the coast in the Forsmark catchment area (Fig. 1).

The advective solute travel time from any mass input location  $a_{gw}$  along the mean groundwater flow direction  $x_{gw}$  to a given control plane location  $x_{CP}$  along that direction (e.g., at the nearest groundwater–stream or groundwater–coast interface), and  $a_s$  along the mean stream/surface water flow direction  $x_s$  to the outlet  $x_{out}$  is quantified as  $\tau_{gw} = \int_{a_{gw}}^{x_{CP}} \frac{dx_{gw}}{v_{gw}(X_{gw})}$  and  $\tau_s = \int_{a_s}^{x_{out}} \frac{dx_s}{v_s(X_s)}$ , with  $v_{gw}(X_{gw})$  and  $v_s(X_s)$  being the local transport velocity in the  $x_{gw}$  and  $x_s$  direction at advective solute transport position  $X_{gw}$  and  $X_s$  along  $x_{gw}$  and  $x_s$ , respectively. For any solute input location at the catchment surface, a total flow-weighted average travel time  $T$  to the recipient can be quantified as  $T = (1 - \beta_{gw})\tau_s + \beta_{gw}(\tau_{gw} + \tau_s)$ , or just  $T = \tau_{gw}$  in near-coastal catchment zones with only groundwater flow to the coast (see Forsmark area in Fig. 1b), where  $\beta_{gw}$  is the flow fraction of the total precipitation surplus (precipitation minus actual evapotranspiration) at the catchment surface that infiltrates the soil–groundwater system, and  $(1 - \beta_{gw})$  is the complementary fraction that flows directly into the recipient through only surface runoff and stream flow. In general,  $\beta_{gw} = 0$  in all catchment area parts that are covered by surface water, while it may generally have different values at different land surface locations. In the present calculations, explained further in the specific catchment sections below,  $\beta_{gw}$  is assumed steady in time and is estimated mainly from available land cover information for the Forsmark catchment area, and both land cover and river network information for the Norrström drainage basin.

The quantification of delivered solute mass fraction from the catchment surface to the coast is made here for solute that undergoes first-order attenuation  $exp(-\lambda_{gw}\tau_{gw})$  in the subsurface and  $exp(-\lambda_s\tau_s)$  in the stream network system of the catchment. For simplicity, because we do not investigate any specific tracer, nutrient or pollutant transport situation, we illustrate results for  $\lambda_{gw} = \lambda_s = \lambda$ , so that the mass delivery fraction  $\alpha$  from any input location to the coast is quantified as  $\alpha = exp(-\lambda T)$ . The total delivered mass fraction from the whole catchment to the coast is quantified by the mean value,  $\bar{\alpha}$ , of  $\alpha$  for uniform mass input over the whole catchment surface.

### 2.3 The Forsmark and Norrström catchment areas

The Forsmark catchment area is relatively small (30 km<sup>2</sup>) and characterized by uniquely high-resolved (on 10 m × 10 m grid cells) measured and modeled hydrological data [25–28]. The Norrström drainage basin is relatively large (22000 km<sup>2</sup>), with much coarser (1 km × 1 km) resolution of available measured and modeled data [19–24]. This section shortly describes the main flow and transport characteristics of these areas. More details on the modeling and calculations for each area are given in Appendix.

### 2.3.1 Forsmark catchment area

The Forsmark catchment area (Fig. 1b) contains the subcatchments (black contours, Fig. 1b) of ten main stream-outlets to the Baltic Sea, with small near-coastal catchment zones in between discharging mainly groundwater to the sea. The Forsmark catchment area is currently of particular interest due to its consideration by the Swedish Nuclear Fuel and Waste Management Company as a possible suitable location for a deep repository for spent nuclear fuel, e.g., [26,56]. Quaternary deposits cover a major part of the surface and are dominated by till (mainly sandy). The land surface is mainly covered by forest. There are also many lakes and wetlands, with the wetlands being sometimes partially forested. Figure 1b shows the ten main connected stream networks (with outlets to the coast shown with black dots) and their catchments (with boundaries drawn with black lines), where the dominating flow and transport pathways from the land surface to the coastal waters go through the coupled groundwater–stream system to the nearest surface water (stream, lake, wetland) and through the associated stream network to the coast. The remaining surface area in the Forsmark catchment represents the about 11% of the total catchment surface area that is covered by the small, near-coastal catchment zones where groundwater discharges directly into the coastal waters.

In general, infiltration excess overland flow may occur in this catchment area but only over short distances [56,57], implying a negligible surface runoff contribution to the total runoff from the catchment and thereby  $\beta_{gw} \approx 1$  in the land surface grid cells, which cover about 85% of the catchment area. The remaining 15% is covered by surface water (streams, lakes and wetlands), for which  $\beta_{gw} = 0$ .

The fine data and model resolution for this catchment area allows us to investigate the role of the groundwater hydraulic gradient quantification, by using the same underlying fine-resolved (10 m  $\times$  10 m grid) ground slope data as in previously reported hydrological modeling [26,28] in two different ways. Specifically, we estimate the hydraulic gradient in each grid cell in the groundwater system as equal to: either (i) the arithmetic mean value of all the local, fine-resolved ground slopes in the subcatchment area of the outlet (to the nearest stream or directly to the sea) that is associated with the grid cell; this slope is then constant among the different grid cells within each subcatchment area and referred to as the subcatchment-average slope and hydraulic gradient; or (ii) the fine-resolved local ground slope at each grid cell location, which we refer to as the local ground slope and groundwater hydraulic gradient. Grid cell lengths through each model cell are generally for both gradient approaches calculated in the horizontal plane, based on estimated flow path directions and the size of model grid cells. Elevation is thus not accounted for in the transport distance calculations, which implies that any result differences between the different gradient estimation approaches depend on associated transport velocity and not transport length differences.

Field measurements of hydraulic conductivity (by 36 slug tests and 2 pumping tests) throughout the Forsmark catchment area yielded highly variable conductivity values, which were generally higher at the interface between the quaternary deposits and the underlying bedrock than in the soil above that interface [57]. For the investigation purposes of the previous hydrological modeling studies of this area [26,28], a uniform hydraulic conductivity value (equal to the reported mean value from measurements [57]) was used to mainly represent the solute transport through the high-conductivity layer at the soil–bedrock interface. The same model representation is used also here, allowing us to investigate the effect of different assumptions with regard to the spatial variability of hydraulic conductivity, by comparison with Norrström basin results under similar mean travel time conditions.

### 2.3.2 Norrström drainage basin

The Norrström drainage basin (Fig. 1c) is defined by the coastal outlet location of Norrström in the Swedish capital, Stockholm, and contains many (sixty shown in Fig. 1c) main sub-catchments that drain their water through the major lake Mälaren to that common outlet and further into the Baltic Sea. The basin is rather flat with a basin-average topographic slope of 1.5% and a steepest topographic slope of 10% in a single 1 km × 1 km model grid cell, and low-lying with numerous lakes, underlain by granitic and gneiss-granitic bedrock covered by clay or till deposits. On the resolution scale of 1 km × 1 km, land-cover is classified to consist of 4% built-up areas, 36% agricultural and open land, 49% forest, 1.5% wetlands and 9.5% major inland surface waters.

Due to the coarse spatial model resolution of this basin, there are generally unresolved streams and other surface water features also within the model grid cells that are classified as land. Given a relevant stream density for these grid cells based on several paper and digital sources for river network delineation [19], the previous hydrological model studies of the Norrström basin [19–24] have quantified the total flow from the land–soil–groundwater system that feeds the surface water system to be, on average, about 75% of the total water flow through the basin. The remaining flow of about 25% goes then only through the surface water system. In these surface water cells defined by land cover and river network information,  $\beta_{gw} = 0$ . In the land–soil–groundwater system grid cells,  $\beta_{gw} = 1$  because the pure surface runoff contribution to the total (surface and land–soil–ground) water flow is negligible (about 0.02%) in Norrström, as in Forsmark.

The previous, underlying hydrological modeling of the Norrström basin [21] conceptualized the groundwater flow to be partitioned between a relatively highly conductive (shallow, e.g., of quaternary deposits) and a less conductive (deeper, e.g., the bedrock) groundwater subsystem with the average total thickness of the two groundwater systems being set to 50 m following de Wit [58]. In this study, we investigate specifically the advective travel time effects of accounting for or neglecting the possible flow partitioning into the groundwater subsystem of slower/deeper flow.

Due to the coarse spatial resolution, the grid cell-average hydraulic gradient quantification for the groundwater system in the Norrström basin is more consistent with the subcatchment-average than with the local gradient estimate in the Forsmark catchment area. In contrast to the Forsmark application, the groundwater hydraulic conductivity in Norrström is modeled to vary between grid cells, depending on the available data of soil characteristics [19–24].

## 3 Results and discussion

Figure 2 illustrates the spatial and statistical distributions of advective travel times through the different water subsystems, and in total through the catchment area to the coast, from all the 10 m × 10 m grid cells in Forsmark, with the different hydraulic gradient quantifications: (i) the subcatchment-average gradient (Fig. 2a, b), and (ii) the local gradient (Fig. 2c, d). The different gradient quantifications yield large travel time differences in both the spatial distribution (Fig. 2a, c) and the spreading of the statistical distribution (Fig. 2b, d) of travel times. The differences depend on the contributions of very long travel time components in the local gradient approach from the large flat-topography parts of the Forsmark area. The arithmetic averaging involved in the subcatchment-average gradient approach reduces the weight of small local gradient values and provides more realistic estimates of the prevailing hydraulic gradient, which is not likely to fluctuate as much as the local ground slope.

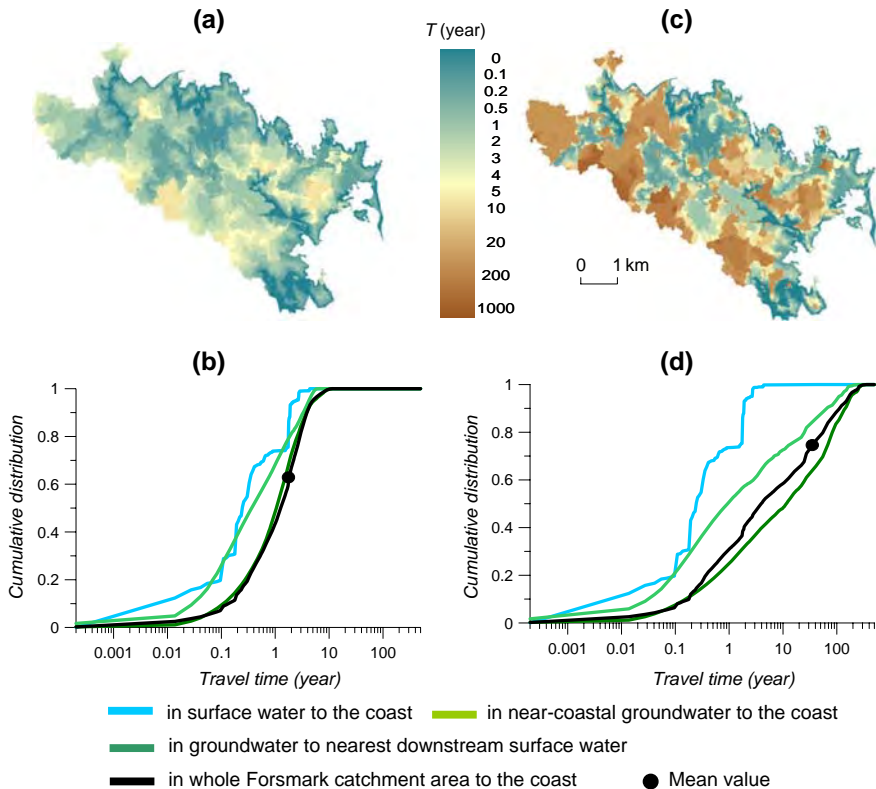


**Fig. 2** Spatial (a, c) and statistical (b, d) distributions of advective travel time from all grid cells in Forsmark catchment area to the coast, for the stream network and groundwater subsystems and the whole catchment, with hydraulic gradient quantification from a, b subcatchment-average ground slope; and c, d local ground slope

The differences in Fig. 2 underline the essential role of the model representation of groundwater hydraulics, here reflected by the different possible approaches to estimate the hydraulic gradient. The fact that infiltration excess overland flow is negligible in Forsmark [56,57] explains the strong hydraulic gradient control on calculated advective travel times through this catchment area, which was also found by McGuire et al. [15]. A contrasting and counter-intuitive positive relationship between catchment transit times and ground slope has been found by Tetzlaff et al. [59] for the flat Swedish Krycklån boreal basin. This result is explained by the total runoff being dominated by relatively fast overland flow, rather than by groundwater flow as in Forsmark, in the flatter, poorly drained peat soils of the Krycklån basin [60].

Figure 3 illustrates the spatial and statistical distributions of advective travel times through the different water subsystems and the whole basin to the coast from all the  $1 \text{ km} \times 1 \text{ km}$  grid cells in Norrström. Results are illustrated for the alternative model representations that neglect (Fig. 3a, b) or account for (Fig. 3c, d) the possible contribution of slow/deep groundwater flow. The travel time differences obtained by these alternative model representations are large in terms of both the spatial distribution (Fig. 3a, c) and the statistical spreading (Fig. 3b, d) of travel times in the basin. Since flow path directions and flow pathway lengths are the same in

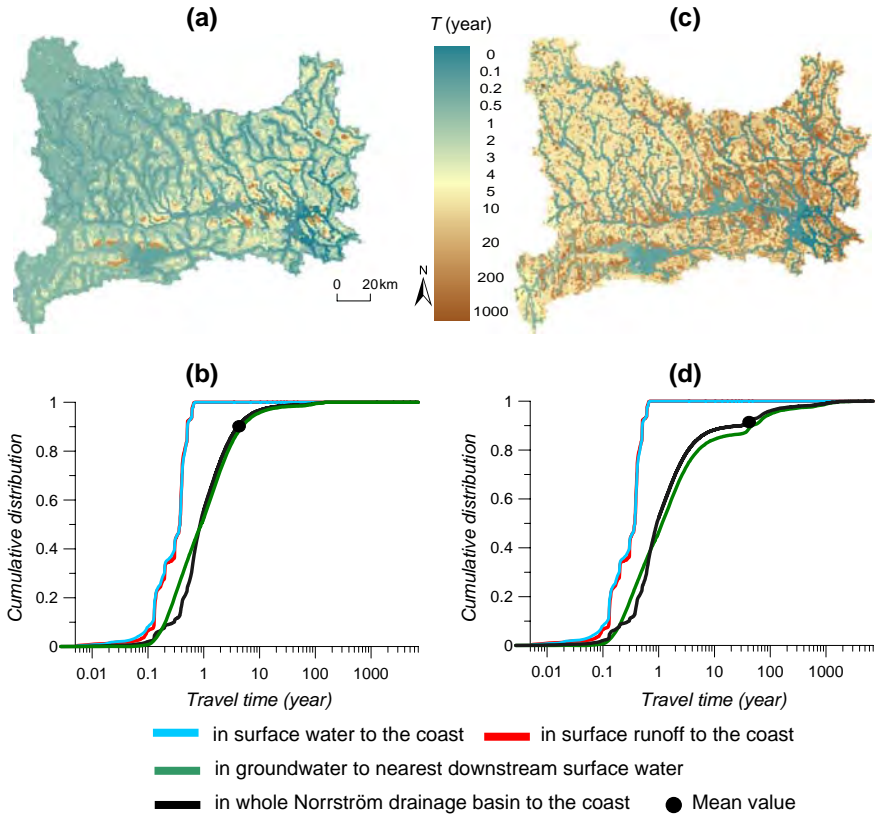


**Fig. 3** Spatial (a, c) and statistical (b, d) distributions of advective travel time from all grid cells in the Norrström drainage basin to the coast, for the surface runoff, surface water and groundwater subsystems and the whole catchment for a, b neglect and c, d account for the possible contribution of a slow/deep groundwater subsystem

both conceptualizations, these travel time distribution differences are only due to the assumed partitioning (in Fig. 3c, d) or the no-partitioning (in Fig. 3a, b) of groundwater flow between the two groundwater subsystems with distinctly different advective velocities. Also these differences emphasize thus the importance of relevant groundwater system characterization for relevant and accurate assessment of solute travel time distributions in catchments.

The importance of groundwater controls on catchment-scale travel times has also been reported in other studies, which have found greater travel time dependence on bedrock seepage [61,62] than on the more directly intuitive catchment size. The results illustrated in Fig. 3 show that also in the Norrström basin, the relatively small proportion of about 12% of the total runoff recharging the slow/deep groundwater subsystem is sufficient for significantly increasing the total mean travel time to the coast. With this deep recharge fraction, the mean total travel time increases from about 3 to about 30 years (Fig. 3). Furthermore, the travel time variability, quantified in terms of the travel time standard deviation, increases from about 10 to about 60 years (Fig. 3).

Table 1 summarizes the most directly comparable catchment-scale travel time statistics for the two catchment areas: those for the case of neglecting the slow/deep groundwater

**Table 1** Catchment-scale mean value, standard deviation and coefficient of variation of advective travel times  $T$  from all grid cells in the Forsmark and Norrström catchment areas to the coast

Advective travel time to the coast in the Forsmark catchment area		Advective travel time to the coast in the Norrström drainage basin	
Mean value (years)	1.7	Mean value (years)	3.4
Standard deviation (years)	1.7	Standard deviation (years)	11.2
Coefficient of variation	1.0	Coefficient of variation	3.3

Travel times in Forsmark are for the subcatchment-average hydraulic gradient quantification. Travel times in Norrström neglect the possible contribution of slow/deep groundwater

flow contribution in Norrström (Fig. 3a, b), and the case of subcatchment-average hydraulic gradient in Forsmark (Fig. 2a, b). Under these conditions, the resulting total mean travel time is similar for both catchment areas. To explain this similarity, Tables 2 and 3 in Appendix summarize some characteristic flow and transport parameter statistics for these Forsmark and Norrström cases, respectively. A comparison between these tables shows that, beyond the similar precipitation surplus because both catchments are in the same hydro-climatic region, the similarity in mean advective travel times between the two cases depends on their similar mean combined times for advective groundwater transport, expressed as the mean value of the ratio between groundwater flow path length and groundwater flow velocity (in turn quantified as the product of hydraulic conductivity and slope divided by porosity). This time scale is similar even though the separate groundwater flow and transport characteristics are quite different between the two cases, and irrespectively of the very different catchment area sizes. The independence of mean travel time on catchment scale is consistent with similar findings for diffuse solute transport by McGuire et al. [15], Tetzlaff et al. [59] and Rodgers et al. [63], however depending on different types of flow and transport controls in the different catchment case studies.

The main groundwater system control of the Forsmark and Norrström travel time results is emphasized by the order-of-magnitude smaller standard deviation and the three times smaller coefficient of variation of advective travel times (from different input positions to the coast) in Forsmark than in Norrström (Table 1). Specifically, comparison between Tables 2 and 3 with regard to the coefficients of variation of different flow and transport parameters shows that the uniform hydraulic conductivity and porosity assumption for the groundwater system in Forsmark is primarily responsible for its small travel time variability (in terms of both standard deviation and coefficient of variation). This variability difference implies a much greater spatio-temporal spreading (macro-dispersion) of solute around its centre of mass in Norrström than in Forsmark, and emphasizes the importance of spatial groundwater variability assumptions for the distributions of advective solute travel time and the associated physical spreading of solute mass in catchment-scale hydrological transport.

Figure 4 finally illustrates the effect of these variability differences for the delivered solute mass fraction from different input locations to the coast in the comparable (in terms of similar mean travel time) Norrström (Fig. 4a–c) and Forsmark (Fig. 4d–f) cases, for different scenarios of the product of catchment-average physical travel time  $\bar{T}$  and biogeochemical attenuation rate  $\lambda$ . For each catchment area and  $\lambda\bar{T}$  scenario, Fig. 4 shows also the total resulting catchment-scale delivery fraction  $\bar{\alpha}$  of solute mass to the coast.

The results in Fig. 4 indicate that the differences in solute travel time variability implied by the different spatial variability assumptions for the groundwater hydraulic parameters in the two catchment case quantifications are primarily important in solute-catchment situations where  $0.1 < \lambda\bar{T} < 10$ . For the interval  $0.1 < \lambda\bar{T} < 10$ , any uniform, instantaneous solute mass

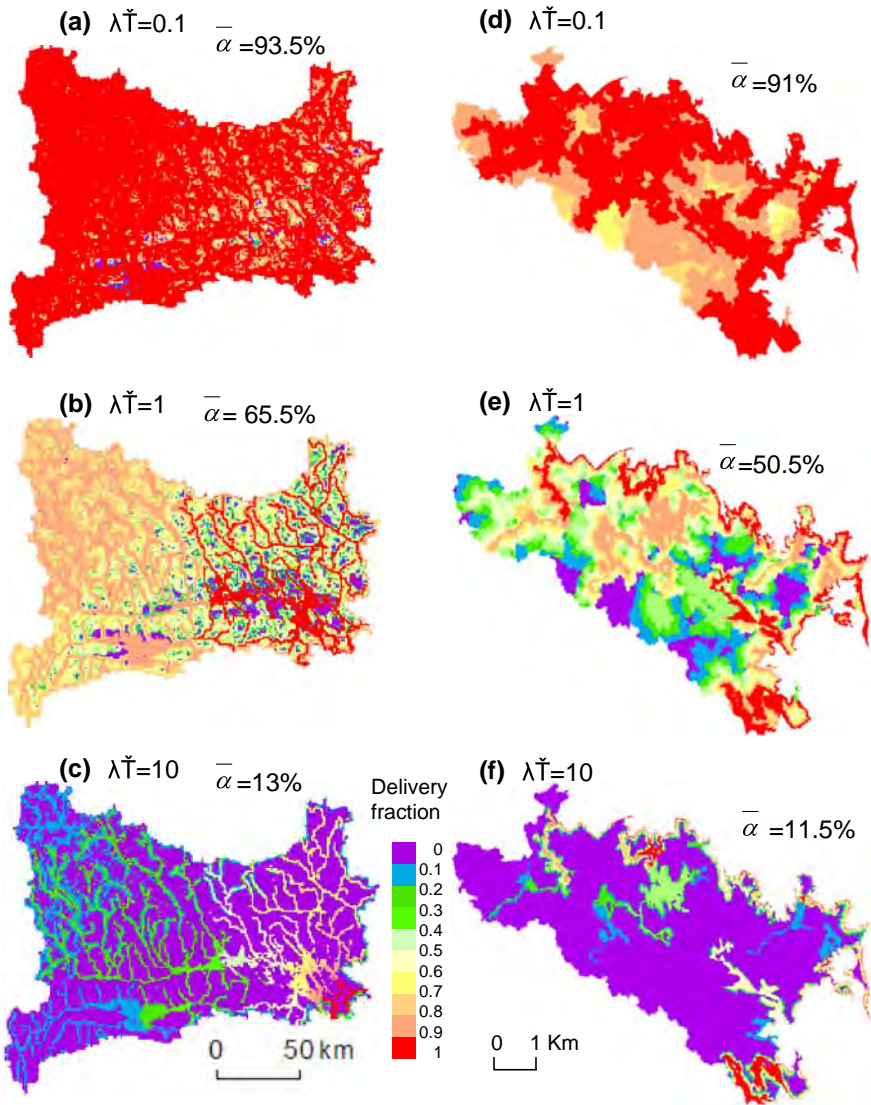


**Fig. 4** Map of delivered mass fraction from each grid cell location to the coast in the Norrström drainage basin (a–c) and Forsmark catchment area (d–f), for different scenarios (0.1, 1 and 10) of the product of catchment-average advective travel time  $\bar{T}$  and attenuation rate  $\lambda$ . The total delivered mass fraction  $\bar{\alpha}$  from the whole catchment area is also quantified in the figure for each  $\lambda\bar{T}$  scenario. Travel times in Norrström (a–c) neglect the possible contribution of slow/deep groundwater. Travel times in Forsmark (d–f) are for the subcatchment-average hydraulic gradient

input leads to a delivered mass fraction that is about 30% (or 15 percentage units) greater for the Norrström case with the larger advective travel time variability than for the Forsmark case with the smaller travel time variability. Smaller or greater mean  $\lambda\bar{T}$  scenarios than this  $0.1 < \lambda\bar{T} < 10$  interval imply nearly non-attenuated or nearly totally attenuated solute mass, respectively, essentially regardless of the prevailing variability of advective solute travel times.

## 4 Conclusion

This study has outlined the possible quantification of advective solute travel-time distributions in different catchment areas. The specific catchment cases in the study differ largely in terms of their scale, data-model resolutions, and process representations in the travel time modeling. Yet the comparative analysis of these cases has provided some important general insights.

The results show that the groundwater system characterization and model representation largely controls the resulting distributions of advective travel times through these hydrological catchments. For groundwater assumptions that yielded similar catchment-average travel times in the different catchment cases, the spatial variability in groundwater hydraulics played an essential role for the travel time variance, which determines the physical spreading (macro-dispersion) of non-reactive solute mass transported through the catchment.

For solute that is physically or biogeochemically attenuated along its different transport pathways through the catchment, the product of the catchment-average advective travel time and the solute-dependent biogeochemical attenuation rate was shown to largely determine the effects of travel time variance on the total solute mass delivery from the catchments. These effects were found to be primarily important for the product interval  $0.1 < \lambda \bar{T} < 10$ . For hazardous contaminants, where even very small solute concentrations and concentration differences may be essential for environmental and health risks, however, the travel time variability effects may be important and need to be further investigated also for  $\lambda \bar{T} \geq 10$ .

Furthermore, the primary importance-interval  $0.1 < \lambda \bar{T} < 10$  applies to the investigated conditions of variability only in the physical, advective travel time  $T$ . The interval may widen significantly if also the attenuation rate  $\lambda$  is variable, and depending on its possible cross-correlation with the advective travel time  $T$  [e.g., 34,64–66]. Further investigations and realistic quantifications are needed for the spatial variability of biogeochemical attenuation rates and their correlation with the physics of flow and transport in both the surface water and not least the groundwater systems of hydrological catchments.

**Acknowledgements** Financial support for this work has been provided by the Swedish Research Council (VR), the Swedish Rescue Services Agency (Räddningsverket), and the Swedish Nuclear Fuel and Waste Management Company (SKB).

## Appendix

### Modeling of the Forsmark catchment area

The previous hydrological modeling of the Forsmark catchment area [25–28], described in detail by Jarsjö et al. [25,26,28], provides the spatial distribution of total (surface and sub-surface) annual average runoff (over 30 years), as estimated from the modeled precipitation surplus, which is the difference between annual average precipitation and modeled actual evapotranspiration in each model cell. The direction of the water flow and solute transport pathway through each cell of the modeled catchment area is estimated from the local ground slope, which is in turn estimated from a detailed digital elevation model of the area, as explained in more detail by Jarsjö et al. [25,26,28]. The present Forsmark application is based on average results from two different empirical approaches [67,68], which were used for actual evapotranspiration calculations in the previous, underlying hydrological modeling and yielded consistent resulting spatial water flow distribution with each other and consistent water flow results with independent runoff data from the catchment area.

To obtain the travel time from each input cell  $a_{gw}$  along the associated groundwater pathway (as estimated from the ground slope direction) to the control plane at distance  $x_{cp}$  (of the nearest stream and/or the coast), the travel time contribution  $\Delta\tau_{gw} = \Delta x_{gw}/v_{gw}$  of each model cell is estimated from the cell length  $\Delta x_{gw}$  and the transport velocity  $v_{gw} = K \cdot I/n$ , where  $K$  is hydraulic conductivity,  $I$  is hydraulic gradient, and  $n$  is effective porosity. The total mean  $\tau_{gw}(a_{gw}, x_{CP})$  is the sum of  $\Delta\tau_{gw}$  for all cells along the transport pathway to  $x_{cp}$ . The hydraulic conductivity and effective porosity are assumed to be  $1.5 \cdot 10^{-5}$  m/s and 0.05, respectively, over the whole catchment area, as reported by Johansson et al. [57] for the quaternary deposits/bedrock interface. In the subcatchment-average gradient approach (i) in the main text, the hydraulic gradient in each grid cell is set equal to the arithmetic average of all the local ground slopes in the subcatchment area of the associated grid-cell outlet to the nearest stream or directly to the sea. The hydraulic gradient is then constant among the different grid-cells within each subcatchment area, including in cells with nearly zero local ground slope. In the local gradient approach (ii) in main text, the local hydraulic gradient in each cell equals the local ground slope in that cell.

The stream network includes all the interconnected bodies of surface water, streams, lakes and wetlands, through which the waterborne solute mass may be transported all the way to the coast. For obtaining the travel time from each input cell  $a_s$  along the associated stream network pathway to the outlet at  $x_{out}$ , the travel time contribution  $\Delta\tau_s = L_s/v_s$  of each stream stretch is estimated from its length  $L_s$  and mean flow velocity  $v_s = Q/A_{cs}$ , where  $Q$  is the mean annual flow rate and  $A_{cs}$  is the mean cross-sectional area of the stream. The total mean  $\tau_s(a_s, x_{out})$  is the sum of  $\Delta\tau_s$  for all the stream stretches, lakes and wetlands along the whole stream network pathway to  $x_{out}$ ; the estimation of  $\Delta\tau_s$  in lakes and wetlands is explained below. In streams where the mean cross-sectional area is measured and known (from 0.29 to 0.43 m<sup>2</sup>),  $Q$  is assumed to be equal to the modeled mean annual water flow at the model cell location where the stream cross-section area was measured. Otherwise, a generic value of  $A_{cs} = 0.3$  m<sup>2</sup> and the modeled [25,26,28] mean annual flow value at the mouth of the stream are used in the calculation of mean flow velocity. The  $\Delta\tau_s$  contribution of a lake or a wetland is estimated as  $\Delta\tau_s = A_{L/W} \cdot d_{eff}/Q$ , where  $A_{L/W}$  is the area of the lake or wetland,  $Q$  is the mean annual flow rate through the lake or wetland, and  $d_{eff}$  is the mean depth in lakes and is defined as the product of the depth and the water content (typically around 0.9) in wetlands. The mean flow rate  $Q$  is the modeled [25,26,28] mean annual runoff (precipitation minus evaporation) generated in the lake or wetland plus the modeled [25,26,28] runoff into the lake or wetland from all upstream cells. For isolated lakes and wetlands that are not part of any connected stream network pathway all the way to the coast, their travel time contribution is calculated from the length of a topographically estimated transport pathway through the lake or wetland divided by an average velocity  $v_{L/W} = Q \cdot \sqrt{[4A_{L/W}/\pi]}/[A_{L/W} \cdot d_{eff}]$ , where  $\sqrt{[4A_{L/W}/\pi]}$  is the diameter of a circle with the same area  $A_{L/W}$  as the lake or wetland. The travel time contribution obtained is added to the total groundwater travel time  $\tau_{gw}$  along the main groundwater pathway that crosses the isolated lake or wetland. Details on measured lake and wetland depths are given by Johansson [69] and Brunberg et al. [70].

### Modeling of the Norrström drainage basin

The previous hydrological modeling of the Norrström drainage basin [19–24], described in detail by Darracq et al. [21] after de Wit [58,71] and Greffe [72], provides the spatial distribution of total (surface and subsurface) annual average runoff (over 30 years),

as estimated from the modeled precipitation surplus in each model cell; as in Forsmark, the precipitation surplus is also here defined as the difference between annual average precipitation and actual evapotranspiration, modeled based on an empirical function of precipitation and potential evapotranspiration [67, 73]. A digital elevation map available at a resolution of  $1 \text{ km} \times 1 \text{ km}$  was used for assigning water flow and solute-transport pathway directions through each cell of the modeled catchment area. Previous hydrological modeling results in the Norrström basin [21] are also used to obtain: the contribution of the flow through the land–soil–groundwater system to the total water flow through the basin, based on the ratio between the long-term average groundwater recharge and the total precipitation surplus in each grid cell, as functions of land cover and topographic slope [68]; and the travel time  $\tau_{gw}(a_{gw}, x_{CP})$  from each grid cell  $a_{gw}$  along the groundwater pathway (as estimated from the ground slope direction) to the control plane at distance  $x_{CP}$  of the nearest stream.

As mentioned also in the main text, the previous hydrological modeling of the Norrström basin [21] conceptualized the groundwater flow to be partitioned between a relatively highly conductive (shallow, e.g., of quaternary deposits) and a less conductive (deeper, e.g., the bedrock) groundwater subsystem, with the groundwater flow depending on aquifer type, soil texture, groundwater level, slope, land use and average January temperature [73] based on empirical estimates by de Wit [58] and Mourad [74]. Following Wendland [68], the travel time  $\tau_{sgw}(a_{gw}, x_{CP})$  from each input cell  $a_{gw}$  along the associated pathway (as estimated from the ground slope direction) in the fast/shallow groundwater subsystem to the nearest stream at  $x_{CP}$  is quantified as:  $\tau_{sgw} = lp/v$ , where  $v$  is the groundwater flow velocity and  $lp$  is the average length of the groundwater flow path, as a function of conductivity of the aquifer  $ca$ , hydraulic gradient  $h$  (with topographic slope in each 1000 m grid cell used as an estimate of  $h$ ), primary effective aquifer porosity  $pp$  and modeled total runoff  $Q$ . Specifically,  $v = ca \cdot h/pp$  and  $lp = 0.5/ns$ , where  $ns$  is stream density quantified as  $ns = 2$  in wetlands and  $(Q/450)^{0.8}$  (with  $Q$  given in  $\text{mm year}^{-1}$ ) elsewhere.

Furthermore, following Meinardi et al. [73], the travel time  $\tau_{dgw}(a_{gw}, x_{CP})$  from each grid cell  $a_{gw}$  along the pathway in the slow/deep groundwater subsystem to the nearest stream at  $x_{CP}$  (the transport length of which is estimated similarly as in the fast/shallow groundwater system, from the ground slope direction) is calculated as the product between total effective porosity of the aquifer  $tp$ , thickness of groundwater flow formation  $at$  and the inverse of the long-term average recharge of the slow/deep groundwater subsystem. The average total thickness of both groundwater systems over the whole Norrström basin is set to 50 m following de Wit [58]. Values for aquifer conductivity, primary and total porosity are empirically related [58, 68, 73] to the aquifer type and the soil and bedrock groundwater flow yields, which were obtained for the Norrström basin from the Swedish Geological Survey mapping of groundwater in soil and bedrock.

The resulting total groundwater travel time  $\tau_{gw}(a_{gw}, x_{CP})$  is quantified as:  $\tau_{gw} = (1 - \beta_{dgw}) \cdot \tau_{sgw} + \beta_{dgw} \cdot \tau_{dgw}$ , where  $\beta_{dgw}$  is the recharge of the slow/deep groundwater subsystem, in terms of flow fraction of the total groundwater flow into the surface water system; that fraction was on average about 12% of the total flow in the previous model simulations [19–24], implying that  $\beta_{dgw} = 0.12$  in the present results that account for the possible slow/deep groundwater flow contribution, and  $\beta_{dgw} = 0$  in the results that neglect it (Tables 2, 3).

The stream network includes all the interconnected bodies of surface water, streams and lakes through which the waterborne mass may be transported all the way to the coast. For obtaining the travel time from each cell  $a_s$  along a stream network pathway to the outlet at  $x_{out}$ , the travel time contribution  $\Delta\tau_s = L_s/v_s$  of each stream stretch is estimated from

**Table 2** Mean value, standard deviation and coefficient of variation of precipitation surplus (i.e., precipitation minus actual evapotranspiration), topographic slope, groundwater system porosity, hydraulic conductivity and flow path length, and the combined characteristic time for groundwater transport expressed by the fraction:  $\frac{\text{groundwater\_flow\_path\_length}}{\text{conductivity} \cdot \text{slope}}$  in the Forsmark catchment area

	Mean value	Standard deviation	Coefficient of variation
Precipitation surplus (mm/year)	226	35	0.2
Slope	0.03	0.01	0.3
Porosity	0.05	0	0
Hydraulic conductivity (m/day)	1.3	0	0
Groundwater flow path length (m)	394	491	1.2
$\frac{\text{groundwater\_flow\_path\_length}}{\text{conductivity} \cdot \text{slope}}$ (years)	1.5	1.8	1.2

**Table 3** Mean value, standard deviation and coefficient of variation of precipitation surplus (i.e., precipitation minus actual evapotranspiration), topographic slope, groundwater system porosity, hydraulic conductivity and flow path length, and the combined characteristic time for groundwater transport expressed by the fraction:  $\frac{\text{groundwater\_flow\_path\_length}}{\text{conductivity} \cdot \text{slope}}$  in the Norrström drainage basin

	Mean value	Standard deviation	Coefficient of variation
Precipitation surplus (mm/year)	233	50	0.2
Slope	0.01	0.01	1.0
Porosity	0.18	0.3	1.6
Hydraulic conductivity (m/day)	125	295	2.4
Groundwater flow path length (m)	1042	299	0.3
$\frac{\text{groundwater\_flow\_path\_length}}{\text{conductivity} \cdot \text{slope}}$ (years)	3.4	12	3.6

its length  $L_s$  and mean flow velocity  $v_s$ , empirically estimated from an expression given in [20, 75], as:  $v_s = 0.36Q^{0.241}$  in streams and  $v_s = 0.36(Q/A_L)^{0.241}$  in lakes, where  $Q$  is mean annual flow rate in  $\text{m}^3/\text{s}$  as obtained from previous hydrological modeling [21] and  $A_L$  is lake surface area. The total  $\tau_s(a_s, x_{out})$  is the sum of  $\Delta\tau_s$  for all the stream stretches and lakes along the whole stream network pathway and topographically estimated transport pathway through lakes to  $x_{out}$ .

The travel time contributions  $\Delta\tau_{sr} = L_{sr}/v_{sr}$  in the surface runoff subsystem is estimated in analogy with the stream network subsystem, from the surface runoff pathway length  $L_{sr}$  and mean flow velocity  $v_s = 0.36(Q)^{0.241}$ , where  $Q$  is modeled surface runoff flow in  $\text{m}^3/\text{s}$ . In the combined total travel time distribution through the whole basin, the weight of the surface runoff contribution is negligible (0.02%) compared to the groundwater flow, so that results are directly comparable between Norrström and Forsmark.

## References

1. McGuire KJ, McDonnell JJ (2006) A review and evaluation of catchment transit time modeling. *J Hydrol* 330:543–563
2. Maloszewski P, Zuber A (1982) Determining the turnover time of groundwater systems with the aid of environmental tracers. 1. Models and their applicability. *J Hydrol* 57:207–231
3. Simic E, Destouni G (1999) Water and solute residence times in a catchment: stochastic model interpretation of 18O transport. *Water Resour Res* 35(7):2109–2120
4. Lindgren GA, Destouni G (2004) Nitrogen loss rates in streams: scale-dependence and up-scaling methodology. *Geophys Res Lett.* doi:[10.1029/2004GL019996](https://doi.org/10.1029/2004GL019996)
5. Lindgren GA, Destouni G, Miller AV (2004) Solute transport through the integrated groundwater–stream system of a catchment. *Water Resour Res.* doi:[10.1029/2003WR002765](https://doi.org/10.1029/2003WR002765)
6. Botter G, Bertuzzo E, Bellin A, Rinaldo A (2005) On the Lagrangian formulations of reactive solute transport in the hydrologic response. *Water Resour Res.* doi:[10.1029/2004WR003544](https://doi.org/10.1029/2004WR003544)
7. Fiori A, Russo D (2008) Travel time distribution in a hillslope: insight from numerical simulations. *Water Resour Res.* doi:[10.1029/2008WR007135](https://doi.org/10.1029/2008WR007135)
8. Schnoor JL (1996) Environmental modeling: fate and transport of pollutants in water, air and soil. Wiley, New York
9. Rinaldo A, Marani A, Rigon R (1991) Geomorphological dispersion. *Water Resour Res* 27(4):513–525
10. White AB, Kumar P, Saco PM, Rhoads BL, Yen BC (2004) Hydrodynamic and geomorphologic dispersion: scale effects in the Illinois River Basin. *J Hydrol* 288:237–257
11. Saco PM, Kumar P (2002) Kinematic dispersion in stream networks 1. Coupling hydraulic and network geometry. *Water Resour Res.* doi:[10.1029/2001WR000695](https://doi.org/10.1029/2001WR000695)
12. Valett HM, Morrice JA, Dahm CN, Campana ME (1996) Parent lithology, surface-groundwater exchange, and nitrate retention in headwater streams. *Limnol Oceanogr* 41(2):333–345
13. Ensign SH, Doyle MW (2005) In-channel transient storage and associated nutrient retention: evidence from experimental manipulations. *Limnol Oceanogr* 50(6):1740–1751
14. Haggerty R, Wondzell SM, Johnson MA (2002) Power-law residence time distribution in the hyporheic zone of a 2nd-order mountain stream. *Geophys Res Lett.* doi:[10.1029/2002GL014743](https://doi.org/10.1029/2002GL014743)
15. McGuire KJ, McDonnell JJ, Weiler M, Kendall C, McGlynn BL, Welker JM, Seibert J (2005) The role of topography on catchment-scale water residence time. *Water Resour Res* 41(5):W05002.1–W05002.14
16. Boano F, Packman AI, Cortis A, Revelli R, Ridolfi L (2007) A continuous time random walk approach to the stream transport of solutes. *Water Resour Res.* doi:[10.1029/2007WR006062](https://doi.org/10.1029/2007WR006062)
17. Wörman A, Packman AI, Marklund L, Harvey J, Stone S (2007) Fractal topography and subsurface water flows from fluvial bedforms to the continental shield. *Geophys Res Lett.* doi:[10.1029/2007GL029426](https://doi.org/10.1029/2007GL029426)
18. Malmström ME, Destouni G, Banwart SA, Strömberg BHE (2000) Resolving the scale-dependence of mineral weathering rates. *Environ Sci Technol* 34:1375–1378
19. Darracq A, Destouni G (2005) In-stream nitrogen attenuation: model-aggregation effects and implications for coastal nitrogen impacts. *Environ Sci Technol* 39(10):3716–3722
20. Darracq A, Destouni G (2007) Physical versus biogeochemical interpretations of nitrogen and phosphorus attenuation in streams and its dependence on stream characteristics. *Glob Biogeochem Cycles.* doi:[10.1029/2006GB002901](https://doi.org/10.1029/2006GB002901)
21. Darracq A, Greffe F, Hannerz F, Destouni G, Cvetkovic V (2005) Nutrient transport scenarios in a changing Stockholm and Mälaren valley region. *Water Sci Technol* 51(3-4):31–38
22. Destouni G, Darracq A (2006) Response to comment on “In-stream nitrogen attenuation: model aggregation effects and implications for coastal nitrogen impacts”. *Environ Sci Technol* 40(7):2487–2488
23. Lindgren GA, Destouni G, Darracq A (2007) The inland subsurface water system role for coastal nitrogen load dynamics and abatement responses. *Environ Sci Technol* 41(7):2159–2164
24. Darracq A, Lindgren GA, Destouni G (2008) Long-term development of phosphorus and nitrogen loads through the subsurface and surface water systems of drainage basins, *Global Biogeochem Cycles.* doi:[10.1029/2007GB003022](https://doi.org/10.1029/2007GB003022)
25. Jarsjö J, Shibuo Y, Destouni G (2004) Using the PCRaster-POLFLOW approach to GISbased modelling of coupled groundwater–surface water hydrology in the Forsmark Area. Swedish Nuclear Fuel and Waste Management Company Report R-04-54, Stockholm, Sweden
26. Jarsjö J, Destouni G, Persson K, Prieto C (2007) Solute transport in coupled inland-coastal water systems. General conceptualization and application to Forsmark. Swedish Nuclear Fuel and Waste Management Company Report R-07-65, Stockholm, Sweden
27. Destouni G, Shibuo Y, Jarsjö J (2008) Freshwater flows to the sea: spatial variability, statistics and scale dependence along coastlines. *Geophys Res Lett.* doi:[10.1029/2008GL035064](https://doi.org/10.1029/2008GL035064)

28. Jarsjö J, Shibuo Y, Destouni G (2008) Spatial distribution of unmonitored inland water discharges to the sea. *J Hydrol* 348(12):59–72
29. Dagan G (1989) Flow and transport in porous formations. Springer Verlag, Berlin
30. Rubin Y (2003) Applied stochastic hydrogeology. Oxford University Press, New York
31. Simmons CS (1982) A stochastic-convective transport representation of dispersion in one-dimensional porous media. *Water Resour Res* 18:1193–1214
32. Shapiro AM, Cvetkovic V (1998) Stochastic analysis of solute travel time in heterogeneous porous media. *Water Resour Res* 24:1711–1718
33. Cvetkovic V, Shapiro AM (1990) Mass arrival of sorptive solute in heterogeneous porous media. *Water Resour Res* 26:2057–2067
34. Destouni G, Cvetkovic V (1991) Field-scale mass arrival of sorptive solute into the groundwater. *Water Resour Res* 27:1315–1325
35. Destouni G (1993) Stochastic modeling of solute flux in the unsaturated zone at the field scale. *J Hydrol* 143:45–61
36. Cvetkovic V, Dagan G (1994) Transport of kinetically sorbing solute by steady random velocity in heterogeneous porous formations. *J Fluid Mech* 265:189–215
37. Destouni G, Sassner M, Jensen KH (1994) Chloride migration in heterogeneous soil: 2, stochastic modeling. *Water Resour Res* 30:747–758 (Correction, *Water Resour Res* 31:1161, 1995)
38. Ginn TR, Simmons CS, Wood BD (1995) Stochastic-convective transport with nonlinear reaction: biodegradation with microbial growth. *Water Resour Res* 31:2689–2700
39. Simmons CS, Ginn TR, Wood BD (1995) Stochastic-convective transport with nonlinear reaction: mathematical framework. *Water Resour Res* 31:2675–2688
40. Berglund S, Cvetkovic V (1996) Contaminant displacement in aquifers: coupled effects of flow heterogeneity and nonlinear sorption. *Water Resour Res* 32:23–32
41. Cvetkovic V, Dagan G (1996) Reactive transport and immiscible flow in geochemical media: 2 applications. *Proc R Soc Lond Ser A* 452:303–328
42. Eriksson N, Destouni G (1997) Combined effects of dissolution kinetics, secondary mineral precipitation, and preferential flow on copper leaching from mining waste rock. *Water Resour Res* 33:471–483
43. Yabusaki SB, Steefel CI, Wood BD (1998) Multidimensional, multicomponent, subsurface reactive transport in nonuniform velocity fields: code verification using an advective reactive streamtube approach. *J Contam Hydrol* 30(3):299–331
44. Foussereau X, Graham W, Aakpoji A, Destouni G, Rao PSC (2001) Solute transport through a heterogeneous coupled vadose-saturated zone system with temporally random rainfall. *Water Resour Res* 37(6):1577–1588
45. Tompson AFB, Bruton CJ, Pawloski GA, Smith DK, Bourcier WL, Shumaker DE, Kersting AB, Carle SF, Maxwell RM (2002) On the evaluation of groundwater contamination from underground nuclear tests. *Environ Geol* 42:235–247
46. Cvetkovic V, Haggerty R (2002) Transport with multiple-rate exchange in disordered media. *Phys Rev E*. doi:[10.1103/PhysRevE.65.051308](https://doi.org/10.1103/PhysRevE.65.051308)
47. Malmström ME, Destouni G, Martinet P (2004) Modeling expected solute concentration in randomly heterogeneous flow systems with multicomponent reactions. *Environ Sci Technol* 38:2673–2679
48. Rinaldo A, Marani A (1987) Basin scale model of solute transport. *Water Resour Res* 23:2107–2118
49. Destouni G, Graham W (1995) Solute transport through an integrated heterogeneous soil–groundwater system. *Water Resour Res* 31:1935–1944
50. Botter G, Bertuzzo E, Bellin A, Rinaldo A (2005) On the Lagrangian formulations of reactive solute transport in the hydrologic response. *Water Resour Res*. doi:[10.1029/2004WR003544](https://doi.org/10.1029/2004WR003544)
51. Dagan G, Fiori A (1997) The influence of pore-scale dispersion on concentration statistical moments in transport through heterogeneous aquifers. *Water Resour Res* 33(7):1595–1606
52. Fiori A, Dagan G (2000) Concentration fluctuations in aquifer transport: a rigorous first-order solution and applications. *J Contam Hydrol* 45:139–163
53. Fiori A, Berglund S, Cvetkovic V, Dagan G (2002) A first-order analysis of solute flux statistics in aquifers: the combined effect of pore-scale dispersion, sampling, and linear sorption kinetics. *Water Resour Res*. doi:[10.1029/2001WR000678](https://doi.org/10.1029/2001WR000678)
54. Janssen GMCM, Cirpka OA, Van der Zee EATM (2006) Stochastic analysis of nonlinear biodegradation in regimes controlled by both chromatographic and dispersive mixing. *Water Resour Res*. doi:[10.1029/2005WR004042](https://doi.org/10.1029/2005WR004042)
55. Malmström ME, Berglund S, Jarsjö J (2008) Combined effects of spatially variable flow and mineralogy on the attenuation of acid mine drainage in groundwater. *Appl Geochem* 23(6):1419–1436

56. Lindborg T (2005) Description of surface systems. Preliminary site description Forsmark area—version 12. Swedish Nuclear Fuel and Waste Management Company Report R-05-03, Stockholm, Sweden
57. Johansson P-O, Werner K, Bosson E, Juston J (2005) Description of climate, surface hydrology, and near-surface hydrology. Preliminary site description. Forsmark area—version 1.2. Swedish Nuclear Waste Management Company (SKB) Report R-05-06, Stockholm, Sweden
58. de Wit MJM (1999) Nutrients fluxes in the Rhine and Elbe basins. Dissertation, Royal Dutch Geographical Society, Utrecht, Netherlands
59. Tetzlaff D, Seibert J, McGuire KJ, Laudon H, Burns DA, Dunn SM, Soulsby C (2009) How does landscape structure influence catchment transit time across different geomorphic provinces? *Hydrol Process* 23:945–953
60. Laudon H, Sjöblom V, Buffam I, Seibert J, Mörth CM (2007) The role of catchment scale and landscape characteristics for runoff generation of boreal streams. *J Hydrol* 344:198–209
61. Asano Y, Uchida T, Ohte N (2002) Residence times and flow paths of water in steep unchannelled catchments, Tanakami, Japan. *J Hydrol* 261:173–192
62. Dunn SM, McDonnell JJ, Vaché KB (2007) Factors influencing the residence time of catchment waters: a virtual experiment research. *Water Resour Res*. doi:[10.1029/2006WR005393](https://doi.org/10.1029/2006WR005393)
63. Rodgers P, Soulsby C, Waldron S (2005) Stable isotope tracers as diagnostic tools in upscaling flow path understanding and residence time estimates in a mountainous mesoscale catchment. *Hydrol Process* 19:2291–2307
64. Jarsjö J, Bayer-Raich M, Ptak T (2005) Monitoring groundwater contamination and delineating source zones at industrial sites: uncertainty analyses using integral pumping tests. *J Contam Hydrol* 79:107–134
65. Jarsjö J, Bayer-Raich M (2008) Estimating plume degradation rates in aquifers: effect of propagating measurement and methodological errors. *Water Resour Res*. doi:[10.1029/2006WR005568](https://doi.org/10.1029/2006WR005568)
66. Cunningham JA, Fadel ZJ (2007) Contaminant degradation in physically and chemically heterogeneous aquifers. *J Contam Hydrol* 94:293–304
67. Turc L (1954) The water balance of soils. Relation between precipitation, evaporation and flow. *Annal Agron* 5:491–569
68. Wendland F (1992) Die Nitratbelastung in den Grundwasserlandschaften der 'alten' Bundesländer (BRD), Berichte aus der Ökologischen Forschung, Band 8, Forschungszentrum Jülich, Jülich
69. Johansson P-O (2003) Drilling and sampling in soil. Installation of groundwater monitoring wells and surface water level gauges. Swedish Nuclear Fuel and Waste Management Company Report P-03-64, Stockholm, Sweden
70. Brunberg A-K, Carlsson T, Blomqvist P, Brydsten L, Strömgren M (2004) Identification of catchments, lake-related drainage parameters and lake habitats. Swedish Nuclear Fuel and Waste Management Company Report P-04-25, Stockholm, Sweden
71. de Wit MJM (2001) Nutrients fluxes at the river basin scale I: the PolFlow model. *Hydrol Process* 15: 743–759
72. Greffe F (2003) Material transport in the Norrström drainage basin: integrating GIS and hydrological process modelling. Master Thesis, Royal Institute of Technology, Stockholm, Sweden
73. Meinardi C, Beusen A, Bollen M, Klepper O (1994) Vulnerability to diffuse pollution of European soils and groundwater. National Institute of Public Health and Environmental Protection (RIVM), Report 4615001002, Bilthoven, Netherlands
74. Mourad DSJ (2002) Application of GIS-based modelling to assess nutrient loads in rivers of the Estonian part of the lake Peipsi basin. MANTRA-East working paper 5.1
75. Alexander RB, Elliott AH, Shankar U, McBride GB (2002) Estimating the sources and transport of nutrients in the Waikato River Basin, New Zealand. *Water Resour Res* 38:1268–1290